GOVERNMENT OF
NEWFOUNDLAND AND LABRADOR
Department of Mines and Energy
Geological Survey

TILL GEOCHEMISTRY OF THE WESTERN AVALON PENINSULA AND ISTHMUS

(All or parts of NTS map sheets 1N/5, 1N/6, 1N/11, 1N/12, 1N/13, 1N/14; 1M/16; 2C/4)

M. Batterson and D.M. Taylor

Open File NFLD 2824

St. John's, Newfoundland
June 4, 2003

NOTE

The purchaser agrees not to provide a digital reproduction or copy of this product to a third party. Derivative products should acknowledge the source of the data.

DISCLAIMER

Cover photo:
View overlooking Bay Roberts.

GOVERNMENT OF
NEWFOUNDLAND AND LABRADOR
Department of Mines and Energy
Geological Survey

TILL GEOCHEMISTRY OF THE WESTERN AVALON PENINSULA AND ISTHMUS

(All or parts of NTS map sheets 1N/5, 1N/6, 1N/11, 1N/12, 1N/13, 1N/14; 1M/16; 2C/4)

M. Batterson and D.M. Taylor

Open File NFLD 2824

St. John's, Newfoundland
June 4, 2003

Recommended citation:
Batterson, M.J. and Taylor, D.M.
2003: Till geochemistry of the western Avalon Peninsula and Isthmus. Newfoundland Department of Mines and Energy, Geological Survey, Open File NFLD 2824, 169 pages.

CONTENTS

FIGURES

TABLES

APPENDICES

INTRODUCTION

This project continues regional surficial and till geochemistry mapping in eastern Newfoundland (Batterson and Taylor, 2003), that began in 2000 on the Bonavista Peninsula (Batterson and Taylor, 2001a, b). The efficacy of this project was demonstrated recently by interest from mineral-exploration companies and prospectors following the Bonavista open-file release (Batterson and Taylor, *op. cit.*), which generated the staking of 1045 new claims having a value of $62 300, within the first 5 days of its release. This response was similar to results from other till geochemistry projects, including those covering Grand Falls–Gander (Batterson *et al.*, 1998), Hodges Hill (Liverman *et al.*, 2000), Roberts Arm (Liverman *et al.*, 1996), and southern Labrador (McCuaig, 2002).

These projects combine surficial mapping (a combination of aerial photograph analysis and field verification), paleo ice-flow mapping and sampling of till for geochemistry analyses. The latter two elements are complete for this project, although further surficial geology mapping is required.

LOCATION AND ACCESS

The Avalon Peninsula is located in the eastern part of the province, comprising an area of about 9700 km^2, and that has a population of about 300 000 (over 60 percent of the total population of the province). The Avalon Peninsula is connected to the rest of the island by the Isthmus, which is only 6.3 km wide at its narrowest point.

This project covered eight 1:50 000-NTS map sheets extending from the Clarenville area across the Isthmus, and continuing north of the Trans-Canada Highway up the Bay de Verde Peninsula to the Victoria–Heart's Content road (Route 74). Map sheets included were: 1N/5, Argentia; 1N/6, Holyrood; 1N/11, Harbour Grace; 1N/12, Dildo; 1N/13, Sunnyside; 1N/14, Heart's Content; 1M/16, Sound Island; and 2C/4, Random Island (Figure 1).

Access to the area was generally good, via a network of paved and gravel roads. The decommissioned Newfoundland railway track also provided access to areas on the Isthmus and the Bay de Verde Peninsula. Parts of the study area, however, were only accessible via helicopter. These included the area between Bull Arm and Southwest Arm, the eastern parts of the Isthmus, the Bellevue Peninsula and parts of the Bay de Verde Peninsula.

The study area is one of variable relief (Figure 2), ranging from the rugged coastal highlands north of Bull Arm to the gently rolling central Avalon lowlands characterized by a well-developed Rogen moraine field. The highest terrain is between Bull Arm and Southwest Arm, where Centre Hill extends to 515 m above sea level (m asl), and Crown Hill to over 365 m asl. Hills over 200 m asl are rare across the remainder of the field area, although the Doe Hills in the central Isthmus are over 350 m asl.

BEDROCK GEOLOGY AND MINERAL POTENTIAL

The study area lies entirely within the Avalon tectonostratigraphic zone. The bedrock consists of late Precambrian igneous and sedimentary rocks overlain by Palaeozoic shallow -marine and

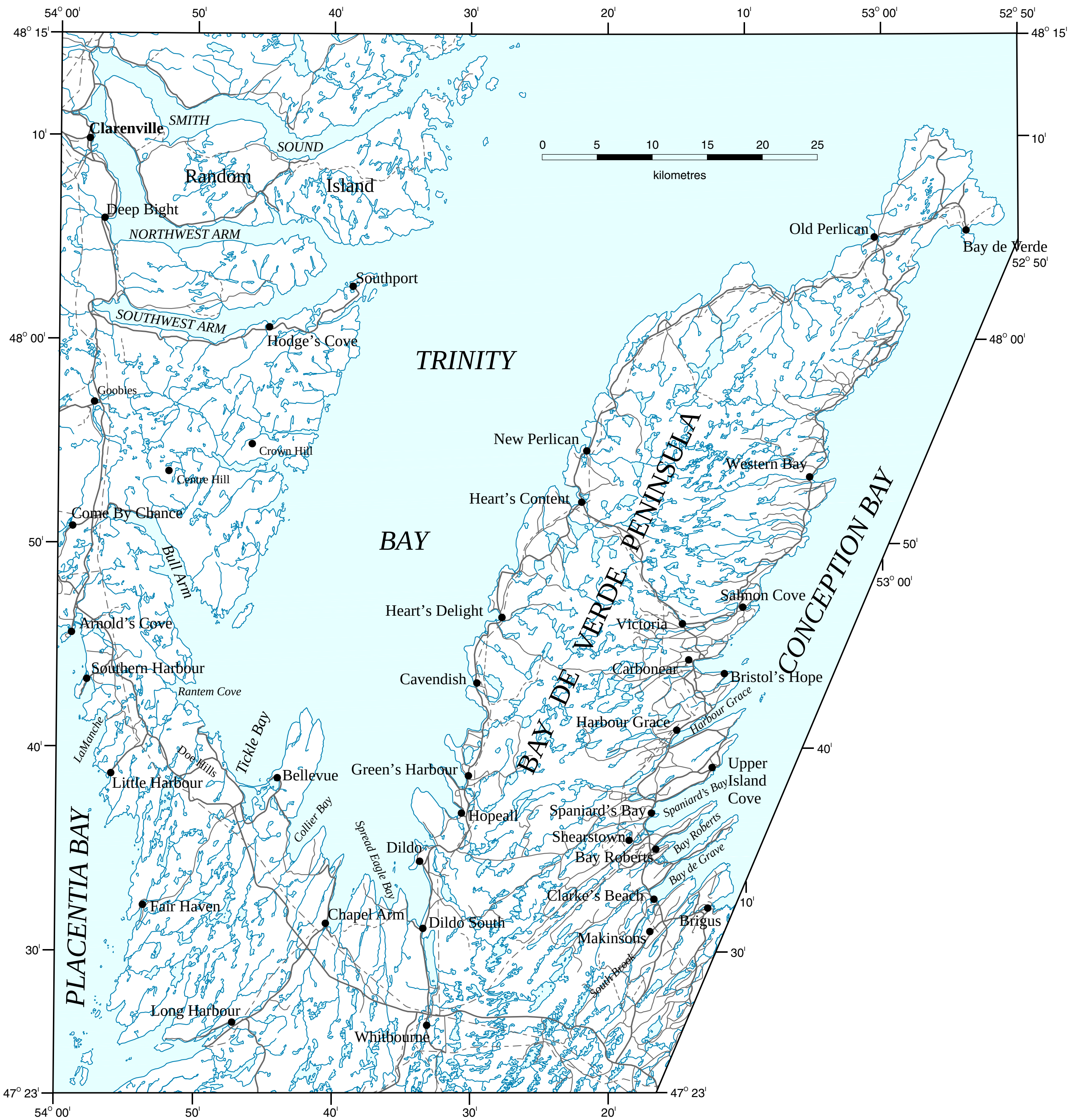

Figure 1. Location of study area and places mentioned in text.

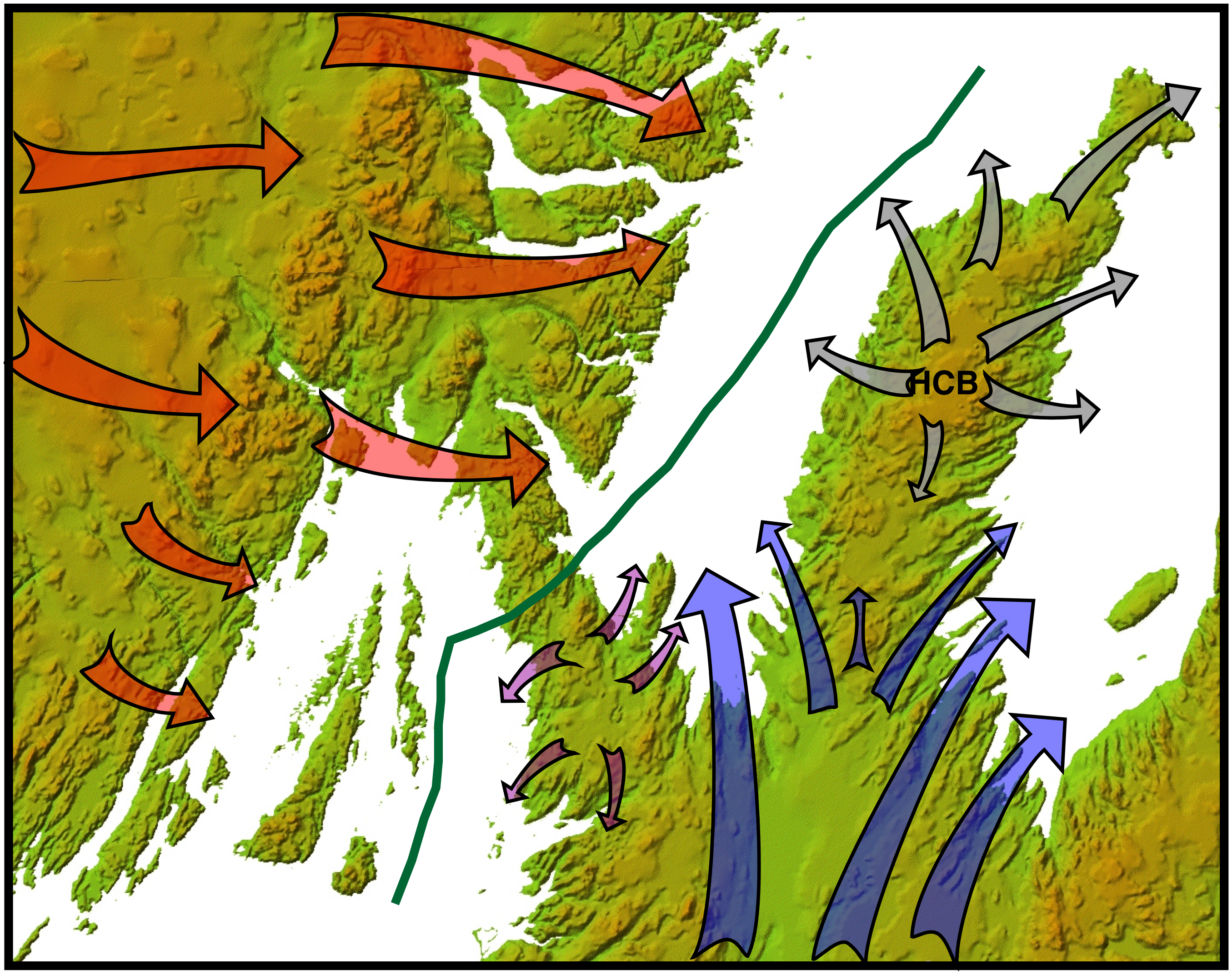

Figure 2: Shaded relief map and patterns of ice flow at the Late Wisconsinan maximum (modified from Catto, 1998). Data shows that the western part of the study area was covered by ice from the main Newfoundland ice dispersal centre (red arrows), likely on Middle Ridge. In contrast, the Avalon Peninsula was covered by radially-flowing ice from a number of small dispersal centres located on the spine of the peninsulas. In the study area, ice flow was from dispersal centres at the head of St. Mary's Bay (blue arrows), Heart's Content barrens (HCB) and Collier Bay Brook (CBB).

terrestrial sedimentary and minor volcanic rocks (O'Brien and King, 2002; O'Brien *et al.*, 1983; King, 1988; Figure 3).

Hadrynian sedimentary sequences of shallow-marine to fluvial rocks underlie most of the study area. The oldest are shallow-marine platformal rocks of the Conception Group, found on the western shore of Conception Bay, which are overlain by deltaic sedimentary rocks of the St. John's Group. The Connecting Point Group consists of early Hadrynian shallow marine sediments of similar age to the Signal Hill and Conception groups and is found in the west of the study area. These are overlain by fluvial sediments of the Signal Hill Group in the east, and the Musgravetown Group in the west. The Musgravetown Group contains felsic and mafic volcanic flows and tuffs found within the Bull Arm Formation. The Bull Arm Formation is intruded by the Hadrynian pink to grey, medium-grained Swift Current Granite.

Much of the remainder of the Avalon Peninsula and the Isthmus are underlain by small areas of younger rocks, the largest of which is shale and limestone of the Early Cambrian to Middle Ordovician Adeytown Group. These rocks are found at the southeast end of Trinity Bay and along its eastern shore.

West of the Isthmus, the Hadrynian rocks are intruded by several granitic bodies, including the Devonian or earlier Clarenville Granite, a pink to red, medium-grained, biotite granite found along the western shore of Northwest Arm, and by the Powder Horn intrusive suite. The Powder Horn intrusive suite is composed mostly of fine- to medium-grained diorite, but also contains gabbro and minor granite (King, 1988).

The now-abandoned lead mine located within Conception Group strata at La Manche (Figure 2) on the north shore of Placentia Bay is one of the oldest mines in Newfoundland, operating from the mid to late 1800s (Martin, 1983). More recently, the open-pit mine at Collier Point (Figure 2) extracted barite for the offshore oil industry. Several other barite showings are found across the Isthmus, mostly within the Connecting Point or Musgravetown groups. Other mineral occurrences include several manganese showings within the Adeytown Group, pyrrhotite found within St. John's Group rocks in the central Bay de Verde Peninsula, and copper exposed on the Heart's Content barrens within the St. John's Group. Recent exploration efforts have focussed on the potential for sediment-hosted or volcanic red-bed copper deposits within the Musgravetown Group (O'Brien and King, 2002). The discovery by Cornerstone Resources of copper mineralization within the Crown Hill Formation on the northern Bonavista Peninsula, and in volcanic rocks of the Bull Arm Formation has prompted exploration activity on the Isthmus and Avalon Peninsula, both of which are underlain by the Crown Hill and Bull Arm formations. Gold is found within the Powder Horn intrusive suite at the Lodestar gold showing, which is currently being prospected by Pathfinder Exploration.

ICE-FLOW HISTORY

PREVIOUS WORK

Much of the early work on the glaciation of the Avalon Peninsula suggested that the area was covered by eastward-flowing ice from central Newfoundland (Murray, 1883; Coleman, 1926; MacClintock and Twenhofel, 1940), although MacClintock and Twenhofel (*op. cit.*) argued that the

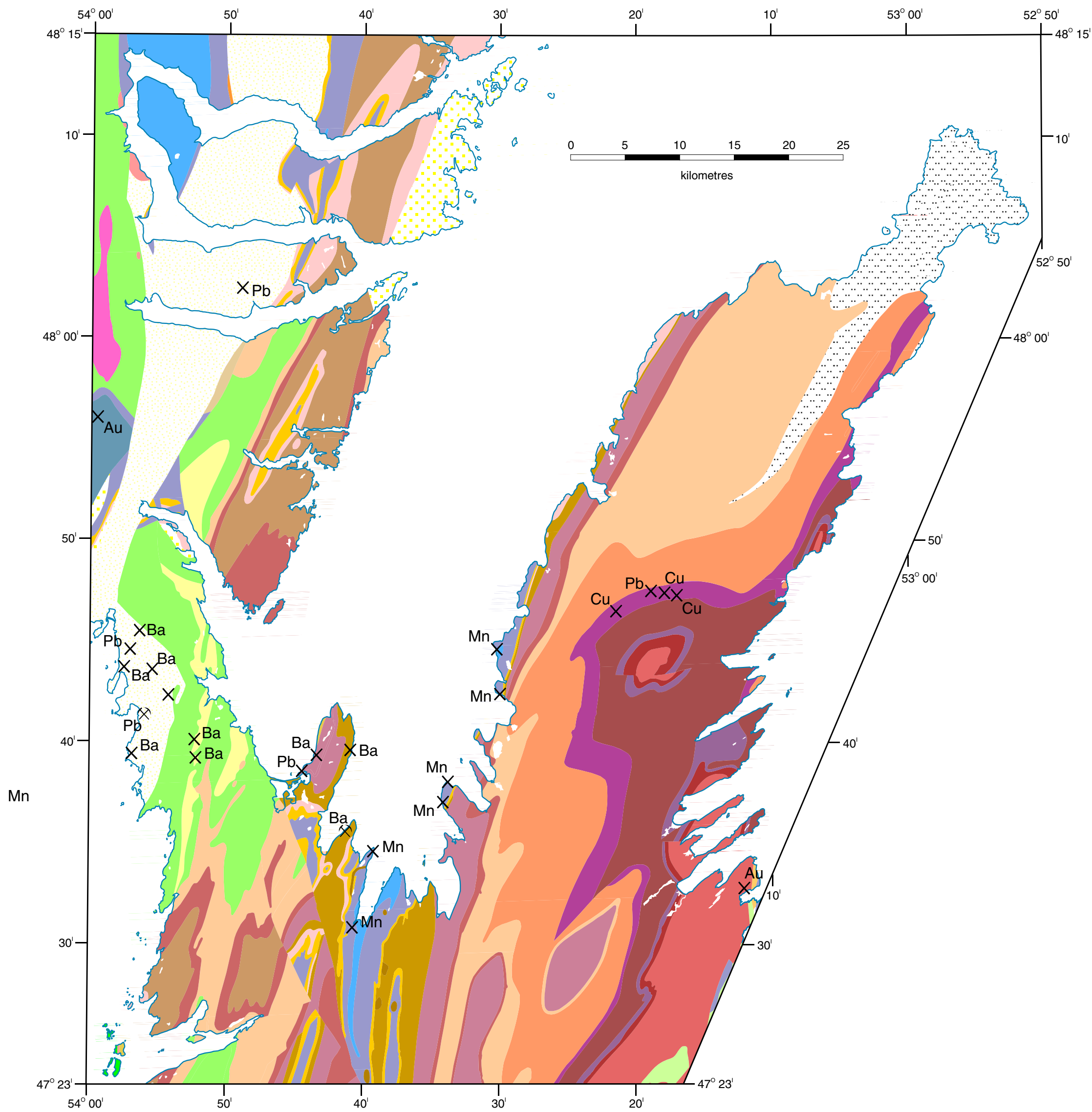

DEVONIAN OR EARLIER

- Clarenville granite: Pink to red, medium grained biotite granite
- Powder Horn Intrusive Suite: Fine to medium grained diorite, gabbro and minor granite

LOWER CAMBRIAN

- *HARCOURT GROUP: Grey to black, micaceous shale; minor siltstone and limestone*
- *ADEYTOWN GROUP*: Green and red shale and slate; thin limestone beds

HADRYNIAN

MUSGRAVETOWN GROUP

- Undivided sedimentary rocks
- *CROWN HILL FORMATION*: Red pebble conglomerate and sandstone
- *TRINNY COVE FORMATION: Olive-green & red sandstone, siltstone & conglomerate*
- *HEART'S DESIRE FORMATION: Olive-green sandstone*
- *HEART'S CONTENT FORMATION: Gray to black shale; beds of wispy sandstone*

BULL ARM FORMATION:

- Mafic to felsic variegated flows, and pyroclastic and sedimentary rocks
- Felsic flows and tuffs, and clastic sedimentary rocks
- *BIG HEAD FORMATION: Wavy bedded, gray to green tuffaceous siltstone and arkose*
- *SWIFT CURRENT GRANITE*: Pink to grey, medium grained granite to granodiorite

SIGNAL HILL GROUP

- *BAY DE VERDE FORMATION:* Red and grey, sandstone, siltstone and red mudstone
- *GIBBET HILL FORMATION*: Thickly bedded, light grey sandstone; siltstone and tuff

ST. JOHN'S GROUP

- *RENEWS HEAD FORMATION: Thin, lenticular bedded, dark grey sandstone and shale*
- *FERMEUSE FORMATION: Gray to black shale; lenses of buff-weathering sandstone*
- *TREPASSEY FORMATION: Medum to thinly bedded, sandstone and shale; minor tuff*

CONNECTING POINT GROUP

- Green, grey and black shale, siliceous siltstone and sandstone; minor conglomerate; numerous mafic dykes and sills

CONCEPTION GROUP

- *DROOK FORMATION: Green siliceous siltstone and sandstone; silicified tuff*
- *MISTAKEN POINT FORMATION: Upper red and green tuffaceous siltstone & sandstone sandstone and shale, with minor tuff and fossiliferous near top in lower part.*

HARBOUR MAIN GROUP

- Green to purple basaltic flows and pyroclastic rocks
- Pink to grey felsic tuff and agglomerate

Past Producing Mine

Mineral Showing

Element List
Au Gold
Ba Barium
Cu Copper
Mn Manganese
Pb Lead

Figure 3. Bedrock geology (after King, 1988)

Avalon Peninsula maintained an independent ice cap during deglaciation. Evidence of ice invading from the west is speculative and mostly based on clast provenance, e.g., Summers (1949) notes the presence of serpentinite clasts near St. John's. This may be sourced off the Avalon Peninsula, although D. Bragg (personal communication, 2001) reports serpentinite-rich veins in the Cochrane Pond area. There is no erosional evidence (e.g., striations) for invasion from the west.

The erosional data suggest that the Avalon Peninsula maintained an independent ice cap during the late Wisconsinan. Chamberlin (1895) was the first to suggest this, but subsequently the idea has been well acknowledged (e.g., Vhay, 1937; Summers, 1949; Jenness, 1963; Henderson, 1972; Catto, 1998). The main ice dome was likely at the head of St. Mary's Bay (Henderson, 1972; Catto, 1998), with ice flowing radially, but particularly over the low cols to the north and northwest into the Trinity and Conception bay watersheds; the Rogen moraines found south of Whitbourne formed during this northward flow. The radial flow from St. Mary's Bay had little effect on intervening peninsulas, which likely maintained their own ice caps (Summers, 1949; Catto, 1998). Similarly, the Isthmus area east of the Doe Hills was covered by ice from a local source. West of the Doe Hills, the area was covered by ice from the main part of the Island (Catto, 1998). This is supported by striations and the provenance of clasts in till.

ICE-FLOW MAPPING

The favoured method of delineating ice flow is by mapping striations on bedrock (Batterson and Liverman, 2001). Striations are excellent indicators of ice flow as they are formed by the direct action of moving ice. Data from individual striations should be treated with caution, as ice-flow patterns can show considerable local variation where ice flow was deflected by local topography. Regional flow patterns can only be deduced after examining numerous striated sites. The orientation of ice flow can easily be discerned from a striation by measuring its azimuth. Determination of the direction of flow can be made by observing the striation pattern over the outcrop. For example, areas in the lee of ice flow may not be striated. The presence of such features as ‘nail-head' striations, miniature crag-and-tails (rat-tails), and the morphology of the bedrock surface may all show the effects of sculpturing by ice (Iverson, 1991). At many sites, the direction of ice flow is unclear and only the overall orientation of ice flow (e.g., north or south) can be deduced. Where striations representing separate flow events are found, the age relationships are based on crosscutting striation sets, and preservation of older striations in the lee of younger striations.

Striation data for Newfoundland and Labrador are compiled in a web-accessible database (Taylor, 2001), which currently contains over 10 700 observations. Ice flow is interpreted from striations and additional data from large-scale landforms such as erosional rôche moutonée features or depositional features such as Rogen moraines. Clast provenance also helped confirm glacial source areas.

RESULTS

Paleo ice-flow history was determined from over 1300 striation observations from across the study area, of which 86 were collected during this project. Striations were fresh, and unweathered. Where two or more sets of striations were found at a site, the older striations showed no evidence (e.g., iron staining) of survival through a non-glacial period. Therefore, all striations were considered to have been produced during the late Wisconsinan. Data are summarized on Figure 2 and generally conform with the detailed ice reconstruction of Catto (1998). Within the study area, Avalon-centred ice extended northwest across the Isthmus to the Doe Hills, north of which, eastward-flowing ice dominates. This is consistent with the reconstruction of Batterson and Taylor (2001) that showed much of the area south and west of Clarenville was covered by eastward-flowing ice from the Middle Ridge area of central Newfoundland. This flow crossed the northern part of Placentia Bay from the Burin Peninsula, as indicated by the presence of eastward-oriented crag-and-tail hills on the west side of the Isthmus (Catto and Taylor, 1998a). Preliminary work shows the presence of granite, mafic volcanic and quartzite clasts in tills, likely derived from the Burin Peninsula.

South of the Doe Hills there is no evidence of ice flow from the area to the west. The striation patterns and the presence of clasts derived from local bedrock suggest that ice flow from 3 separate local sources covered the study area during the late Wisconsinan. The southern parts of the Bay de Verde Peninsula, Trinity Bay and Conception Bay were covered by northward-flowing ice from the main Avalon ice centre at the head of St. Mary's Bay. On the Bay de Verde Peninsula, topography had a profound influence on ice-flow patterns, and in particular by the configuration of bays and inlets. Ice-flow indicators are consistently oriented parallel to major, bedrock-controlled embayments, e.g., Harbour Grace, Bay Roberts, Bay de Grave.

The Isthmus and the Bay de Verde Peninsula both maintained their own ice caps, from which ice flow was radial. The Isthmus ice cap was centred on the Collier Bay Brook area, and the Bay de Verde ice cap was located on the barrens to the east of Heart's Content (Catto, 1998). Within these areas, clasts found in till are consistently locally derived.

SURFICIAL GEOLOGY

The surficial geology of much of the study area was mapped by Catto and Taylor (1998a to f). These maps are being revised, based on field work from this study. Section descriptions of Quaternary exposures will be completed in subsequent years. The following discussion is based on the work of Catto and Taylor (*op. cit.*) and supplemented by recent observations.

The surficial geology within the study area is summarized in Figure 4. It is subdivided into 5 main categories, viz., bedrock, till, glaciofluvial, raised marine and modern sediments.

BEDROCK

Outcrops of bedrock are found over much of the study area, although large expanses of bedrock-dominated terrain are restricted to the higher parts of the Isthmus and the highlands between Bull Arm and Northwest Arm, most of the Bellevue Peninsula, and the west side of Conception Bay. Bedrock exposed at the surface is commonly streamlined. Bedrock outcrop is rare within the Rogen moraine field (*see below*) that extends southward across the central Avalon lowland.

TILL

Till, of varying thickness and composition, is by far the most aerially extensive unit on the Avalon Peninsula. It commonly occurs as a veneer over bedrock, particularly over the Bay de Verde Peninsula and the central Isthmus and has numerous bedrock outcrops exposed within it. An examination of tills indicates that they have consistent characteristics over a wide area. On the Bay

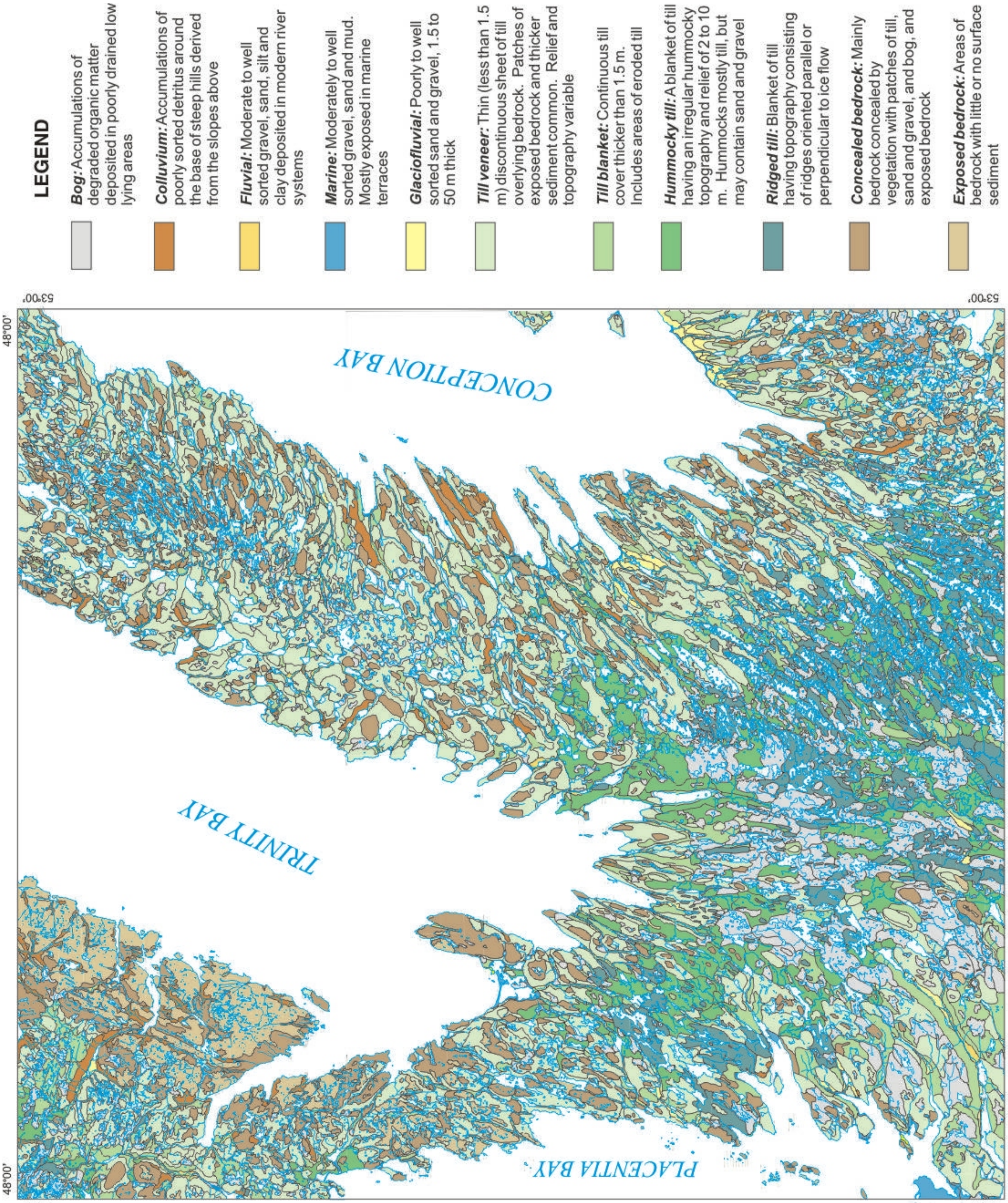

Figure 4. Surficial geology (after Catto and Taylor, 1998a-f).

de Verde Peninsula, for instance, tills are commonly poorly consolidated, very poorly sorted to unsorted, with a silty sand matrix. Clast content varies from 30 to 60 percent by volume, and clast rock types are derived mainly from the underlying bedrock. Fine-grained rocks are commonly striated. Exotic clasts were rare to absent. In contrast, tills to the west of the Doe Hills are commonly finer grained, and contain numerous exotic clasts reflective of dispersal from the west. These observations agree with those of Catto (1998).

Till mostly forms either a veneer or blanket over bedrock and few areas of constructional landforms were found. The west side of the Isthmus contains crag-and-tail hills, up to 800 m long, 300 m wide and 30 m high. These are oriented northeastward, in agreement with the local striation record, but in contrast to the reconstruction of Catto (1998). The southern part of the Bay de Verde Peninsula contains part of the central Avalon Rogen moraine field. The moraines are commonly crescent-shaped, and curved in the direction of glacial movement, which was northward from the St. Mary's Bay ice-dispersal centre. The Rogen moraines are up to 30 m high, and are spaced 200 to 400 m apart. They are composed mostly of till, although some sorted sand and gravel is present. They are commonly found adjacent to small ponds. These features are formed beneath actively flowing ice, although the actual method of formation has been the subject of considerable debate. Lundqvist (1969) argues for squeezing of sediment into subglacial cavities; Boulton (1987) suggests wholesale deformation of subglacial sediment; a melt-out hypothesis is favoured by Bouchard (1989) and Aylsworth and Shilts (1989); and formation by subglacial meltwater is proposed by Fisher and Shaw (1992), based on work on the Avalon moraines.

GLACIOFLUVIAL SEDIMENT

Small areas of glaciofluvial sand and gravel are exposed on the Bay de Verde Peninsula, all of which are currently being exploited for granular aggregate production. Both ice-contact and ice-distal glaciofluvial deposits were identified. At Makinsons, extensive pits within the broad South Brook valley expose ice-contact sediments. The sediments display considerable vertical and lateral variation in both texture and sedimentary structures. These include high-angle, poorly sorted, coarse gravelly sand beds and horizontal rhythmically bedded silt and fine sand. Faulted beds and slump features were noted on pit walls. The faults, slumps and high-angle beds are consistent with collapse from melting of ice blocks, and the fine-grained beds were likely deposited within small ponds on the disintegrating glacier surface.

In the Shearstown Brook valley, which opens into Spaniard's Bay, aggregate operations reveal flat-lying terraced sand and gravel deposits. The sediment is a moderately sorted, roughly horizontally bedded to crossbedded, coarse sandy gravel. Crossbeds indicate paleo flow to the northeast (down-valley). Clasts range up to about 15 cm diameter and the sediment lacks the large boulders characteristic of the Makinsons exposures. These sediments were likely deposited in an ice-distal glaciofluvial environment.

RAISED MARINE SEDIMENT

The paleo sea-level history of the Avalon Peninsula is poorly understood. Grant (1987) suggested that the 0 m isopleth crosses the Avalon Peninsula and lies roughly between Long Harbour and Chapel Arm, extending northward along the western shore of the Bay de Verde Peninsula. The area to the west of this line, therefore, has a Type B paleo sea-level history (Quinlan and Beaumont, 1981), with a period of raised sea levels following deglaciation and a subsequent fall to a lowstand position from which sea level has gradually recovered to the present. To the east, the paleo sea-level history is characterized as being always below modern levels, with no raised marine features occurring. However, this hypothesis has been challenged by Catto and Taylor (1998a) who mapped raised marine sediments in the Argentia area and at the head of St. Mary's Bay.

Within the study area, raised marine deposits were found at several localities on the Isthmus and Bay de Verde Peninsula. At Southern Harbour, a raised beach having a surface elevation of 13 m asl was noted. The beach consists of open work gravels containing angular to subangular clasts up to 10 cm diameter, and a mean of 3 cm diameter. At Dildo South, raised beach sediments were found with a surface elevation of 14.5 m asl, and raised marine terraces were noted at Heart's Delight (11 to 12 m asl) and Heart's Content (9 m asl). The age of these surfaces remains speculative as no marine shells were found within the Quaternary deposits.

MODERN SEDIMENT

Modern sediments include fluvial sand, gravel and silt (alluvium) found adjacent to modern streams, colluvium at the base of steep hills, modern marine deposits such as beaches and tidal flats, and aeolian deposits. Each of these sediment classes is found in small areas across the study area. The most aerially extensive modern fluvial deposits are found in the Shearstown Brook valley and the South Brook valley, which opens into Bay de Verde. Rivers in these valleys have partially reworked their thick glaciofluvial sediments. Other thin veneers of alluvium were identified by Catto and Taylor (1998c, d), including those along the South River, Island Pond Brook and Mosquito Brook valleys draining into Conception Bay, and Murphy's Cove Brook and Collier Bay Brook draining into Trinity Bay. Many other small, unnamed stream valleys also contain thin fluvial deposits over bedrock.

The largest areas of colluvium were identified on the highlands between Bull Arm and Northwest Arm, and on the eastern side of the Bay de Verde Peninsula between Spaniard's Bay and Carbonear. Several of these areas contain active slopes, including that at Upper Island Cove, where a rockfall in 1999 damaged a house and car.

Much of the coastline in the study area is steep and bedrock-dominated. Beaches are commonly restricted to small, gravel-dominated, high-energy, pocket beaches. Barachois beaches were identified at several localities, including Southern Harbour, Rantem Cove, Spread Eagle Bay, Chapel Arm, Cavendish Bay, Clarke's Beach, Bay Roberts and Bristol's Hope (Figure 1). All are gravel-dominated, commonly less than 500 m long, and exhibit a variety of structures, including small- and large-scale cuspate features, and beach berms where the backbeach areas commonly exhibit overwash fans. Sand components commonly exhibit wave ripples. The largest barachois beach and spit complex is Bellevue Beach, which is over 1 km long. This area has an extensive backbeach system, with well-developed overwash fans and active sand dunes. An unusual tidal flat complex is found at the head of Come-by-Chance, where large boulders are littered over a sand-dominated flat. Catto and Thistle (1993) suggest that this is an eroded glaciofluvial fan from which all but the boulders have been re-worked by the tide.

Several small areas of aeolian sediment were located at Bellevue and Hodge's Cove, mostly as a veneer over till. Active sand dunes are present in the backbeach area of Salmon Cove (Figure 1).

Areas of organic accumulation are common across the entire area, mostly less than 50 cm thick, although pockets of bog likely extend beyond 3 m in depth.

REGIONAL TILL SAMPLING

A regional till-sampling program was conducted using the surficial geology as a guide. Glaciofluvial, fluvial, marine, and aeolian sediments were excluded. Most samples were from the C- or BC-soil horizon, taken at about 0.5 m depth in test pits, or 0.5 to 1.0 m depth in quarries or road cuts. In rare instances, the lack of surface sediment necessitated the sampling of bedrock detritus. Sample spacing was controlled by access as well as surficial geology. In areas with good access, the sample density was about 1 sample per 1 km2, increasing to about 1 sample per 4 km^2 in areas where helicopter support was required. Samples were passed through a 5 mm-mesh sieve and approximately 1 kg of the sample was retained for analysis.

A total of 1042 samples were collected, including field duplicates, and submitted to the Geological Survey's geochemical laboratory in St. John's for major- and trace-element analysis. Data quality was monitored using field and laboratory duplicates (analytical precision only) and standard reference materials. In all cases, the silt–clay fraction (less than 0.063 mm) was analyzed.

IMPLICATIONS FOR MINERAL EXPLORATION

For the purposes of discussion, the study area is divided into 4 discrete subareas: north of the Doe Hills; southern Isthmus; southern Bay de Verde Peninsula; and central Bay de Verde Peninsula.

NORTH OF THE DOE HILLS

Paleo ice-flow indicates that during the late Wisconsinan the area north of the Doe Hills was covered by eastward-flowing ice, likely from the main Newfoundland dispersal centre on Middle Ridge. Till contains clasts derived from the west. Transportation distances are commonly greater than 5 km. Batterson and Taylor (2001a) documented dispersal of granite clasts on the Bonavista Peninsula by eastward-flowing ice at least 50 km from their source in the Clarenville area.

SOUTHERN ISTHMUS

The southern part of the Isthmus was covered by a small ice cap during the late Wisconsinan centred on the Tickle Harbour Station–Collier Bay Brook area (Figure 2). Paleo ice-flow radiated from this centre into Placentia Bay and Trinity Bay. Diamictons are characteristically dominated by locally derived clasts, and distances of transport are considered to be less then 5 km.

SOUTHERN BAY DE VERDE PENINSULA

Ice from the St. Mary's Bay dispersal centre covered much of the southern part of the Bay de Verde Peninsula. The influence of topography is noted by the movement of ice into Trinity Bay on the west and Conception Bay on the east side of the peninsula. Ice flow commonly was parallel to the orientation of the major bays on both coasts. Northward-flowing St. Mary's Bay ice produced the Rogen moraines that characterize the central Avalon Peninsula. The mode of formation of these moraines may be unimportant to prospecting in the area. If formed of diamicton during active subglacial ice flow by a compressive flow regime, these features may reflect local derivation. If, however, they were formed by erosion during a subglacial flood event they are likely also composed of locally derived material, although partially transported in a glaciofluvial system. Further work on these features is required to determine their mode of formation.

CENTRAL BAY DE VERDE PENINSULA

The central part of the Bay de Verde Peninsula maintained its own ice cap during the late Wisconsinan. Paleo ice-flow from this centre was radial. Diamictons characteristically contain clasts from the underlying bedrock and erratics are absent from this area. Dispersal distances are therefore considered to be less than 5 km.

Areas of glaciofluvial sedimentation are well defined on published surficial maps and should be treated separately from diamictons in a regional till-geochemistry program. Much of the coastline shows evidence of having been raised up to about 15 m above modern sea level following deglaciation. Marine sediments, due to the uncertainty in source directions and distances of transport (e.g., possibly iceberg derived), should be avoided in exploration programs. Colluvium is derived from the overlying slopes and therefore provides point source geochemical data.

TILL GEOCHEMISTY

SAMPLING AND SAMPLE PREPARATION METHODS

Sediment sampling was conducted across the entire peninsula, guided by the surficial geology. Marine and fluvial/glaciofluvial sediment was avoided during the sampling programme. Most samples were BC- or C-soil horizon samples from tills, although in rare cases the lack of surface sediment necessitated the sampling of bedrock detritus. A total of 1042 samples were collected, including field duplicates (Figure 5a, b and c). This provided a sample density ranging from 1 sample per 1 km^2 for road accessible areas to 1 sample per 4 km^2 for helicopter-supported sampling. In the field, samples were placed in kraft-paper sample bags, and sent to the Geological Survey's Geochemical Laboratory in St. John's, where they were air-dried in ovens at 40°C and dry-sieved through 63 µm stainless steel sieves. The <63 µm till fraction was used for geochemical analysis.

GEOCHEMICAL ANALYSIS

Analytical work was carried out at the Geological Survey's Geochemical Laboratory, with additional analyses from a commercial laboratory. The appended data listings contain all the field and analytical data from the till survey. To distinguish the different analytical methods/laboratories, the trace element variables are labeled with a combination of the element name, a numeric code and the unit of measurement.

A complete list of variables is given in Table 1, and a full listing of field and geochemical data is contained in Appendix A.

Figure 5a. Distribution of till sample sites

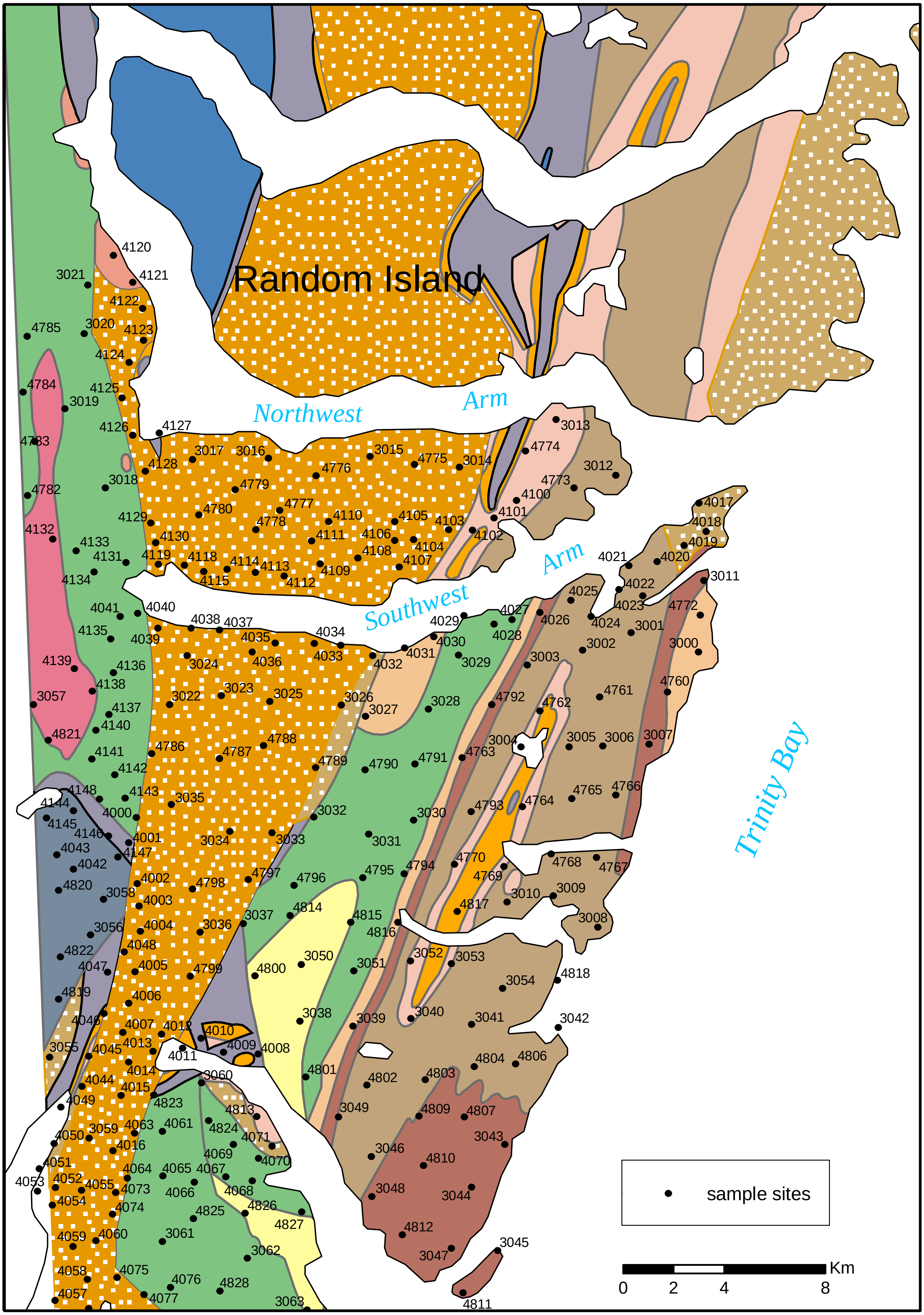

Figure 5b. Distribution of till sample sites

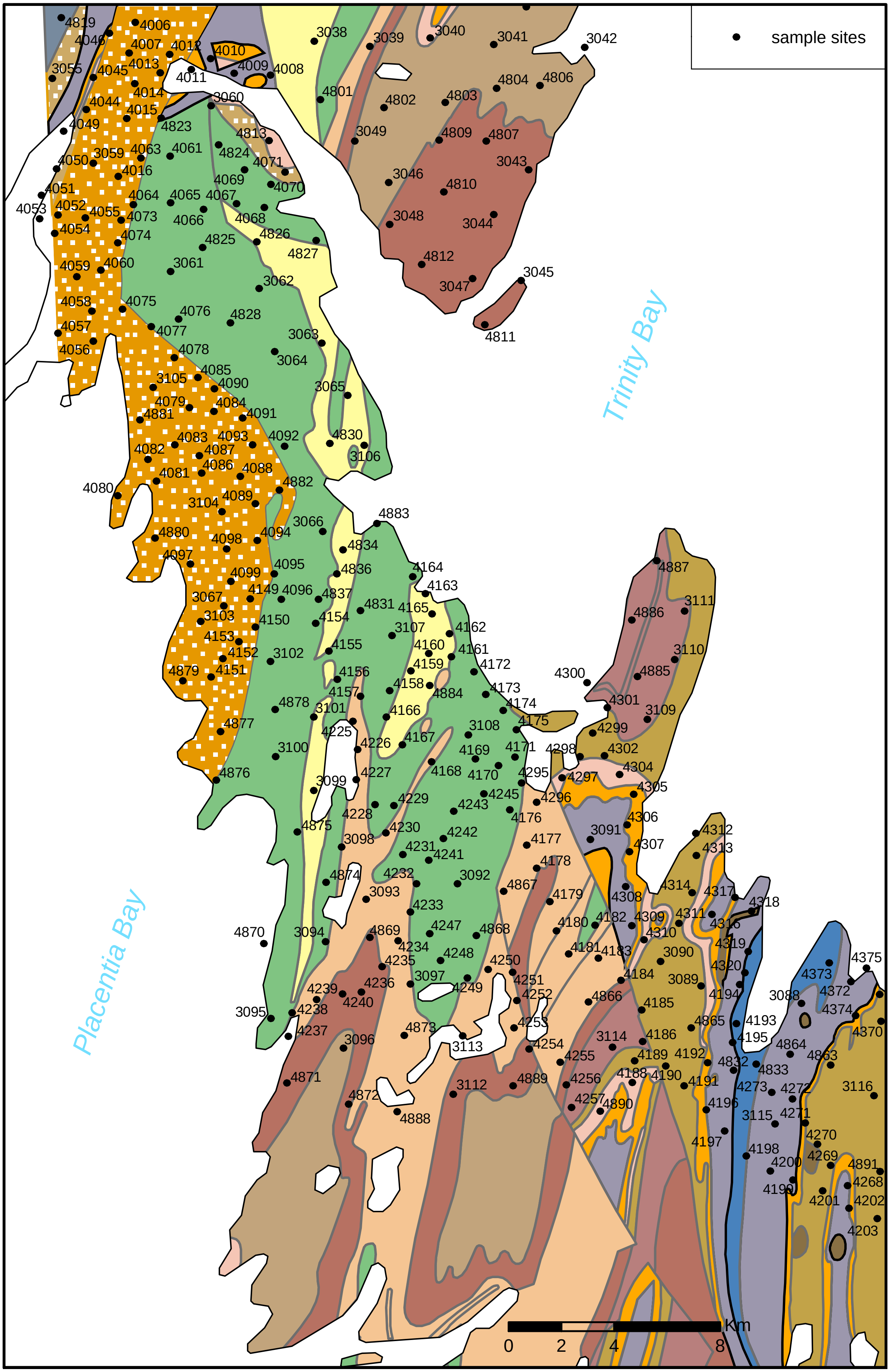

Figure 5c. Distribution of till sample sites

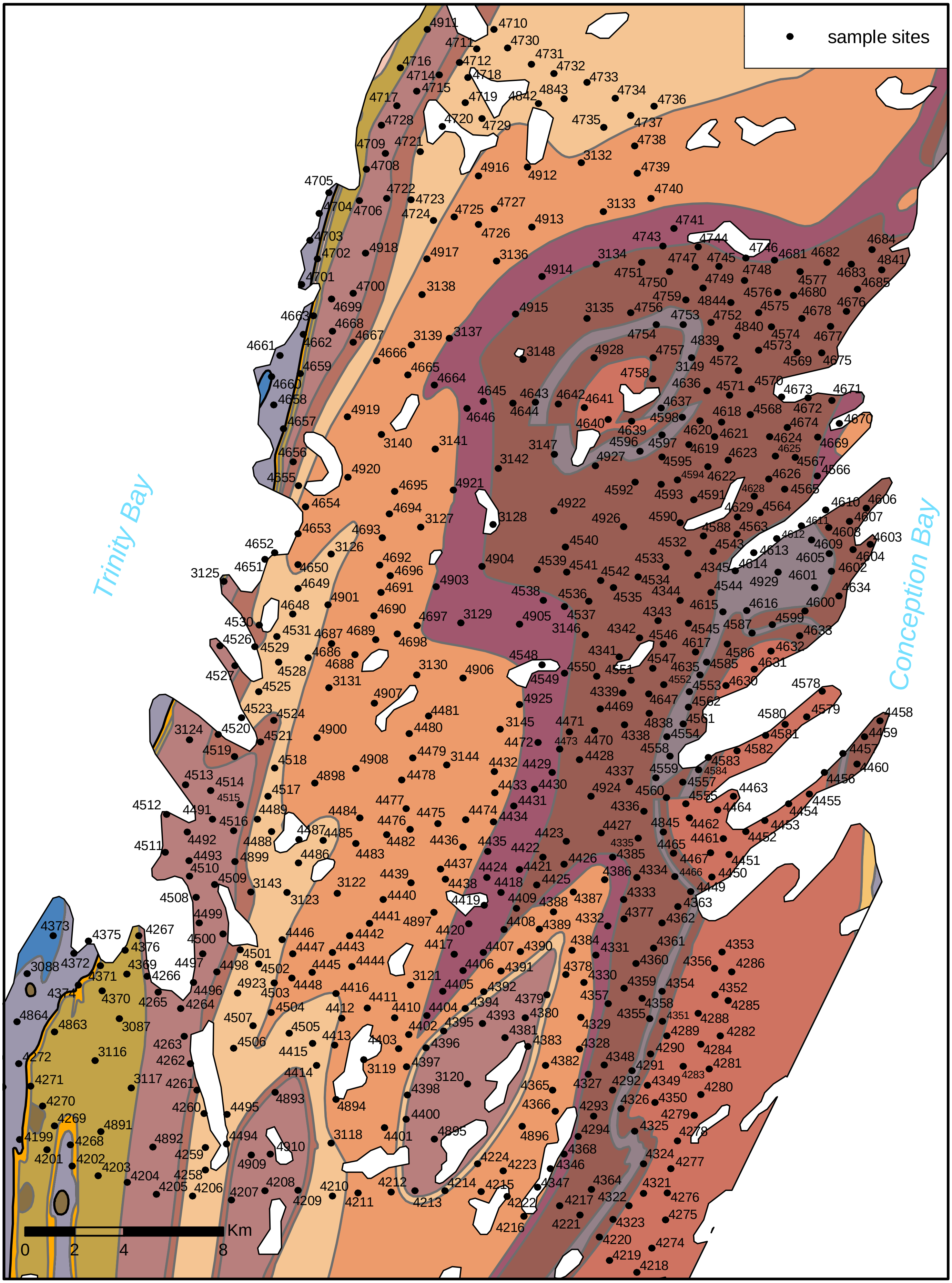

Table 1. Variable list and description of data

VARIABLE	DESCRIPTION
Sample	Unique sample ID
NTS	NTS sheet (1:50 000)
Easting	UTM map coordinate
Northing	UTM map coordinate
Al2 pct	Aluminium, %, by ICP
As2 ppm	Arsenic, ppm, by ICP
Ba2 ppm	Barium, ppm, by ICP
Be2 ppm	Beryllium, ppm, by ICP
Ca2 pct	Calcium, %, by ICP
Cd2 ppm	Cadmium, ppm, by ICP
Ce2 ppm	Cerium, ppm, by ICP
Co2 ppm	Cobalt, ppm, by ICP
Cr2 ppm	Chromium, ppm, by ICP
Cu2 ppm	Copper, ppm, by ICP
Dy2 ppm	Dysprosium, ppm, by ICP
Fe2 pct	Iron, %, by ICP
K2 pct	Potassium, %, by ICP
La2 ppm	Lanthanum, ppm, by ICP
Li2 ppm	Lithium, ppm, by ICP
Mg2 pct	Magnesium, %, by ICP
Mo2 ppm	Molybdenum, ppm, by ICP
Mn2 ppm	Manganese, ppm, by ICP
Na2 pct	Sodium, %, by ICP
Nb2 ppm	Niobium, ppm, by ICP
Ni2 ppm	Nickel, ppm, by ICP
P2 ppm	Phosphorus, ppm, by ICP
Pb2 ppm	Lead, ppm, by ICP
Sc2 ppm	Scandium, ppm, by ICP
Sr2 ppm	Strontium, ppm, by ICP
Ti2 ppm	Titanium, ppm, by ICP
V2 ppm	Vanadium, ppm, by ICP
Y2 ppm	Yttrium, ppm, by ICP
Zn2 ppm	Zinc, ppm, by ICP
Zr2 ppm	Zirconium, ppm, by ICP
As1 ppm	Arsenic, ppm, by INAA
Au1 ppb	Gold, ppb, by INAA
Ag1 ppm	Silver, ppm, by INAA
Ba1 ppm	Barium, ppm, by INAA
Br1 ppm	Bromine, ppm, by INAA
Ca1 pct	Calcium, %, by INAA
Ce1 ppm	Cerium, ppm, by INAA
Co1 ppm	Cobalt, ppm, by INAA

Table 1. Continued

VARIABLE	DESCRIPTION
Cr1 ppm	Chromium, ppm, by INAA
Cs1 ppm	Cesium, ppm, by INAA
Eu1 ppm	Europium, ppm, by INAA
Fe1 pct	Iron, %, by INAA
Hf1 ppm	Hafnium, ppm, by INAA
Hg1 ppm	Mercury, ppm, by INAA
Ir1 ppm	Iridium, ppm, by INAA
La1 ppm	Lanthanum, ppm, by INAA
Lu1 ppm	Lutetium, ppm, by INAA
Mo1 ppm	Molybdenum, ppm, by INAA
Na1 pct	Sodium, %, by INAA
Nd1 ppm	Neodymium, ppm, by INAA
Ni1 ppm	Nickel, ppm, by INAA
Rb1 ppm	Rubidium, ppm, by INAA
Sb1 ppm	Antimony, ppm, by INAA
Sc1 ppm	Scandium, ppm, by INAA
Se1 ppm	Selenium, ppm, by INAA
Sm1 ppm	Samarium, ppm, by INAA
Sn1 ppm	Tin, ppm, by INAA
Sr1 ppm	Strontium, ppm, by INAA
Ta1 ppm	Tantalum, ppm, by INAA
Tb1 ppm	Terbium, ppm, by INAA
Th1 ppm	Thorium, ppm, by INAA
U1 ppm	Uranium, ppm, by INAA
W1 ppm	Tungsten, ppm, by INAA
Yb1 ppm	Ytterbium, ppm, by INAA
Zn1 ppm	Zinc, ppm, by INAA
Zr1 ppm	Zirconium, ppm, by INAA
Ag6 ppm	Silver by AAS
Rb6 ppm	Rubidium by AAS
LOI pct	Loss-on-ignition, %, gravimetric
Site	Sample site number
Zone	UTM zone
Horizon	Soil horizon sampled
Depth	Sample depth (cm)

ANALYTICAL METHODS

Atomic Absorption Spectrophotometry (AAS)

Silver (Ag6) was determined on 0.5g aliquots of sample following digestion in 2 ml of concentrated HNO_3 overnight at room temperature, and then in a water bath at 90°C for 2 h (Wagenbauer *et al.*, 1983). For till the results maybe somewhat less than total (Table 2). At the time of publication, silver data were unavailable and will be released at a later date.

Gravimetric Analysis (LOI)

Organic carbon content was estimated from the weight loss on ignition (LOI) during a controlled combustion in which 1g aliquots of sample were gradually heated to 500°C in air over a 3 h period. Accuracy can be judged from the results for reference materials (Table 2).

Inductively Coupled Plasma Emission Spectrometry (ICP)

For these analyses, the residue of the 1g aliquot of sample remaining from the LOI determination at 500°C was digested in a mixture of 15mL of concentrated HF, 5mL of concentrated HCl and 5 mL of 50 volume percent $HClO_4$ in a 100 mL teflon beaker, which was allowed to stand overnight before being heated to dryness on a hot-plate. The residue was taken up in 10 volume percent HCl by gentle heating on the hot plate, allowed to cool and made up to 50 mL with 10 volume percent HCl (Wagenbauer *et al.*, 1983). For most elements dissolution is total; exceptions are Cr from chromite, Ba from barite and Zr from zircon as these minerals are not usually completely dissolved. Accuracy can be judged from the results for reference materials (Table 2)

The following elements were determined: Aluminium, barium, beryllium, calcium, cerium, cobalt, chromium, copper, dysprosium, iron, gallium, potassium, lanthanum, lithium, magnesium, manganese, molybdenum, sodium, niobium, nickel, phosphorus, lead, scandium, strontium, titanium, vanadium, yttrium, zinc and zirconium (Al2, Ba2, Be2, Ca2, Ce2, Co2, Cr2, Cu2, Dy2, Fe2, Ga2, K2, La2, Li2, Mg2, Mn2, Mo2, Na2, Nb2, Ni2, P2, Pb2, Sc2, Sr2, Ti2, V2, Y2, Zn2 and Zr2, respectively).

Instrumental Neutron Activation Analysis (INAA)

These analyses were carried out at Activation Laboratories Ltd., Ancaster, Ontario. On average 24g of sample was used for analysis, and the samples (with duplicates and control reference materials included incognito) were weighed and encapsulated in the Geochemical Laboratory of the Department of Mines and Energy in St. John's (*see* Table 3). Total contents of the following elements were determined quantitatively: silver, arsenic, gold, barium, bromine, calcium, cerium, cobalt, chromium, cesium, europium, iron, hafnium, mercury, iridium, lanthanum, lutetium, molybdenum, sodium, neodymium, nickel, rubidium, antimony, scandium, selinium, samarium, tin, strontium, tantalum, terbium, thorium, uranium, tungsten, ytterbium, zinc and zirconium. (Ag1, As1, Au1, Ba1, Br1, Ca1, Ce1, Co1, Cr1, Cs1, Eu1, Fe1, Hf1, Hg1, Ir1, La1, Lu1, Mo1, Na1, Nd1, Ni1, Rb1, Sb1, Sc1, Se1, Sm1, Sn1, Sr1, Ta1, Tb1, Th1, U1, W1 Yb1, Zn1, and Zr1 respectively).

Table 2. Accuracy of till geochemical data by ICP. Results of analyses of CANMET Reference samples TILL-1 to -4. Observed values (Obs.) are compared against recommended values (Rec). Recommended values are from Lynch (1996). In all cases number of observations = 16

		TILL-1		TILL-2		TILL-3		TILL-4	
		Obs.	**Rec.**	**Obs**	**Rec.**	**Obs**	**Rec.**	**Obs**	**Rec.**
Al2	**%**	6.4	7.3	7.5	8.5	5.9	6.5	6.8	7.6
As2	**ppm**	18		28		88		111	
Ba2	**ppm**	705	702	538	540	494	489	397	396
Be2	**ppm**	1.4	2.4	3.2	4.0	1.2	2.0	3	3.7
Ca2	**%**	1.77	1.94	0.87	0.91	1.76	1.88	0.86	0.89
Cd2	**ppm**	0.2	?	0.23	?	0.01	?	0.01	?
Ce2	**ppm**	60	71	83	98	36	42	69	78
Co2	**ppm**	19	18	16	15	16	15	8	8
Cr2	**ppm**	54	65	59	74	97	123	38	53
Cu2	**ppm**	43	47	164	150	20	22	274	237
Dy2	**ppm**	4.3	?	3.7	?	2	?	3.2	?
Fe2	**%**	4.78	4.81	3.81	3.84	2.73	2.78	4.01	3.97
K2	**%**	1.65	1.84	2.24	2.55	1.8	2.01	2.34	2.70
La2	**ppm**	28	28	46	44	21	21	43	41
Li2	**ppm**	16	15	47	47	22	21	30	30
Mg2	**%**	1.19	1.30	1.02	1.1	0.96	1.03	0.7	0.76
Mn2	**ppm**	1530	1420	829	780	536	520	528	490
Mo2	**ppm**	0.56	2	14	14	1.14	16.9	15	
Na2	**%**	2.05	2.01	1.69	1.62	1.94	1.96	1.84	1.82
Nb2	**ppm**	11	10	18	20	7	7	15	15
Ni2	**ppm**	24	24	32	32	39	39	18	17
P2	**ppm**	890	930	694	750	477	490	852	880
Pb2	**ppm**	22	22	31	31	26	26	50	50
Sc2	**ppm**	14	13	12	12	10	10	11	10
Sr2	**ppm**	296	291	150	144	309	300	119	109
Ti2	**ppm**	5608	5990	5235	5300	2956	2910	4916	4840
V2	**ppm**	100	99	78	77	61	62	67	67
Y2	**ppm**	27	38	19	40	13	17	17	33
Zn2	**ppm**	94	98	124	130	56	56	71	70
Zr2	**ppm**	102	502	99	390	82	390	89	385

Table 3. Accuracy of till geochemical data by INAA and gravimetry. Results of analyses of CANMET Reference samples TILL-1 to -4. Observed values (Obs.) are compared against recommended values (Rec). Recommended values are from Lynch (1996). In all cases number of observations = 16

		TILL-1		TILL-2		TILL-3		TILL-4	
		Obs.	**Rec.**	**Obs**	**Rec.**	**Obs**	**Rec.**	**Obs**	**Rec.**
As1	**ppm**	19	18	28	26	95	87	119	111
Au1	**ppb**	11	13	2	2	3	6	2	5
Ba1	**ppm**	661	702	657	540	475	489	449	395
Br1	**ppm**	6.4	6.4	12.2	12.2	4.7	4.5	8.4	8.6
Ca1	**%**	1.7		0		2.1		0	
Ce1	**ppm**	74	71	107	98	43	42	93	78
Co1	**ppm**	18	18	15	15	14	15	8	8
Cr1	**ppm**	64	65	77	74	123	123	50	53
Cs1	**ppm**	0	1.0	10	12.0	1.9	1.7	10.3	12.0
Eu1	**ppm**	1.8	1.3	1.6	1.0	1	0.5	1.4	0.5
Fe1	**%**	4.9	4.8	4.1	3.8	2.9	2.8	4.2	4.0
Hf1	**ppm**	14.1	13.0	11.4	11.0	6.8	8.0	11.7	10.0
La1	**ppm**	31	28	53	44	21	21	49	41
Lu1	**ppm**	0.6	0.6	0.6	0.6	0.3	<0.5	0.6	0.5
Mo1	**ppm**	<5	<5	16	14	<5	<5	16	16
Na1	**%**	2.16	2.01	1.82	1.62	2.07	1.96	1.98	1.82
Nd1	**ppm**	27	26	42	36	17	16	37	30
Rb1	**ppm**	44	44	136	143	47	55	143	161
Sb1	**ppm**	7.5	7.8	1.1	0.8	1	0.9	1.4	1.0
Sc1	**ppm**	14	13	13	12	10	10	11	10
Sm1	**ppm**	6.2	5.9	8	7.4	3.5	3.3	7	6.1
Ta1	**ppm**	0	0.7	1.4	1.9	<0.5	<0.5	0.3	1.6
Tb1	**ppm**	0.9	1.1	1.2	1.2	<0.5	<0.5	0.1	1.1
Th1	**ppm**	5.8	5.6	18.3	18.4	4.8	4.6	17.5	17.4
U1	**ppm**	2	2.2	5	5.7	1.9	2.1	4.6	5.0
W1	**ppm**	<1	<4	3.8	<2	<1	<4	175	204
Yb1	**ppm**	4.1	3.9	4.2	3.7	1.7	1.5	3.8	3.4
Zn1	**ppm**	53		114		24		99	
Zr1	**%**	0.03		0.02		0.01		0.01	
LOI	**%**	6.5	6.3	7.1	6.8	3.9	3.6	4.8	4.4

QUALITY CONTROL

Data quality was monitored using laboratory duplicates (analytical precision only), estimates of which are given in Table 4. Accuracy estimates are provided by the results from standard reference materials analysed with them (Tables 2 and 3). These data show that for almost all elements, with Zr2 as an exception, all data is of high quality.

It should be emphasized that for mineral exploration, the relative variation of an element is of primary concern. Of the 44 elements determined, 15 were determined by both ICP and INAA (As, Ba, Ca, Ce, Co, Cr, Fe, La, Mo, Na, Ni, Sc, Sr, Zn, Zr), and two by INAA and AAS (Ag, Rb). To reduce the size of the data for presentation and statistical analysis, for these 17, the data from the method with the best quality determined from comparison with laboratory and field duplicates have been used (Ag6, As1, Ba2, Ca2, Ce2, Co2, Cr2, Fe2, La2, Mo2, Na2, Ni2, Rb6, Sc2, Sr2, Zn2, Zr2), although all are presented in the data listing (Appendix A). A summary of duplicate and control data is included in this report, and detailed data are available on request.

STATISTICAL ANALYSIS – FREQUENCY DISTRIBUTIONS

The frequency distributions of the geochemical data were examined using the Jenks optimization method, also known as the goodness of variance fit (Jenks, 1967) found within the ArcMap GIS application. The method identifies natural breaks in the data set, and has replaced the selection of breaks using cumulative frequency plots (cf., Batterson and Taylor, 2001). Comparison of the two method produced similar subdivisions of the data. Breaks in slope of the curves were used to subdivide the element values into 4-6 natural population groups. These groups are represented by symbols that increase in size with increasing element levels in Figure 6 to Figure 16. Statistics (maximum, minimum, median, mean, standard deviation) were generated from the Excel computer application, and are presented in Table 4.

INTERPRETATION OF GEOCHEMICAL DATA

Dot plot maps of selected elements (As, Au, Ba, Cr, Cu, Mn, Ni, Pb, Sb, V, Yb and Zn) are presented in Figures 6 to 16 respectively. Other element plots are not presented in this open file, but are available on request. A list is included in Appendix F. Individuals and companies are encouraged to undertake their own interpretation of the presented data, the following being a preliminary guide.

COPPER

Exploration for copper in eastern Newfoundland has been a focus of activity in the mineral industry for the past several years. The Cornerstone Resources Red Cliff and Princess Group properties on the Bonavista Peninsula have shown promising indications of extensive copper mineralisation (Cornerstone Resources, 2000). Exploration was enhanced by the 2001 till geochemistry release (Batterson and Taylor, 2001) which generated approximately $62 000 worth of staking activity, focusing mostly on copper exploration.

Copper in till (Figure 10) data failed to highlight the Crown Hill Formation south of Southwest Arm, although this formation hosts significant copper mineralisation on the Bonavista Peninsula. This is similar to the findings of the 2001 till geochemistry survey. In that case it was argued that

Table 4. Units, detection limits, ranges, medians and standard deviations of geochemical data. Values below detection are coded as half of the detection limit value

		Detection limit	Minimum	Maximum	Median	Mean	St. Dev.
Ag1	ppm	5	<5	7	<5	<5	0.2
Ag6	ppm	0.1					
Al2	%	0.01	3.4	9.9	6.3	6.4	0.7
As1	ppm	0.5	0.7	110	7.3	8.8	6.8
As2	ppm	1	1	119	8	9.4	7.2
Au1	ppb	1	<1	32	<1	2.3	2.9
Ba1	ppm	50	<50	19000	400	465	764
Ba2	ppm	50	76	2923	408	448	196
Be2	ppm	0.2	0.7	4.5	1.4	1.5	0.4
Br1	ppm	0.5	0.5	280	16	28.2	34.8
Ca1	%	1	<1	4	<1	<1	0.5
Ca2	%	0.01	0.1	4.4	0.7	0.8	0.5
Cd2	ppm	0.1	<0.1	1.9	0.05	0.1	0.09
Ce1	ppm	3	7	350	60	66	33.7
Ce2	ppm	2	3	287	56	60	29
Co1	ppm	1	<1	70	10	11.4	7
Co2	ppm	2	<1	88	12	13.5	8.6
Cr1	ppm	5	<5	160	33	34.7	14
Cr2	ppm	2	2	153	29	30.5	11.4
Cs1	ppm	1	<1	26	2	2.9	1.8
Cu2	ppm	2	<2	262	19	23.3	18.3
Dy2	ppm	0.2	0.8	18.9	4.2	4.3	1.5
Eu1	ppm	0.5	<0.5	5.3	1.4	1.4	0.4
Fe1	%	0.1	0.4	12.8	3	3.1	1
Fe2	%	0.01	0.3	11.9	3	3.2	1
Hf1	ppm	1	2	24	8	7.7	1.9
Hg1	ppm	1	<1	2	<1	<1	0.1
Ir1	ppb	5	<5	5	<5	<5	0.2
K2	%	0.01	0.2	4.1	1.4	1.4	0.3
La1	ppm	1	2.9	90	22	23	8.5
La2	ppm	1	2	85	23	23	8.3
Li2	ppm	0.2	1.1	87.8	22.9	25.6	11.4
LOI	%	0.01	0.6	45.6	3.5	5.3	5.1
Lu1	ppm	0.05	0.3	2.6	0.5	0.5	0.1

		Detection limit	Minimum	Maximum	Median	Mean	St. Dev.
Mg2	%	0.01	0.1	2.7	0.5	0.6	0.2
Mn2	ppm	2	54	4765	780	870	488
Mo1	ppm	1	<1	12	<1	1.4	1.7
Mo2	ppm	1	<1	9	<1	1.1	0.9
Na1	%	0.1	0.5	4.1	2.2	2.1	0.4
Na2	%	0.01	0.5	3.5	2.2	2.1	0.4
Nb2	ppm	2	4	45	13	13.7	3
Nd1	ppm	5	<5	91	19	20	9
Ni1	ppm	2	10	240	10	13	20
Ni2	ppm	2	<2	99	14	14.7	6.3
P2	ppm	5	38	1815	518.5	536	224
Pb2	ppm	2	<2	399	17.5	23.3	23.5
Rb1	ppm	5	<5	220	50	51	20
Rb6	ppm	10	7	269	48	49	16
Sb1	ppm	0.1	<0.1	3.3	0.6	0.6	0.3
Sc1	ppm	0.1	2.1	47	11	11.8	3.2
Sc2	ppm	1	1.6	53	12.2	12.6	3.1
Se1	ppm	1	<1	6	<1	<1	0.4
Sm1	ppm	0.1	0.7	20	4.9	5	1.8
Sn1	%	1	<1	<1	<1	<1	0
Sr1	%	0.05	<0.05	0.09	<0.05	<0.05	0.01
Sr2	ppm	2	23	644	173	179	68
Ta1	ppm	0.2	<0.2	2.9	<0.2	0.5	0.6
Tb1	ppm	0.5	<0.5	3.4	0.7	0.7	0.4
Th1	ppm	0.2	0.8	24	7	7.1	1.7
Ti2	ppm	5	823	14120	5604	5806	1208
U1	ppm	0.5	<0.5	9.2	1.8	1.9	0.8
V2	ppm	5	8	551	68	74	32.8
Y2	ppm	2	8	87	25	25.2	6.7
W1	ppm	1	<1	4	<1	<1	0.4
Yb1	ppm	0.2	2	17.5	3.2	3.3	0.8
Zn1	ppm	5	25	499	25	60	47
Zn2	ppm	2	10	550	57	65.6	37.6
Zr1	%	0.01	<0.01	0.07	<0.01	<0.01	0.01
Zr2	ppm	2	44	235	99	101	18.4

surface rocks are barren red sandstone, with the mineralisation being found in reduced layers only visible in coastal cliffs. The same can be suggested for the Isthmus area.

Data from the Isthmus area shows slightly elevated copper values (median=19 ppm; mean = 23 ppm) compared with the Bonavista Peninsula (median=14 ppm; mean=18 ppm), although the Bonavista Peninsula dataset had the highest value (307 ppm compared with 262 ppm in the Isthmus dataset). Several clusters of high values were noted in the Isthmus area dataset. The contact between the Bull Arm Formation and the Connecting Point Group shows a cluster of samples with values between 60 and 183 ppm. Ice flow in this area is southwestward. Till samples overlying parts of the Connecting Point Group on the Bonavista Peninsula showed copper anomalies (Batterson and Taylor, 2001). Areas of enriched copper values are found overlying Bull Arm Formation rocks west and southwest of Southwest Arm, with a cluster of values between 59 and 106 ppm. Similar results from the Bull Arm Formation were revealed from the Bonavista survey (Batterson and Taylor, 2001). An area of enriched copper in till is found over the St. John's Group on the east side of the Bay de Verde Peninsula. Most samples show copper values of over 32 ppm, with highs of 65 to 77 ppm. Several copper showings are located on the Heart's Content barrens, but none have been located elsewhere in the St. John's Group. The highest copper value was 262 ppm, found in till overlying rocks of the Bull Arm Formation north of the Doe Hills. Field and laboratory duplicates showed a high degree of correlation, and the data is thus considered accurate and precise.

LEAD

The distribution of lead within till (Figure 13) is similar to that expressed for copper. High values are found along the contact between Bull Arm Formation and Connecting Point Group rocks near Placentia Bay where values up to 399 ppm are found; and in till overlying rocks of the St. John's Group (Fermeuse Formation), where values up to 274 ppm are recorded. These are considerably higher than values found during the Bonavista survey (maximum 172 ppm). Lead was mined at the turn of the century from Connecting Point rocks at La Manche, and a lead showing is found in the Renews Formation on the Heart's Content barrens. No lead showings have been reported from the Fermeuse Formation. All of these areas should be considered prospective environments. Field and laboratory duplicates showed a high degree of correlation, and the data is thus considered accurate and precise.

Similar distributions are also found for **cobalt** (Figure 24), **nickel** (Figure 12) and **zinc** (Figure 17) in till. This suggests base metal exploration is warranted in this area.

GOLD

The gold in till (Figure 7) data is difficult to interpret, and shows a spotty distribution. The sample size is likely a factor. Caution must be exercised when interpreting anomalies, due to the ‘nugget effect'. The highest value recorded within the study area is 32 ppb, found in till overlying the Powder Horn intrusive suite adjacent to the Lodestar gold showing. A cluster of samples, showing results up to 27 ppb, are found in tills overlying the Big Head and Heart's Content formations of the Musgravetown Group, along the northern edge of sampling. Till sampling in 2003 will extend to the northern part of the Bay de Verde Peninsula, and should delineate the extent of this area of potential mineralisation. Field and laboratory duplicates showed a low degree of correlation.

ARSENIC

Arsenic (Figure 6) is considered a pathfinder for gold. Although arsenic values generally bear little areal relationship to the distribution of gold anomalies in the Isthmus area, the highest values for gold and arsenic are found in till from adjacent to the Lodestar gold showing (As=110 ppm and Au=32 ppb). Relatively high arsenic values are found in the eastern part of the study area, in areas underlain by the St. John's Group. Field and laboratory duplicates showed a high degree of correlation, and the data is thus considered accurate and precise.

Arsenic is also a factor in human health. The Canadian soil quality guidelines indicate values below 12 ppm are acceptable. About 20% of data points are above this value within the study area. In particular the western side of Conception Bay is enriched in arsenic. Coincidentally, this area has the greatest concentration of communities within the study area. The proximity of sites with high arsenic values to local or regional water supplies should be examined with a view to further testing of water quality in the region.

YTTERBIUM

Ytterbium (Figure 16) has a high values of 17.5 ppm, found adjacent to the Swift Current granite south of Clarenville. The data also shows some distinct clustering in tills overlying the St. John's Group, and in the area around Heart's Content. Similar distributions are found for other light rare earths, including cerium (Figure 23), dysprosium (Figure 26), europium (Figure 27) and lutetium (Figure 36). Field and laboratory duplicates showed a high degree of correlation, and the data is thus considered accurate and precise.

BARIUM

Values of barium (Figure 8) show a strong relationship with bedrock. The highest value is 2923 ppm found in tills overlying felsic flows of the Bull Arm Formation. High values for barium are clustered within the southern part of the Bull Arm Formation on the Isthmus. The area contains numerous barium showings, as well as a barite mine at Colliers Point. Several of the geochemical highs are adjacent to known showings, although many are not. Till samples from near the barite mine were not anomalous, likely due to a lack of surface exposure of the barite. Field and laboratory duplicates showed a high degree of correlation, and the data is thus considered accurate and precise.

CHROMIUM

The highest value for chromium (Figure 9) was 153 ppm, and show a cluster of values between 73 and 153 ppm. All are from tills underlain by Lower Cambrian Harcourt and Adeytown group sediments. High nickel values are also recorded from this area. Field and laboratory duplicates showed a high degree of correlation, and the data is thus considered accurate and precise.

OTHER ELEMENTS

Antimony (Figure 14) values are low across the area, with a maximum value of only 3.3 ppm. **Vanadium** (Figure 15) has a maximum value of 551 ppm, and shows clusters in the Musgravetown Group and the Bull Arm Formation. **Calcium** (Figure 21) shows distinct regional differences being relatively enriched in the west, particularly in tills overlying the Bull Arm Formation, compared to the values within tills overlying the older Conception and St. John's group rocks to the east. **Strontium** (Figure 48) shows a distinct cluster of samples up to 644 ppm in tills overlying the southern part of the Bull Arm Formation.

SUMMARY

The till geochemistry highlights distinct differences in bedrock across the study area. The St. John's Group is considered a prospective area for base metals, with enrichment of copper, lead, zinc and nickel identified from the survey results. These data will be supplemented by sampling in 2003 which will include coverage of the northern part of the Bay be Verde Peninsula. The relationship to **manganese** (Figure 11) will require examination to determine the effects of post-depositional scavenging.

Barium showed several high values not associated with known mineral occurrences. Gold results were generally low, although a small cluster of relatively higher values near Heart's Content may warrant further examination.

Regional and local ice flow had an influence on dispersal patterns. In the north, regional ice flow was eastward; dispersal from which was well illustrated by Batterson and Taylor (2001). Ice flow on the Isthmus and Bay de Verde Peninsula was generally from small, local ice centres. The pattern of striations suggested short distances of transport were likely. The till geochemistry data supports this contention. Data commonly shows a strong affinity to underlying bedrock chemistry with little down-ice transport away from the source, e.g., strontium, chromium, calcium.

Work planned for summer 2003 should more clearly define geochemical patterns in the area between Placentia and Whitbourne (NTS map sheets 1N/5 and 1N/6), and in the northern half of the Bay de Verde Peninsula. Data release from this survey is expected in June 2004.

ACKNOWLEDGMENTS

We would like to thank the following for their contribution to the project. Sid Parsons and Gerry Hickey provided logistical support while we were in the field. Shirley McCuaig, Amy Newport, Trevor Bell, Andrea Bassan and Larry Nolan assisted with the helicopter component of till sampling. Terry Sears produced the figures. Andrea Bassan and Larry Nolan provide invaluable help with the GIS component of the project. The manuscript was reviewed by Dave Liverman.

REFERENCES

Aylsworth, J.M. and Shilts, W.W.
1989: Glacial features around the Keewatin Ice Divide, Districts of Mackenzie and Keewatin. Geological Survey of Canada, Paper 88-24.

Batterson, M.J. and Liverman, D.G.E.
2001: The contrasting styles of glacial dispersal in Newfoundland and Labrador: Methods and case studies. Geological Society of London, Special Publication 185, pages 267-285.

Batterson, M.J. and Taylor, D.M.

2001a: Quaternary geology and till geochemistry of the Bonavista Peninsula. *In* Current Research. Newfoundland and Labrador Department of Mines and Energy, Geological Survey, Report 01-1, pages 267-278.

2001b: Till geochemistry of the Bonavista Peninsula area. Newfoundland and Labrador Department of Mines and Energy, Geological Survey, Open File Nfld 2734, 181 pages.

2003: Regional till geochemistry and surficial geology of the western Avalon Peninsula and Isthmus. *In* Current Research. Newfoundland and Labrador Department of Mines and Energy, Geological Survey, Report 03-1, pages 259-272.

Batterson, M.J., Taylor, D.M. and Davenport, P.H.

1998: Till geochemistry of the Grand Falls-Mount Peyton area. Newfoundland Department of Mines and Energy, Geological Survey, Open File NFLD/2664.

Bouchard, M.A.

1989: Subglacial landforms and deposits in central and northern Quebec, Canada, with emphasis on Rogen moraines. Sedimentary Geology, Volume 62, pages 293-308.

Boulton, G.S.

1987: A theory of drumlin formation by subglacial sediment deformation. *In* Drumlin Symposium. *Edited by* J. Menzies and J. Rose. A.A. Balkema, Rotterdam, pages 25-80.

Catto, N.R.

1998: The pattern of glaciation on the Avalon Peninsula of Newfoundland. Géographie physique et Quaternaire, Volume 52, pages 23-45.

Catto, N.R. and Taylor, D.M.

1998a: Landforms and surficial geology of the Argentia map sheet (NTS 1N/05), Newfoundland. Scale 1:50 000. Newfoundland Department of Mines and Energy, Geological Survey, Open File 001N/05/0637.

1998b: Landforms and surficial geology of the Holyrood map sheet (NTS 1N/06), Newfoundland. Scale 1:50 000. Newfoundland Department of Mines and Energy, Geological Survey, Open File 001N/06/0638.

1998c: Landforms and surficial geology of the Harbour Grace map sheet (NTS 1N/11), Newfoundland. Scale 1:50 000. Newfoundland Department of Mines and Energy, Geological Survey, Open File 001N/11/0640.

1998d: Landforms and surficial geology of the Dildo map sheet (NTS 1N/12), Newfoundland. Scale 1:50 000. Newfoundland Department of Mines and Energy, Geological Survey, Open File 001N/12/0641.

1998e: Landforms and surficial geology of the Sunnyside map sheet (NTS 1N/13), Newfoundland. Scale 1:50 000. Newfoundland Department of Mines and Energy, Geological Survey, Open File 001N/13/0642.

1998f: Landforms and surficial geology of the Heart's Content map sheet (NTS 1N/14), Newfoundland. Scale 1:50 000. Newfoundland Department of Mines and Energy, Geological Survey, Open File 001N/14/0643.

Catto, N.R. and Thistle, G.
1993: Geomorphology of Newfoundland. International Geomorphological Congress Guidebook, August 1993.

Chamberlin, T.C.
1895: Notes on the glaciation of Newfoundland. Bulletin of the Geological Society of America, Volume 6, page 467.

Coleman, A.P.
1926: The Pleistocene of Newfoundland. Journal of Geology, Volume 34, pages 193-223.

Colman-Sadd, S.P., Hayes, J.P. and Knight, I.
1990: Geology of the Island of Newfoundland. Map 90-01, Newfoundland Department of Mines and Energy, Geological Survey, 1:1 000 000 scale.

Fisher, T.G. and Shaw, J.
1992: A depositional model for Rogen moraine, with examples from the Avalon Peninsula, Newfoundland. Canadian Journal of Earth Sciences, Volume 29, pages 669-686.

Grant, D.R.
1989: Quaternary geology of the Atlantic Appalachian region of Canada. *In* Quaternary Geology of Canada and Greenland. *Edited by* R.J. Fulton. Geological Survey of Canada, Geology of Canada no. 1, pages 391-440.

Henderson, E.P.
1972: Surficial geology of the Avalon Peninsula, Newfoundland. Geological Survey of Canada, Memoir 368, 121 pages.

Iverson, N.R.
1991: Morphology of glacial striae: Implications for abrasion of glacier beds and fault surfaces. Geological Society of America Bulletin, Volume 103, pages 1308-1316.

Jenks, G.F.
1967: The data model concept in statistical mapping. International Yearbook of Cartography, Volume 7, pages 186-190.

Jenness, S.E.
1963: Terra Nova and Bonavista map-areas, Newfoundland (2D E1/2 and 2C). Geological Survey of Canada, Memoir 327, 184 pages.

King, A.F.
1988: Geology of the Avalon Peninsula, Newfoundland. Newfoundland Department of Mines and Energy, Geological Survey Branch, Map 88-01, scale 1:250 000.

Liverman, D.G.E., Klassen, R.A., Davenport, P.H. and Honovar, P.
1996: Till geochemistry, Buchans-Roberts Arm Belt (NTS 2E/5, 2E/12, 12A/15, 12A/16, 12H/1 and 12H/8). Newfoundland Department of Mines and Energy, Geological Survey, Open File NFLD/2596.

Liverman, D., Taylor, D., Sheppard, K. and Dickson, L.
2000: Till geochemistry, Hodges Hill area, central Newfoundland. Newfoundland Department of Mines and Energy, Geological Survey, Open File NFLD/2704, 51 pages.

Lundqvist, J.
1969: Problems of the so-called Rogen moraine. Sveriges Geologiska Undersökning, Ser. C, No. 648.

Lynch, J.
1996: Provisional elemental values for four new geochemical soil and till reference materials, Till-1, Till-2, Till-3 and Till-4. Geostandards Newsletter, Volume 20, pages 277-287.

Martin, W.
1983: Once Upon A Mine: Story of pre-confederation mines on the Island of Newfoundland. Special Volume 26, The Canadian Institute of Mining and Metallurgy, Montreal, Quebec, 98 pages.

MacClintock, P. and Twenhofel, W.H.
1940: Wisconsin glaciation of Newfoundland. Bulletin of the Geological Society of America, Volume 51, pages 1729-1756.

McCuaig, S.
2002: Till geochemistry of the Alexis River region (NTS map areas 13A/10, 14 and 15). Newfoundland and Labrador Department of Mines and Energy, Geological Survey, Open File 013A/0046.

Murray, A.
1883: Glaciation in Newfoundland. Proceedings and Transactions of the Royal Society of Canada, Volume 1, pages 55-76.

O'Brien, S.J. and King, A.F.
2002: Neoproterozoic stratigraphy of the Bonavista Peninsula: Preliminary results, regional correlations and implications for sediment-hosted stratiform copper exploration in the Newfoundland Avalon zone. *In* Current Research. Newfoundland and Labrador Department of Mines and Energy, Geological Survey, Report 02-1, pages 229-244.

O'Brien, S.J., Wardle, R.J. and King, A.F.
1983: The Avalon Zone: A Pan-African Terrane in the Appalachian Orogen of Canada. Geological Journal, Volume 18, pages 195-222.

Quinlan, G. and Beaumont, C.
1981: A comparison of observed and theoretical postglacial relative sea level in Atlantic Canada. Canadian Journal of Earth Sciences, Volume 18, pages 1146-1163.

Summers, W.F.
1949: Physical geography of the Avalon Peninsula of Newfoundland. Unpublished M.Sc. Thesis, McGill University, Montreal.

Taylor, D.M.
2001: Newfoundland and Labrador Striation Database. Newfoundland Department of Mines and Energy, Geological Survey, Open File NFLD/2195, version 4.

Vhay, J.S.
1937: Pyrophyllite deposits, Manuels, Conception Bay, Newfoundland. Newfoundland Geological Survey, Bulletin 7, 133 pages.

Wagenbauer, H.A., Riley, C.A. and Dawe, G.
1983: The Geochemicial Laboratory. *In* Current Research. Newfoundland and Labrador Department of Mines and Energy, Mineral Development Division, Report 83-1, pages 133-137.

Till Geochemistry Maps

Page

Figure 6. Distribution of Arsenic in till

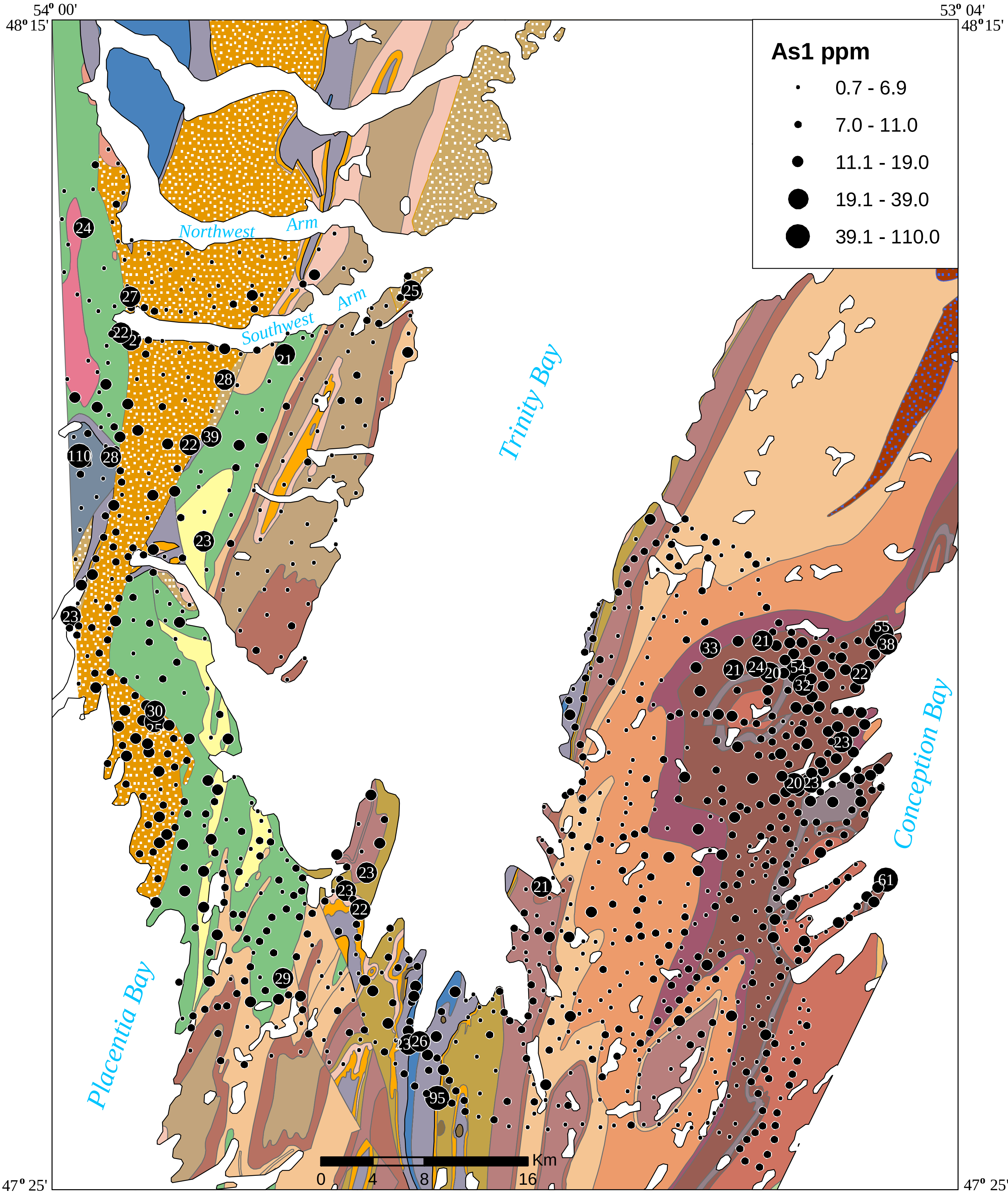

Open File NFLD 2824

Figure 7. Distribution of Gold in till

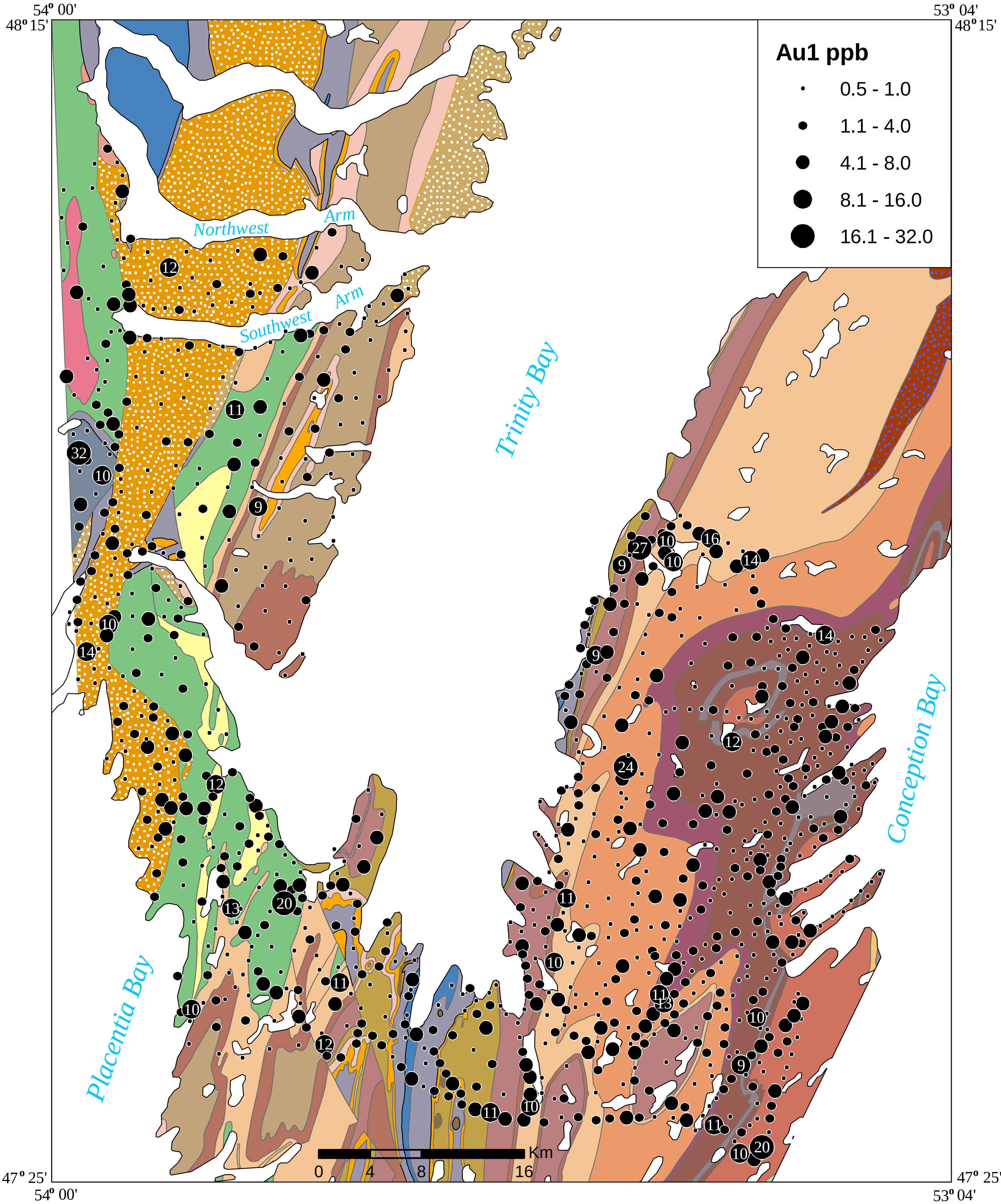

Open File NFLD 2824

Figure 8. Distribution of Barium in till

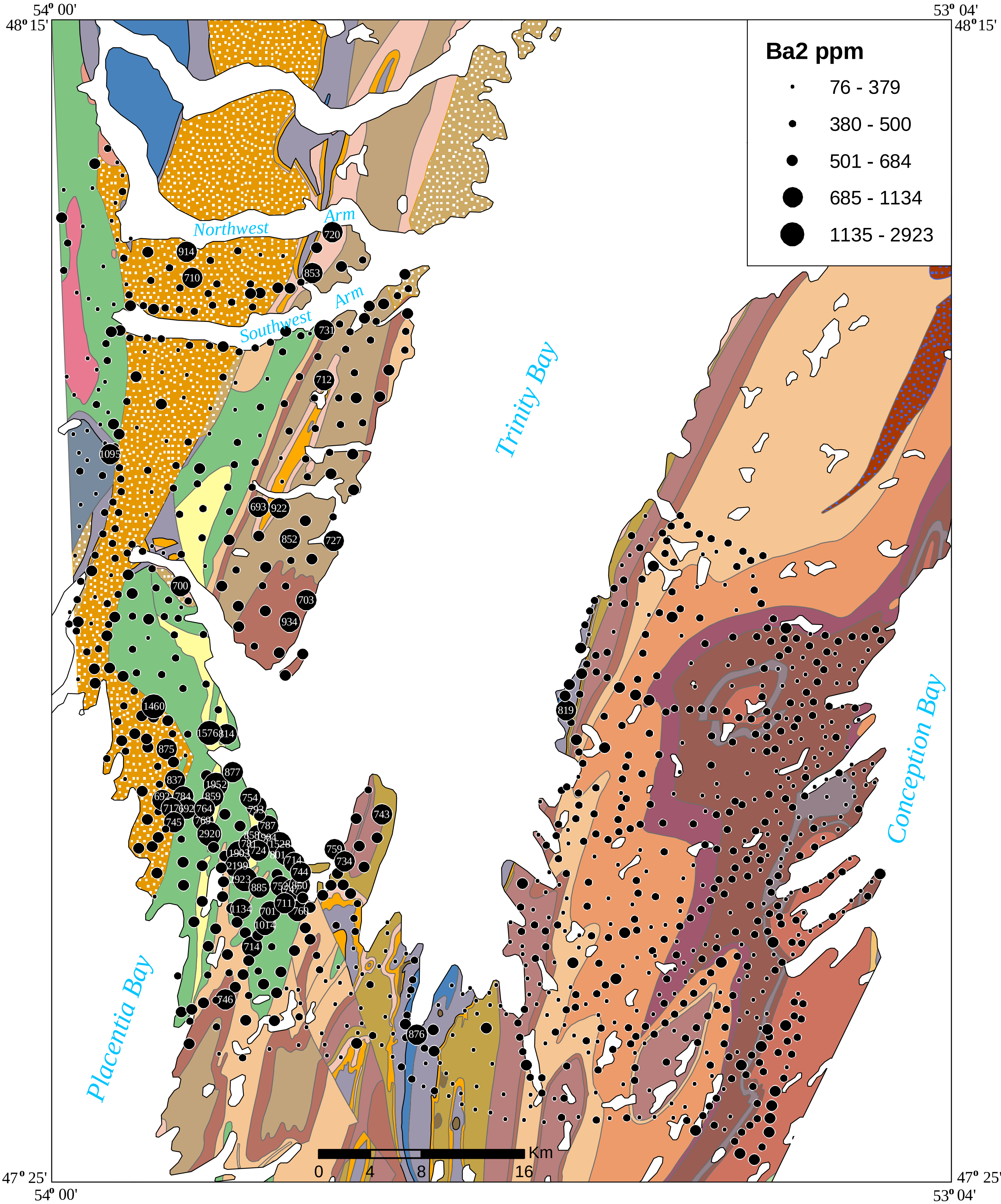

Open File NFLD 2824

Figure 9. Distribution of Chromium in till

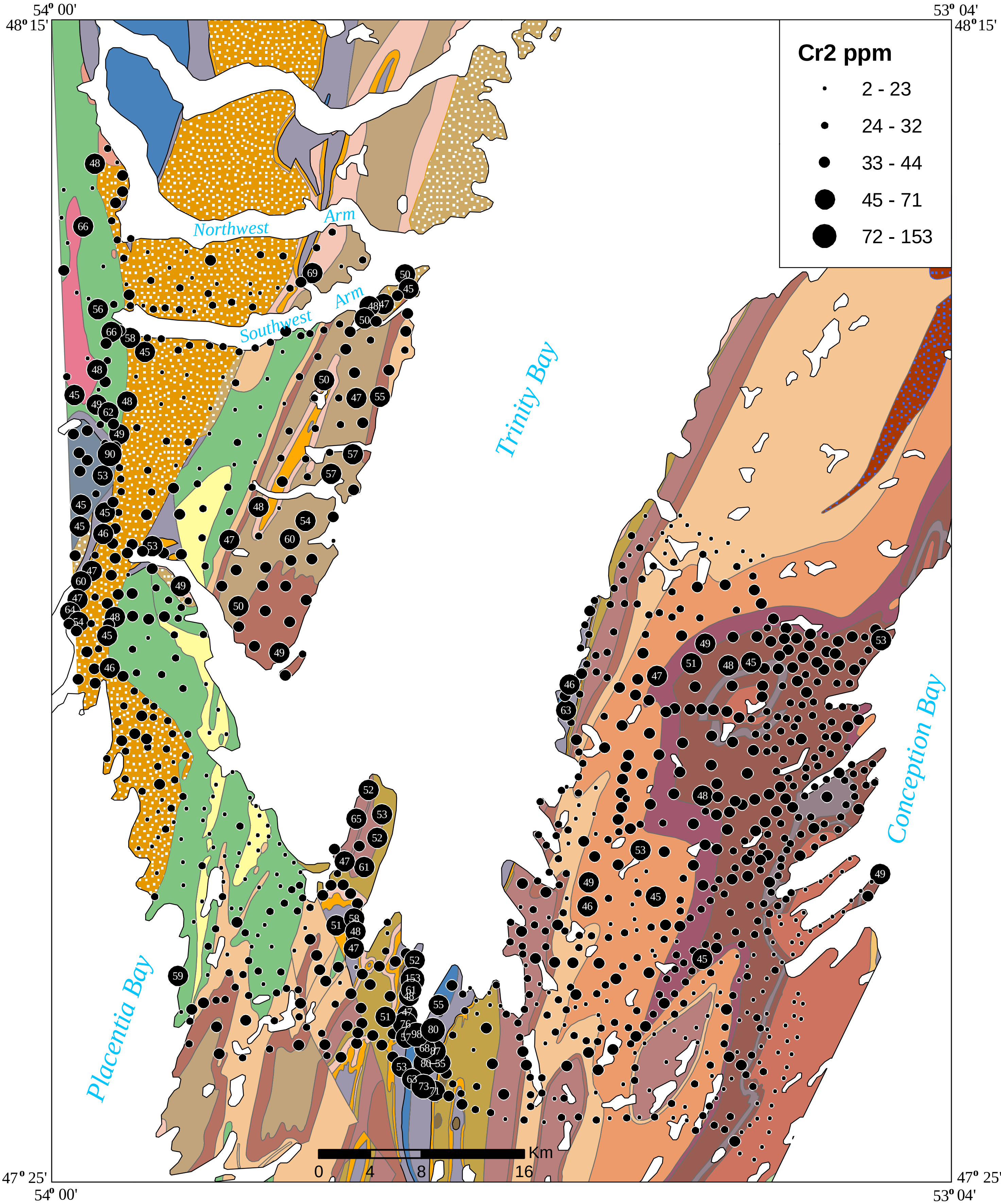

Open File NFLD 2824

Figure 10. Distribution of Copper in till

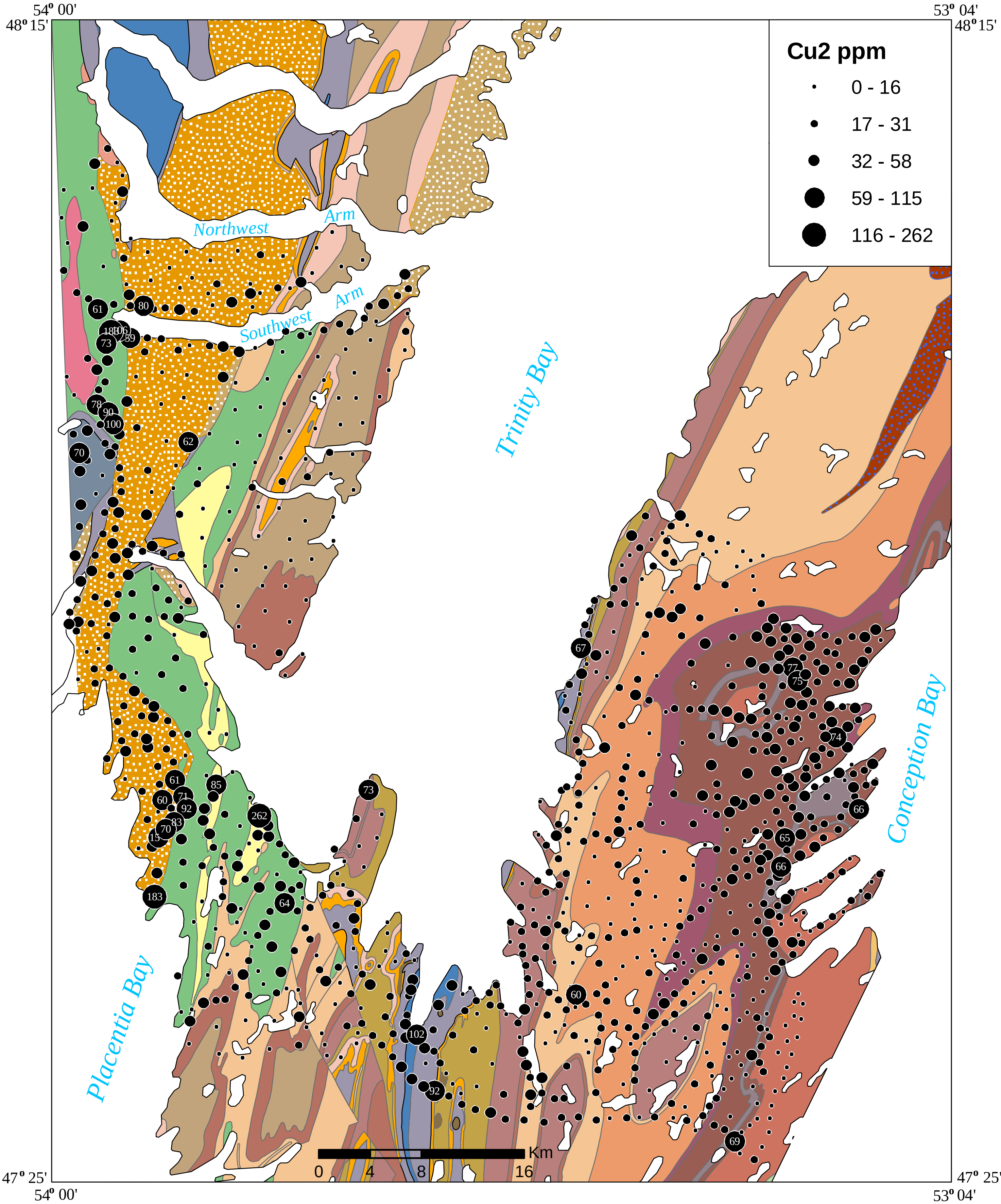

Open File NFLD 2824

Figure 11. Distribution of Manganese in till

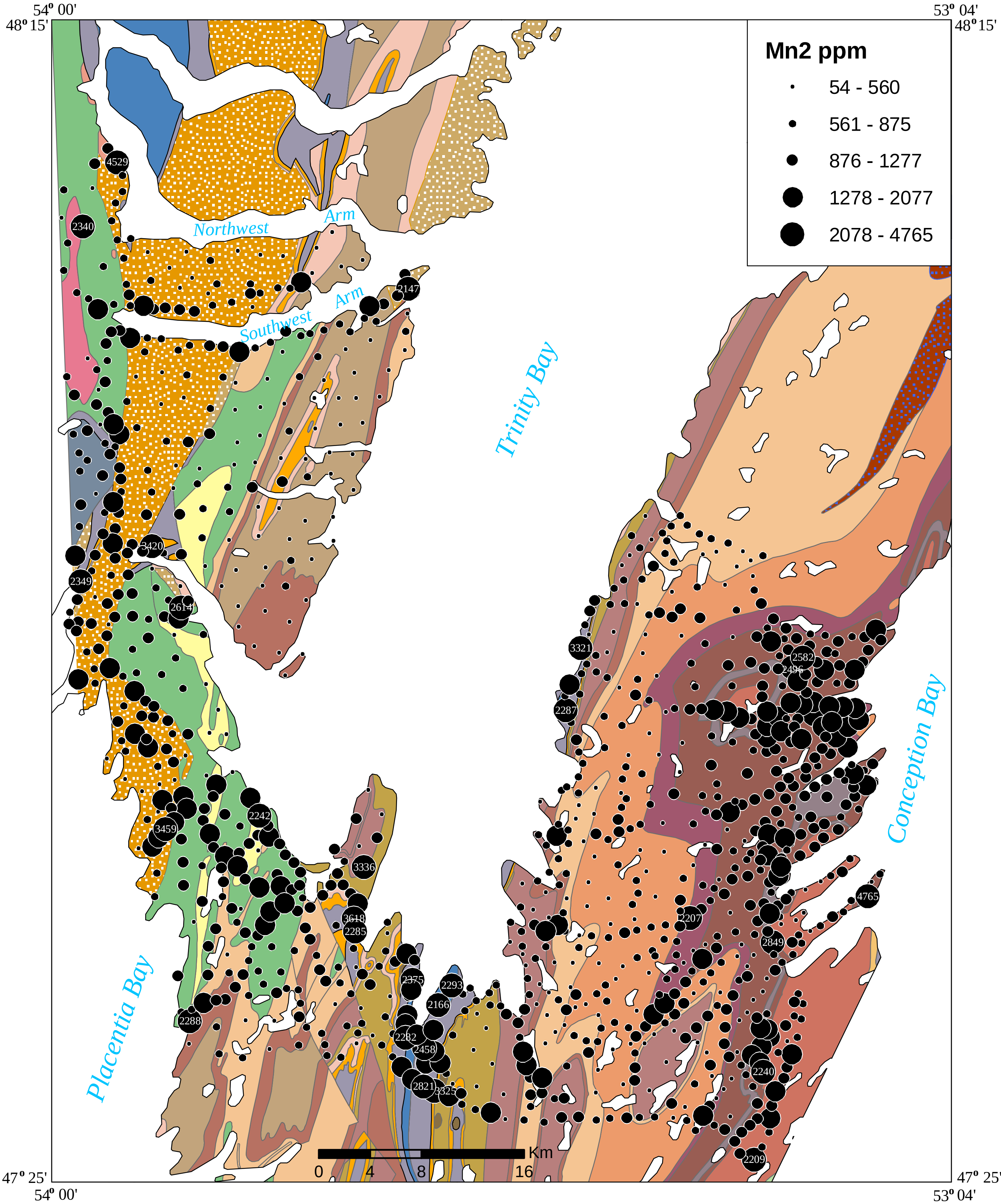

Open File NFLD 2824

Figure 12. Distribution of Nickel in till

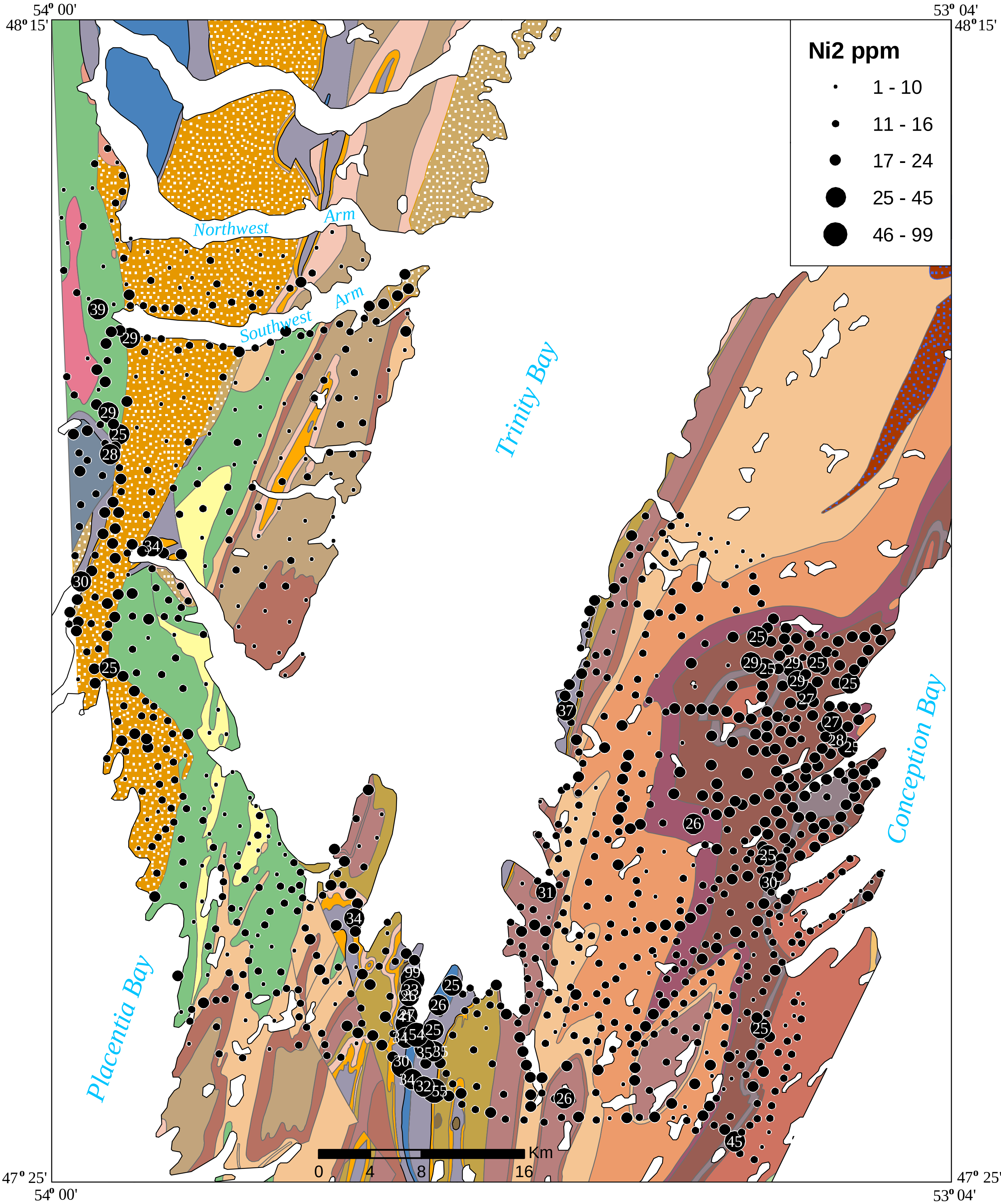

Open File NFLD 2824

Figure 13. Distribution of Lead in till

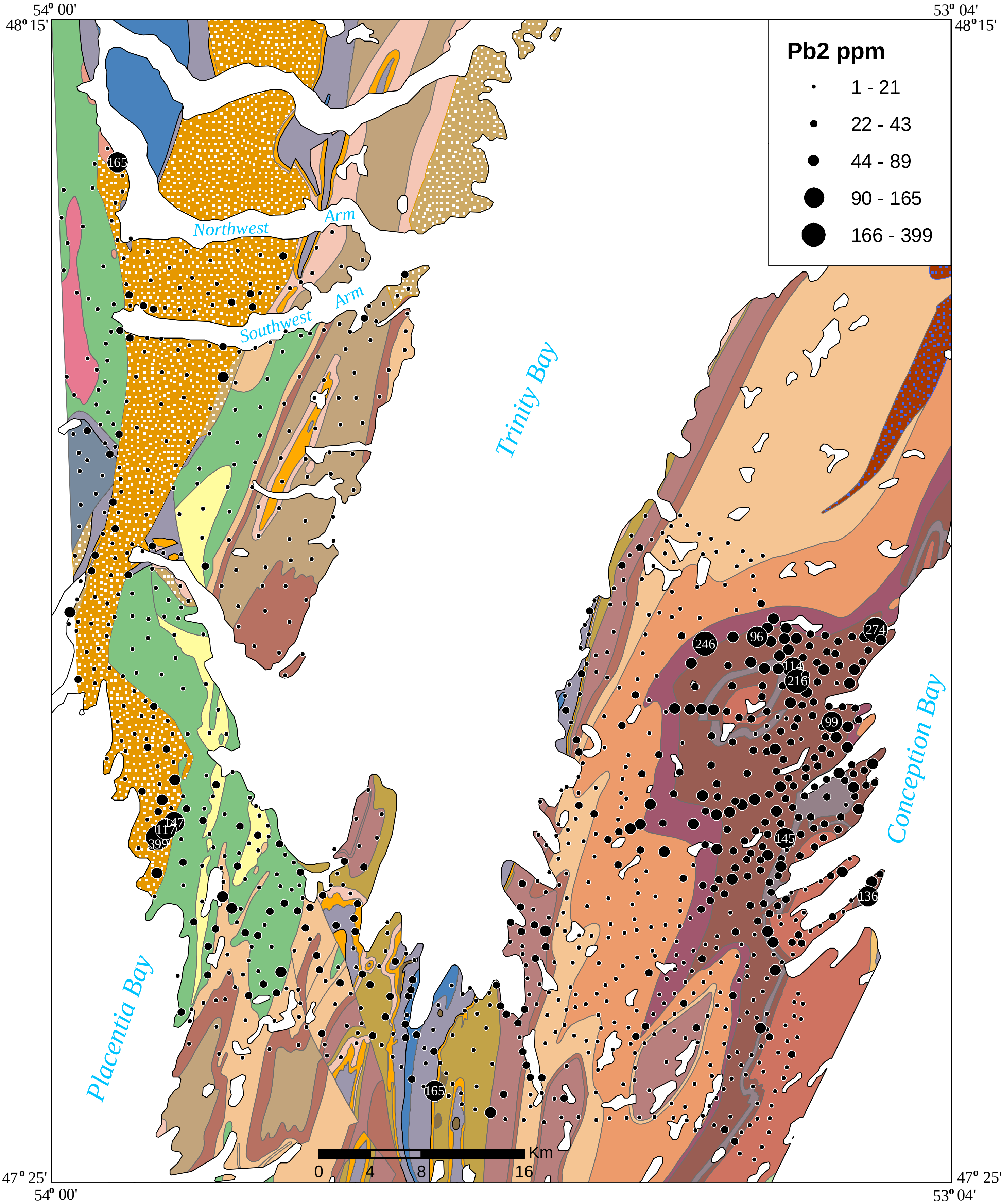

Open File NFLD 2824

Figure 14. Distribution of Antimony in till

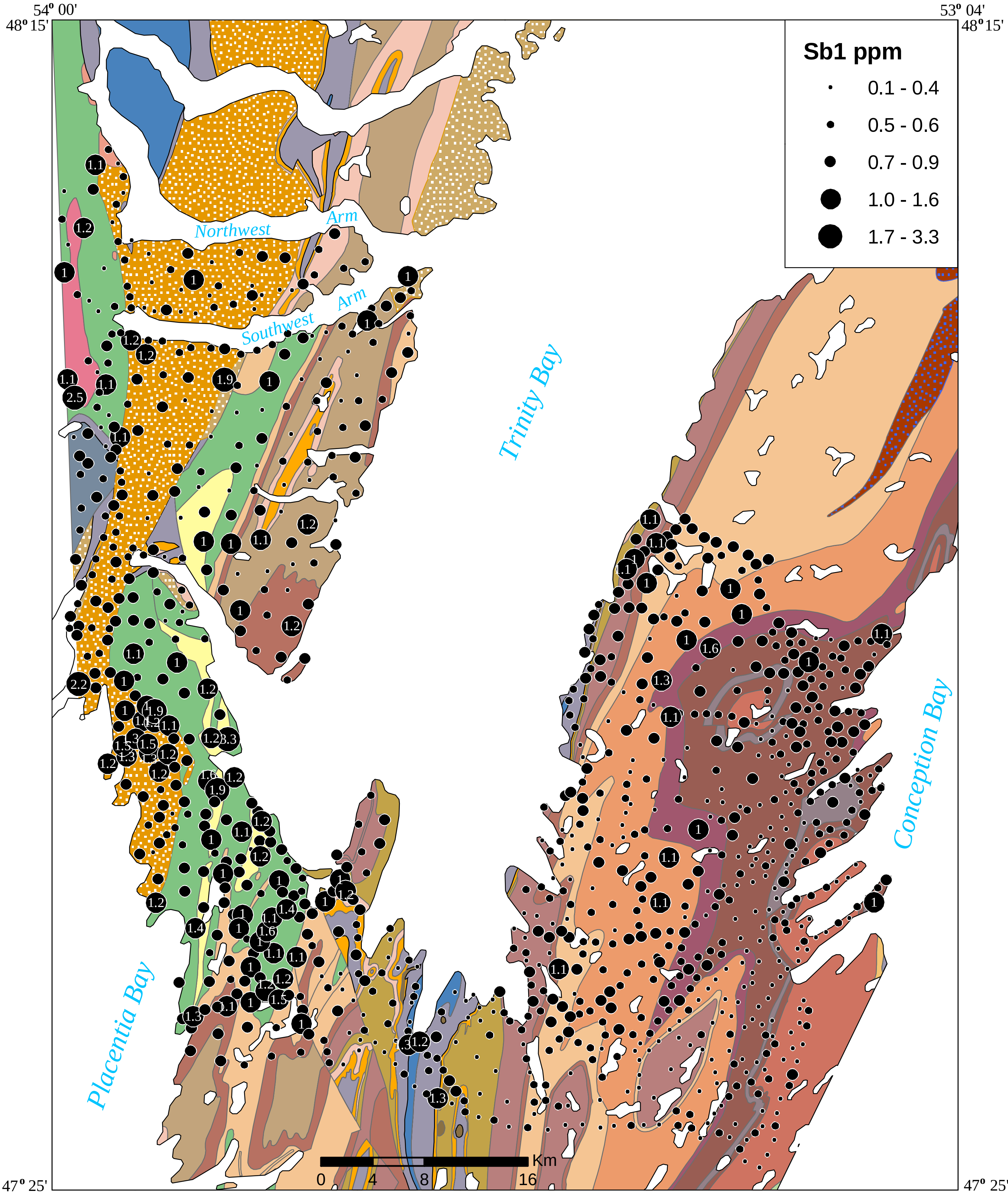

Open File NFLD 2824

Figure 15. Distribution of Vanadium in till

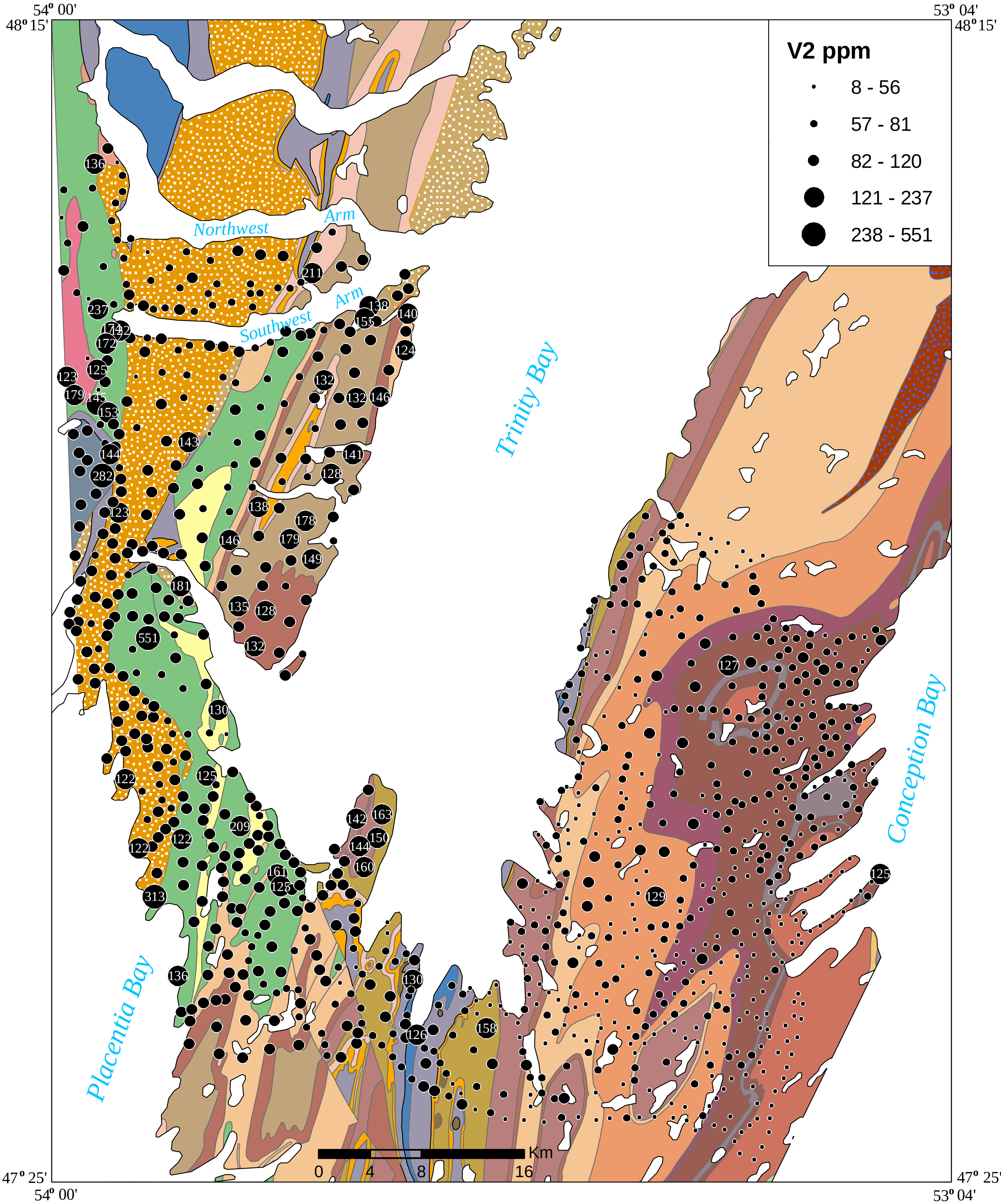

Open File NFLD 2824

Figure 16. Distribution of Ytterbium in till

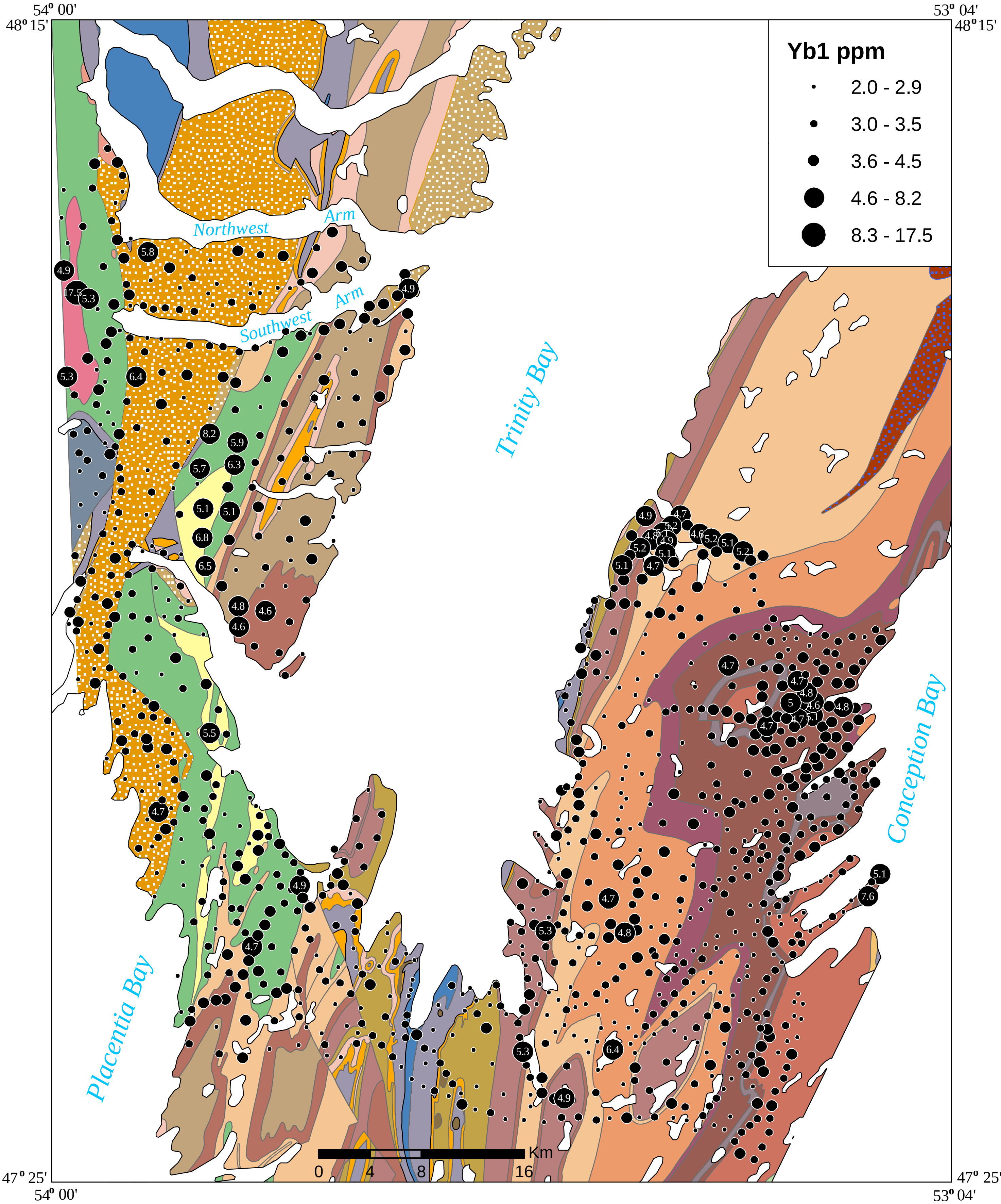

Open File NFLD 2824

Figure 17. Distribution of Zinc in till

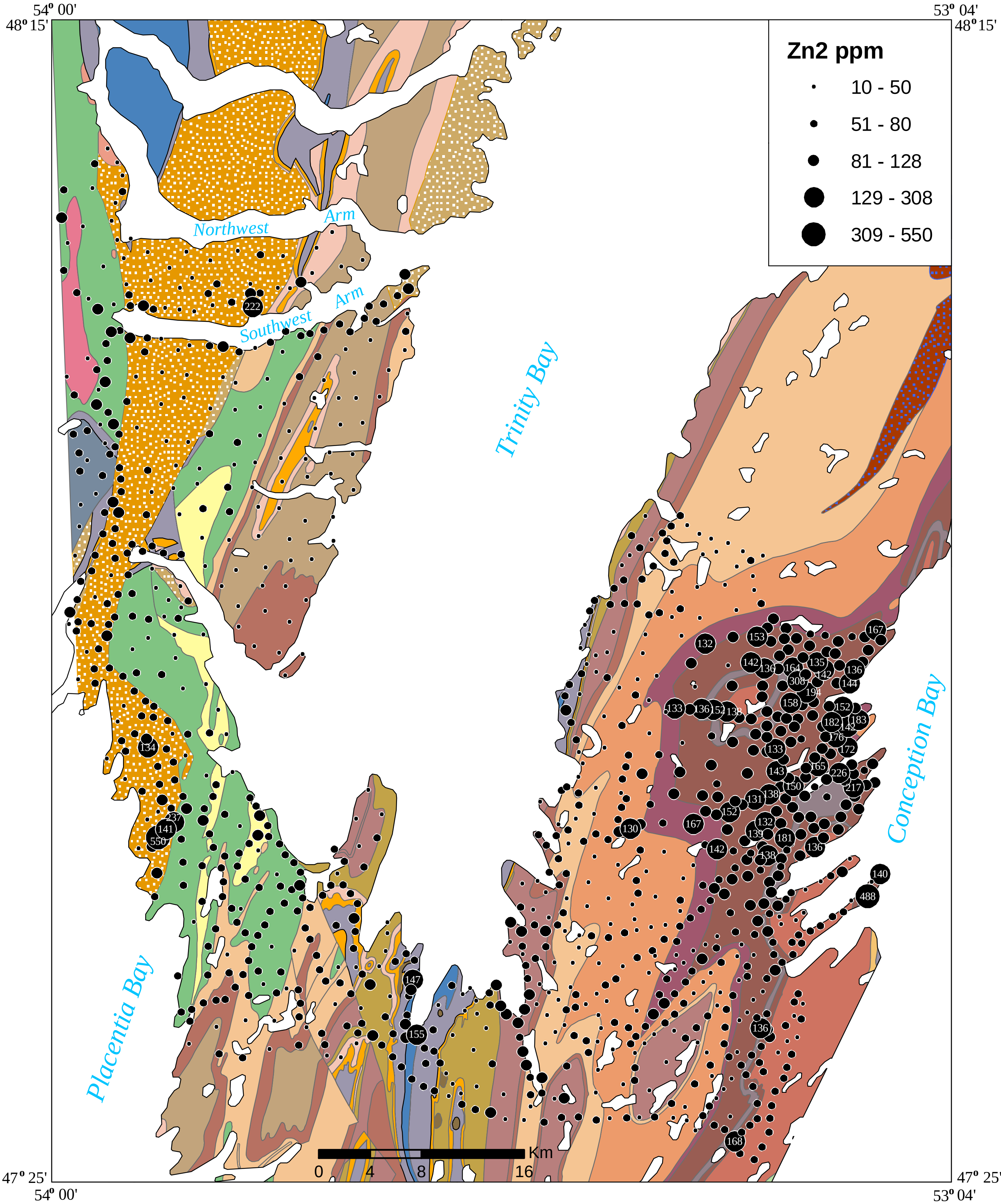

Open File NFLD 2824

Appendices

Appendix A

For the data shown on pages 47-154 please see the data files (nfld2824data.csv or nfld2824data.xls) included on this CD.

Appendix B: Comparison plots of laboratory duplicates for elements analysed by INAA.

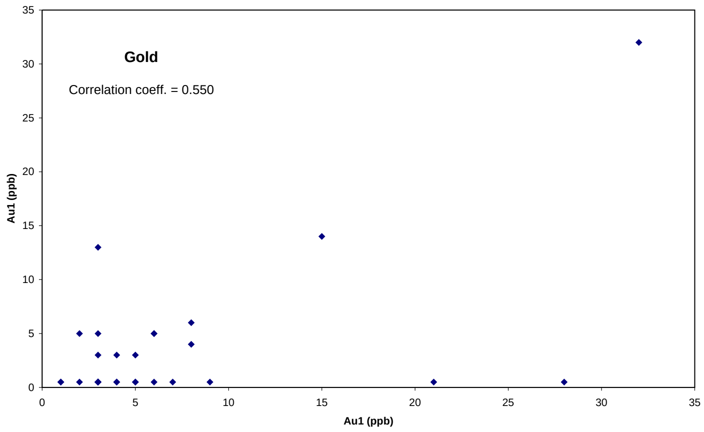

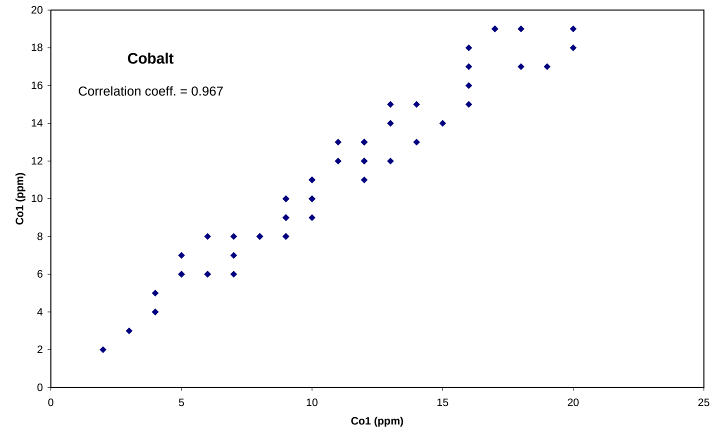

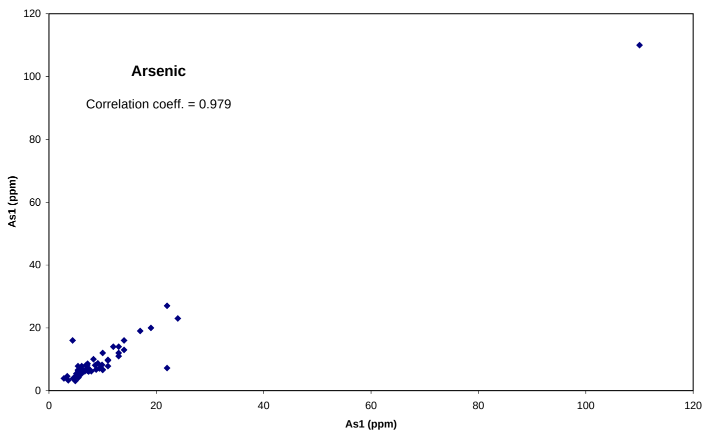

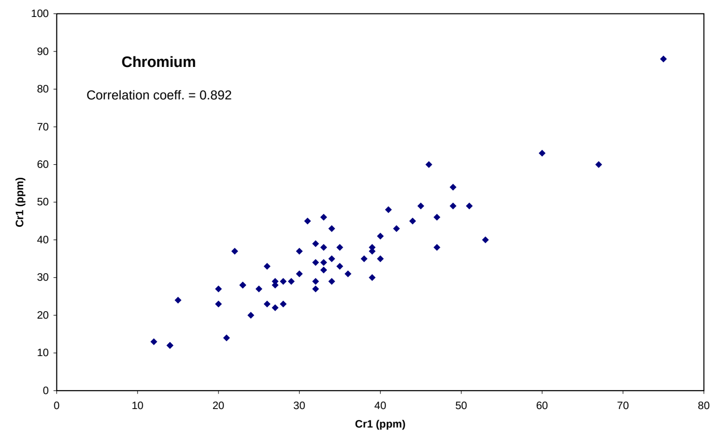

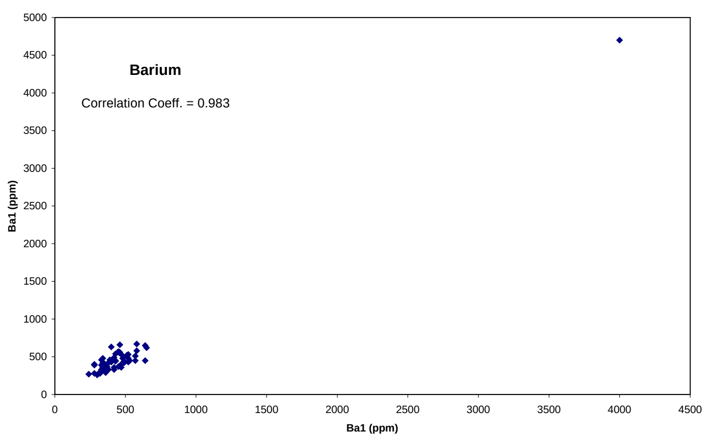

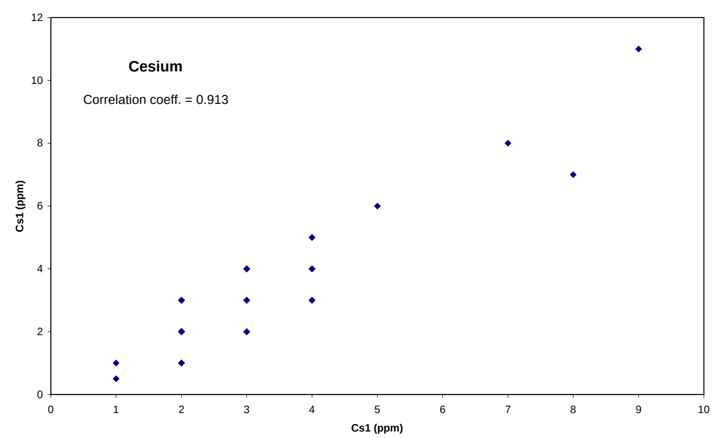

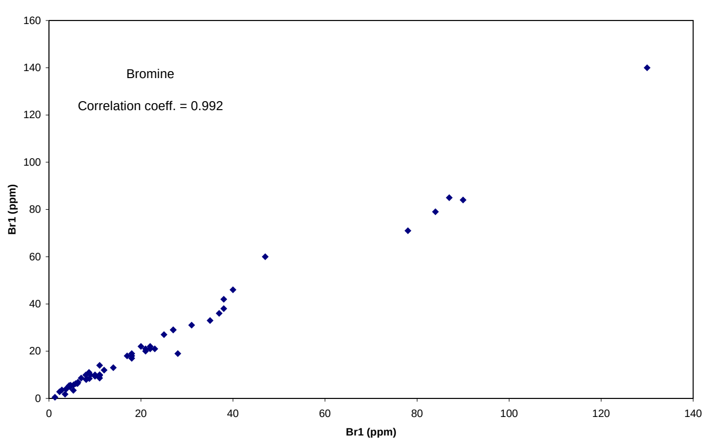

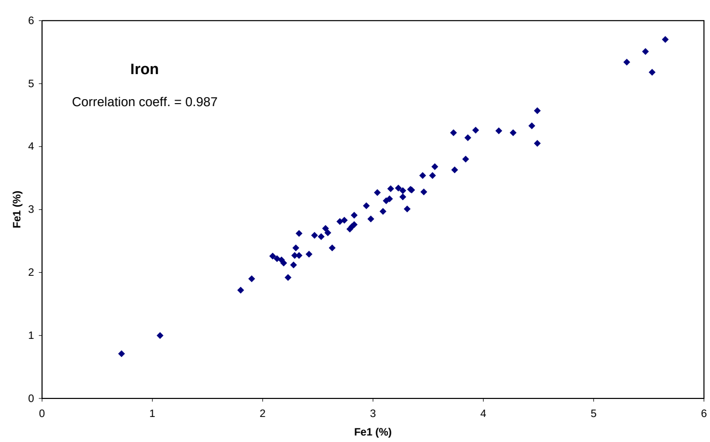

Appendix B cont.

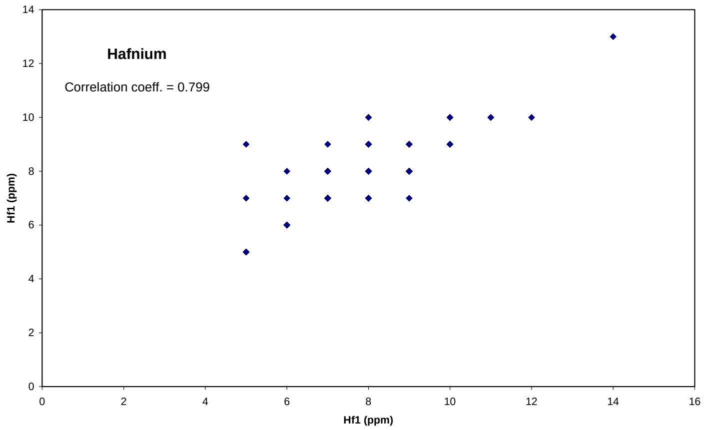

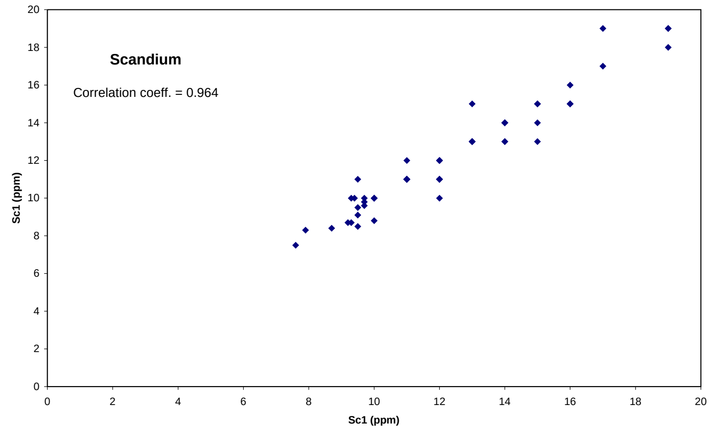

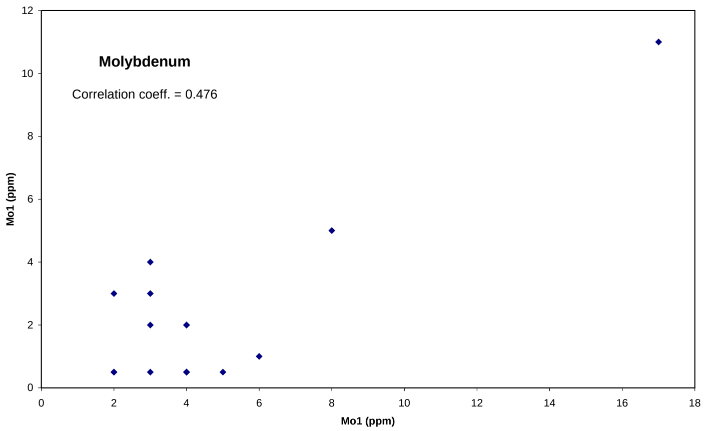

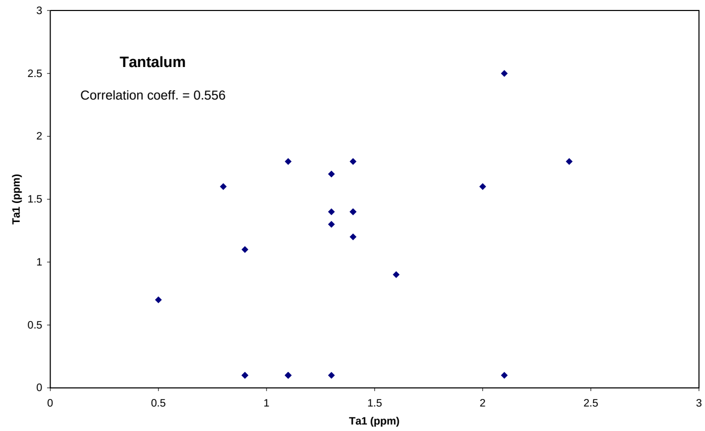

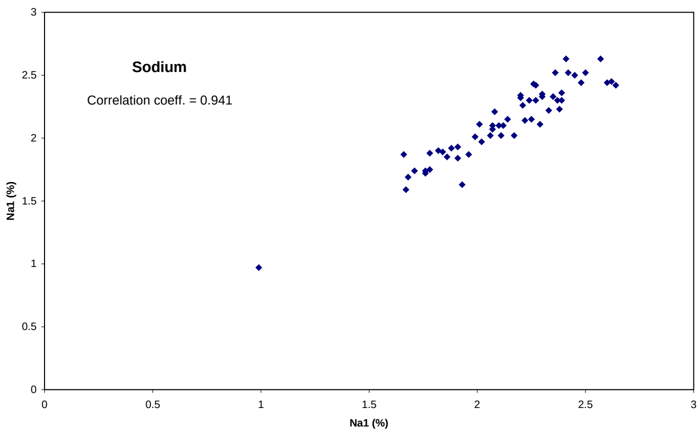

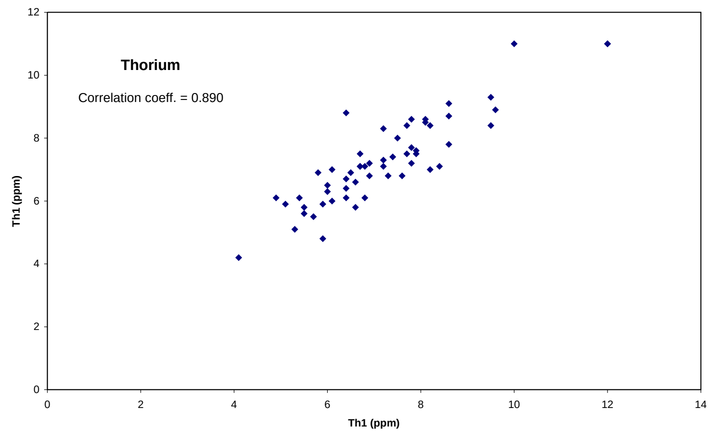

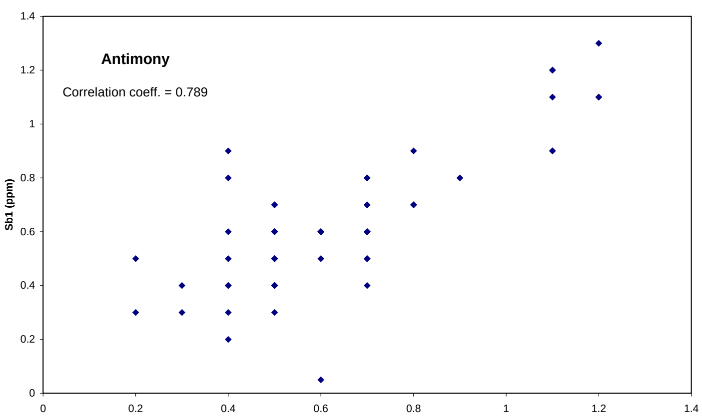

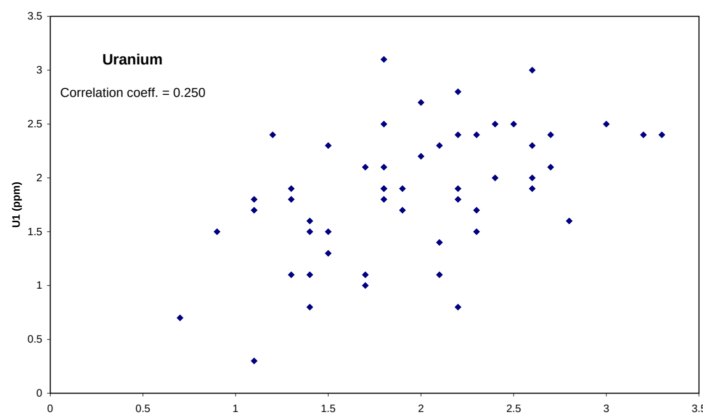

Appendix B cont.

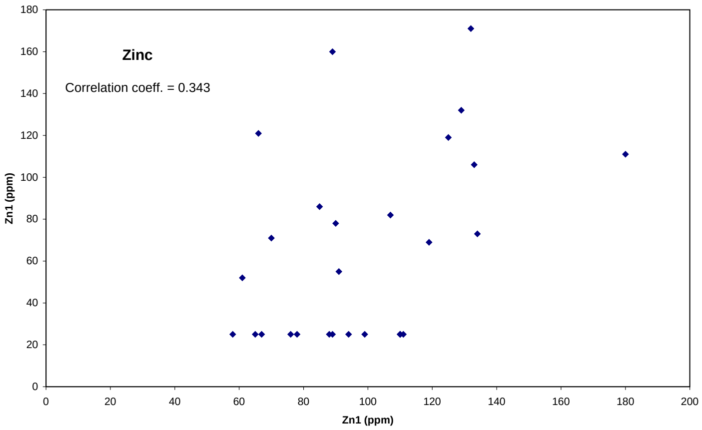

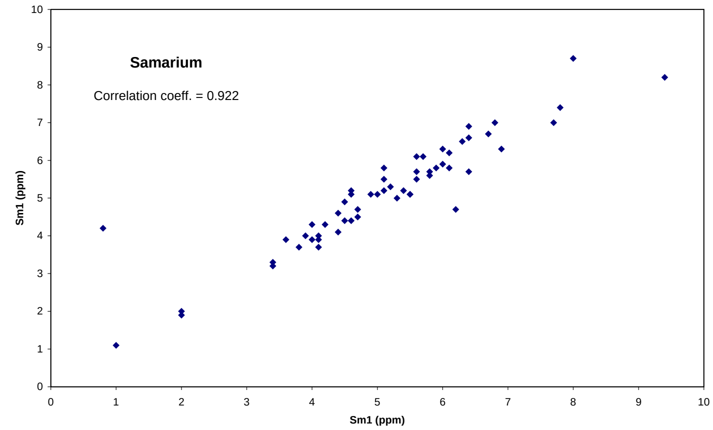

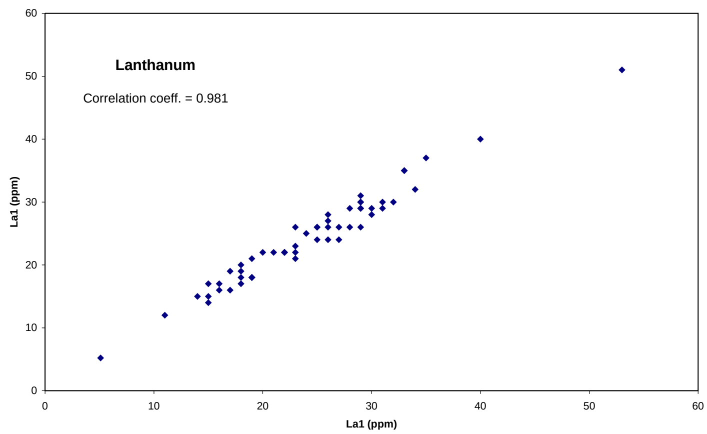

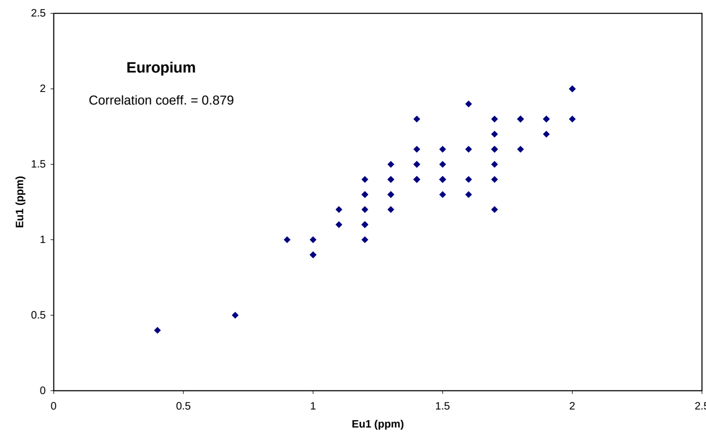

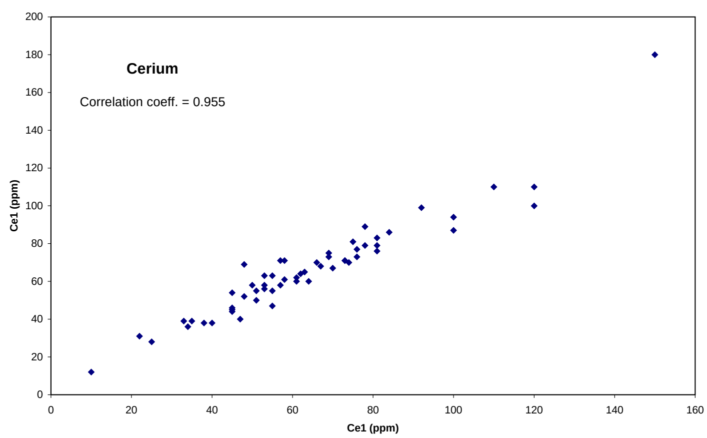

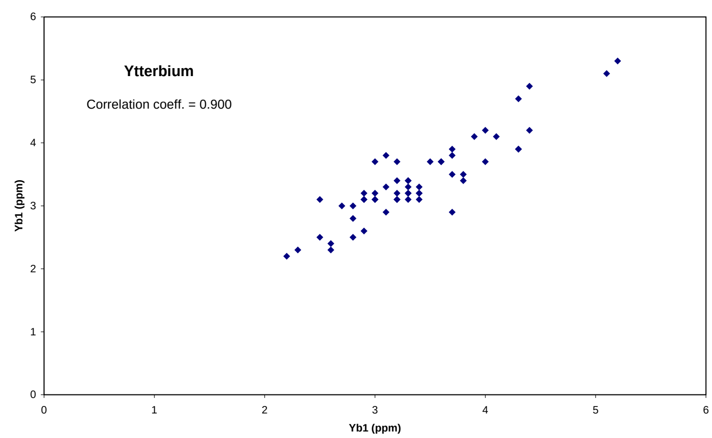

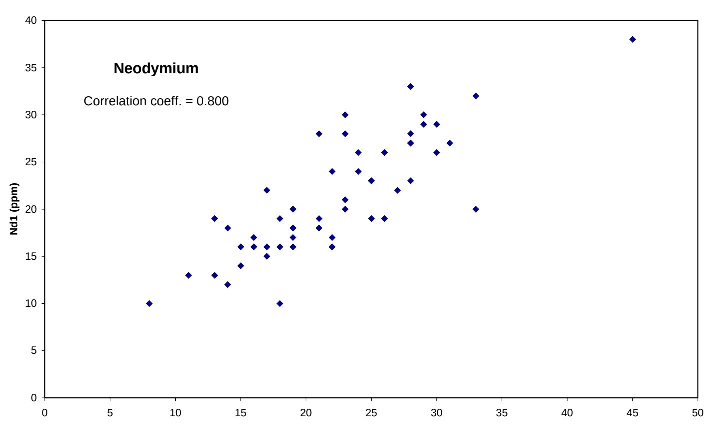

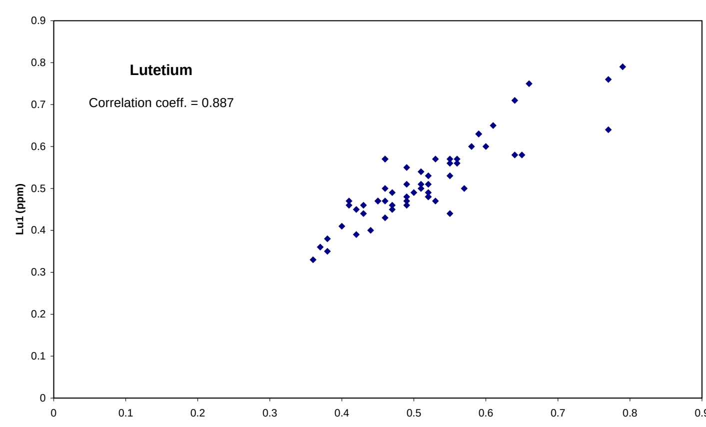

Appendix C: Comparison plots of laboratory duplicates for elements analysed by ICP

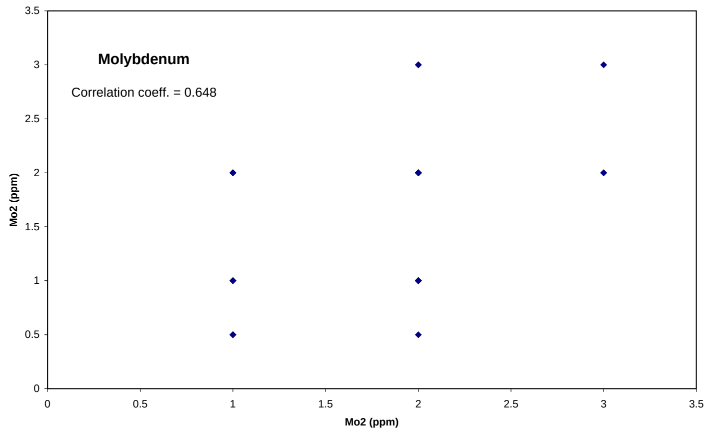

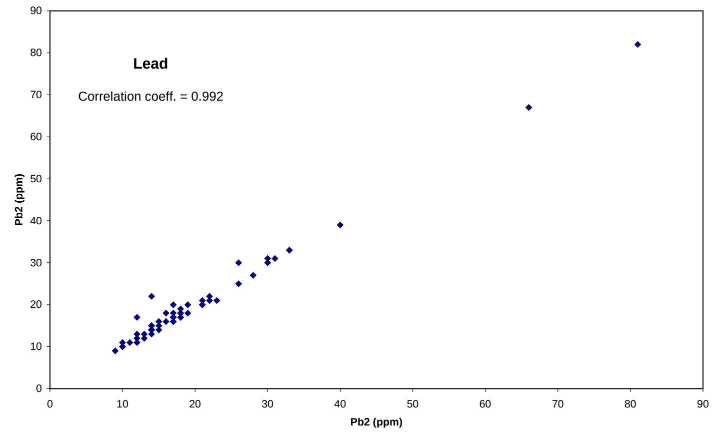

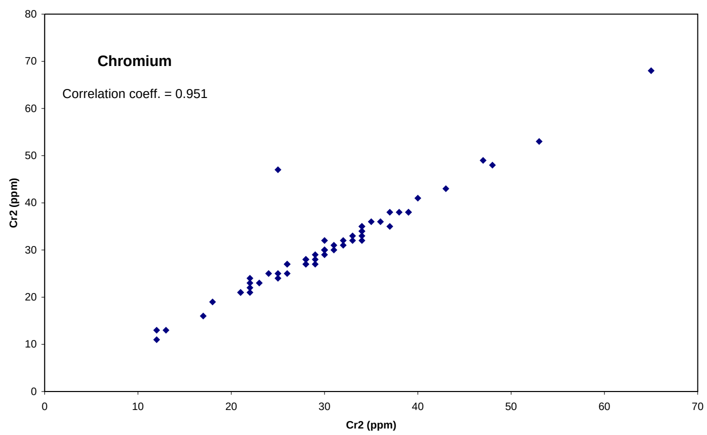

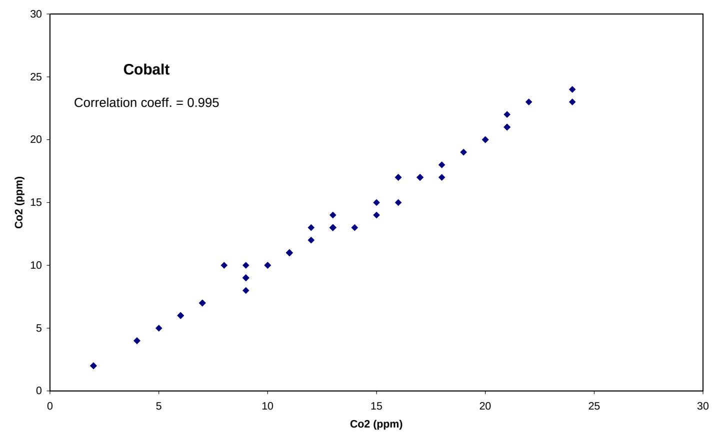

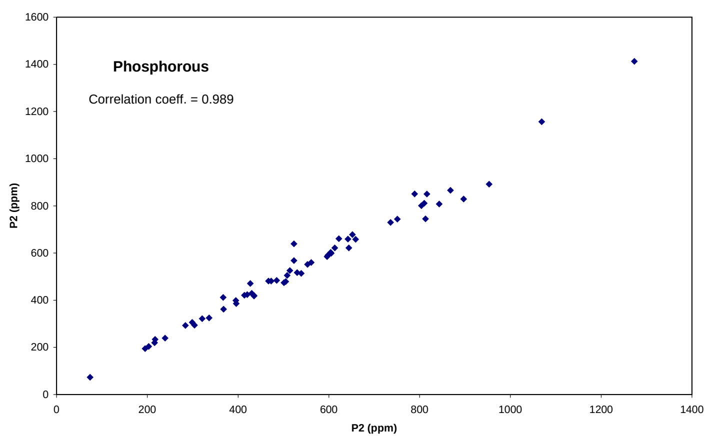

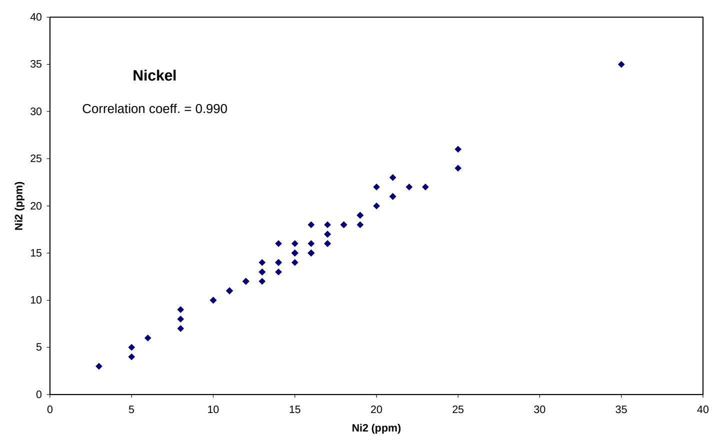

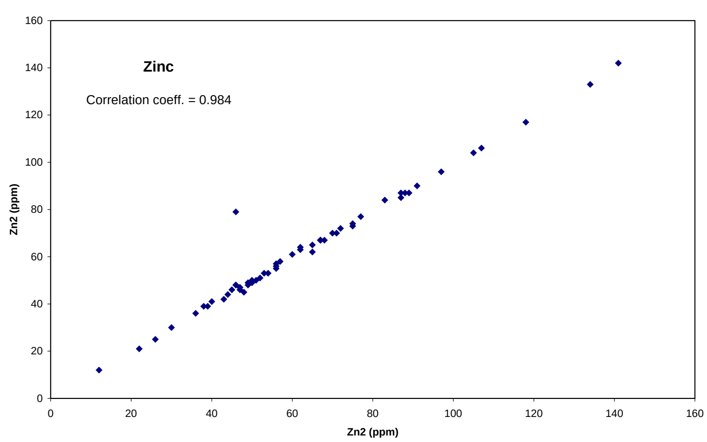

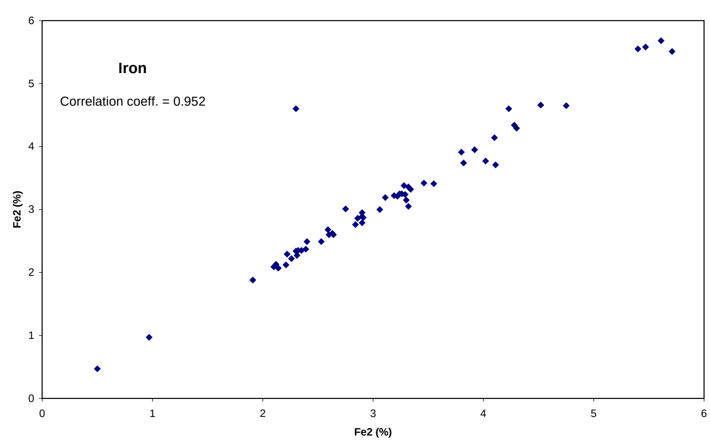

Appendix C cont.

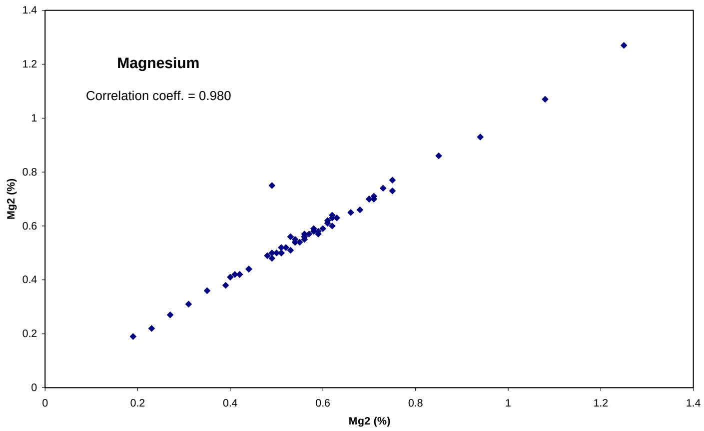

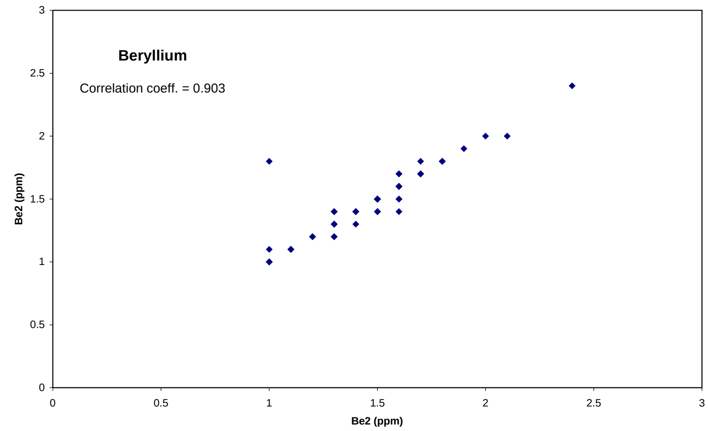

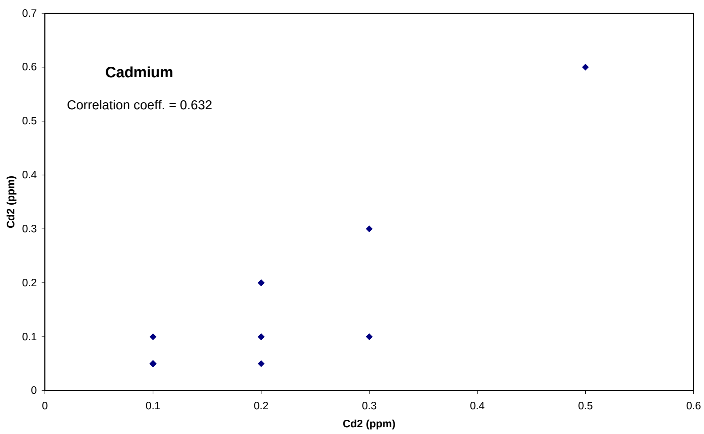

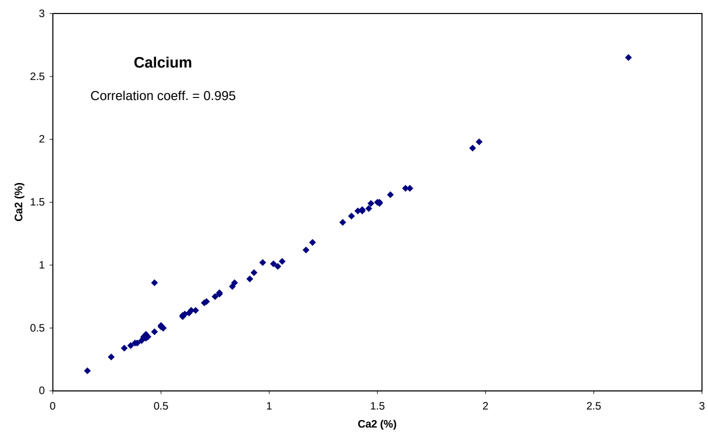

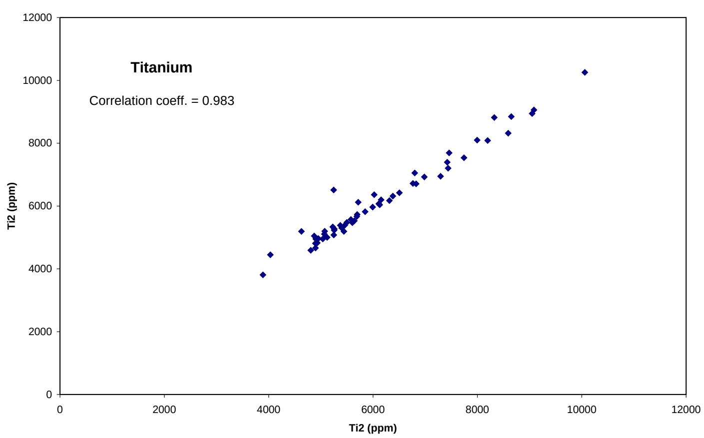

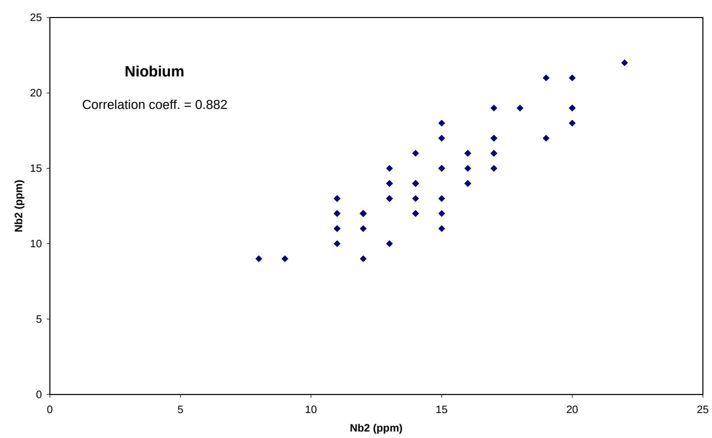

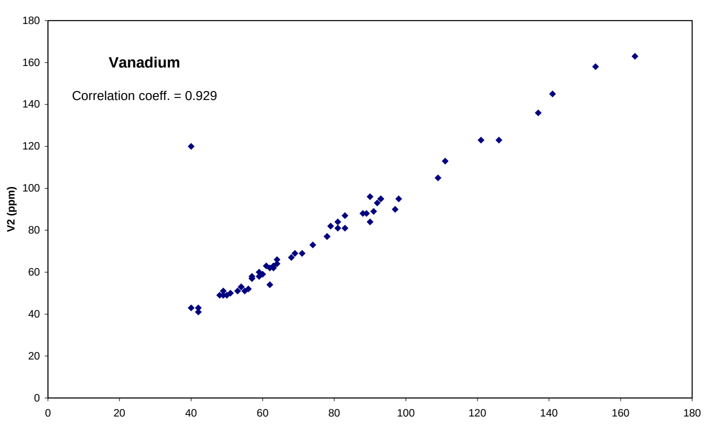

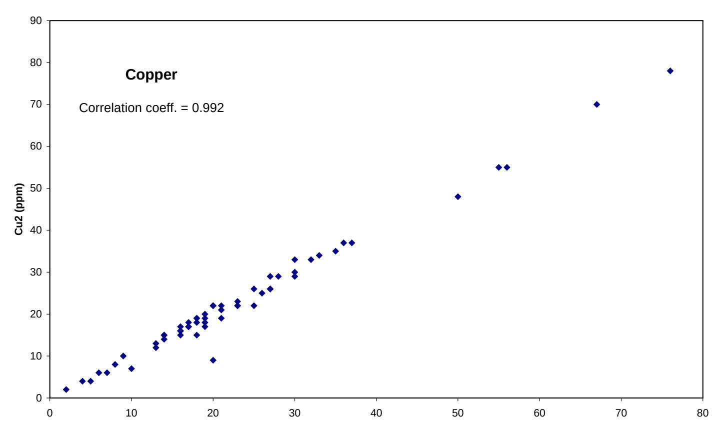

Appendix C cont.

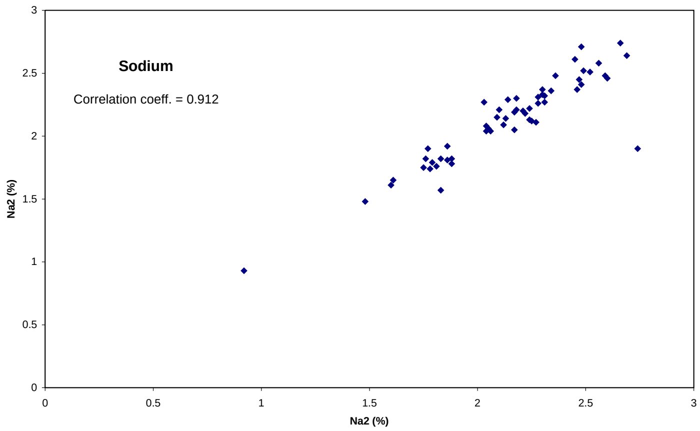

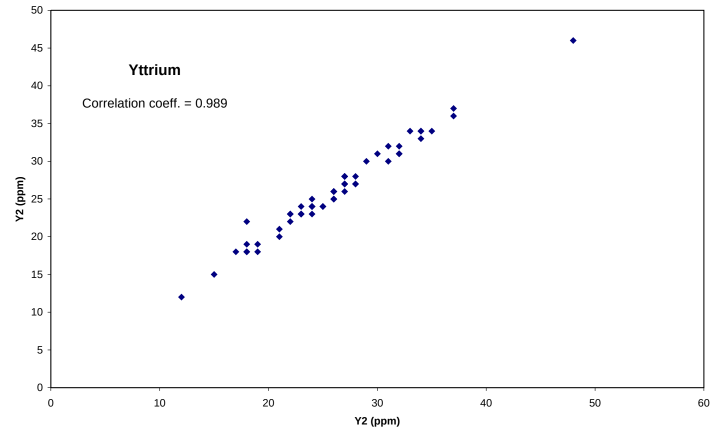

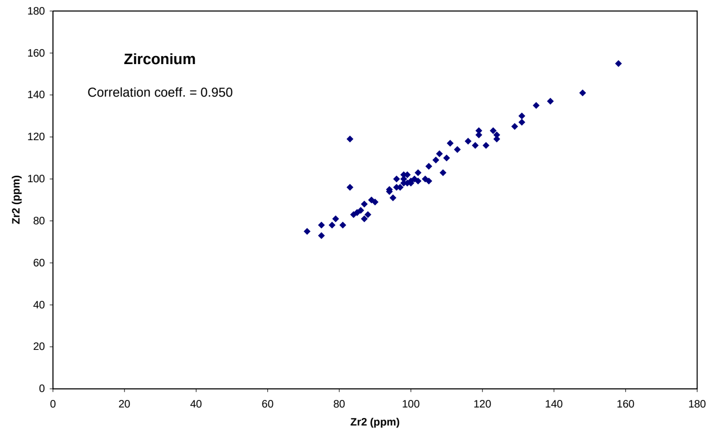

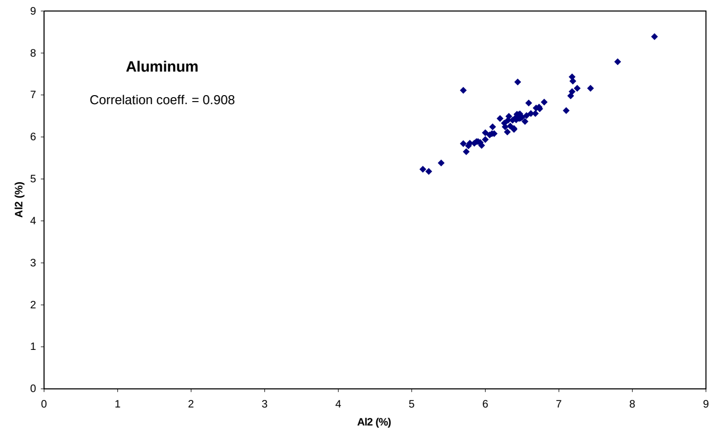

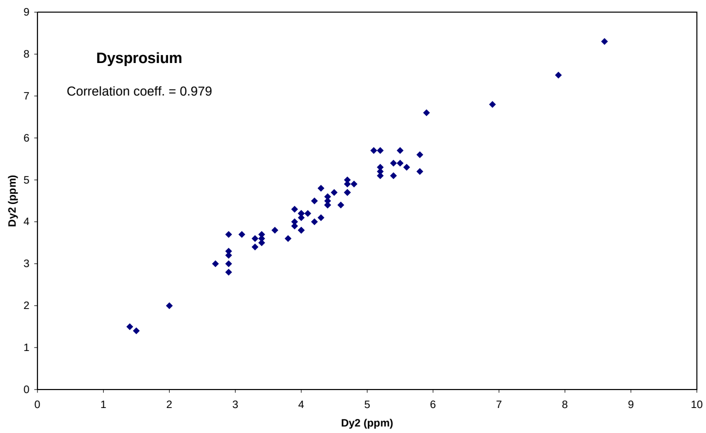

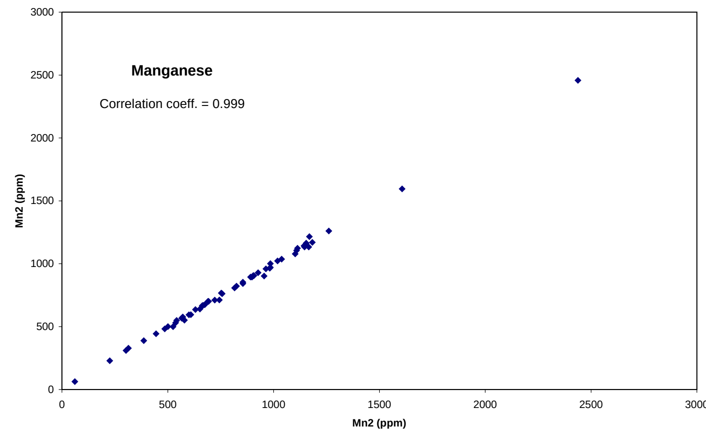

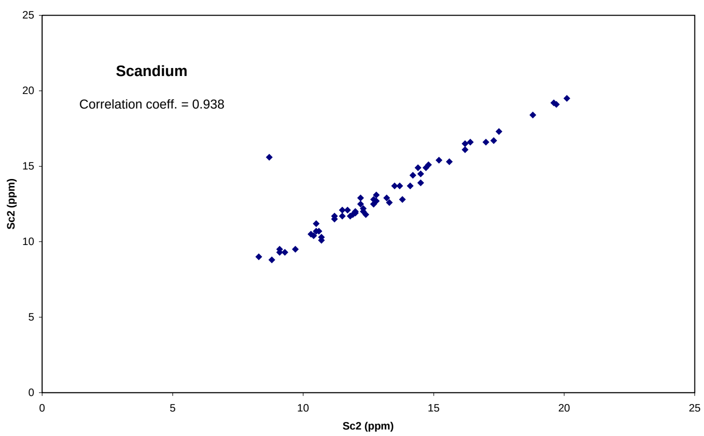

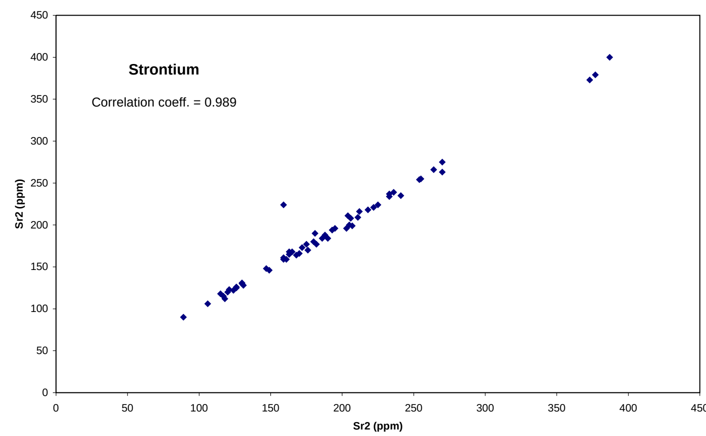

Appendix C cont.

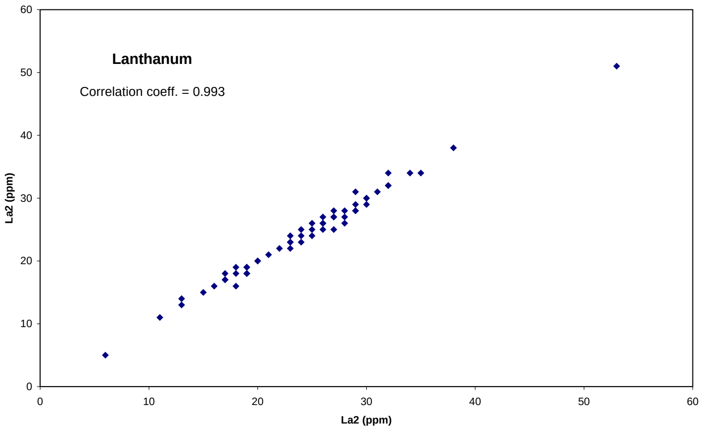

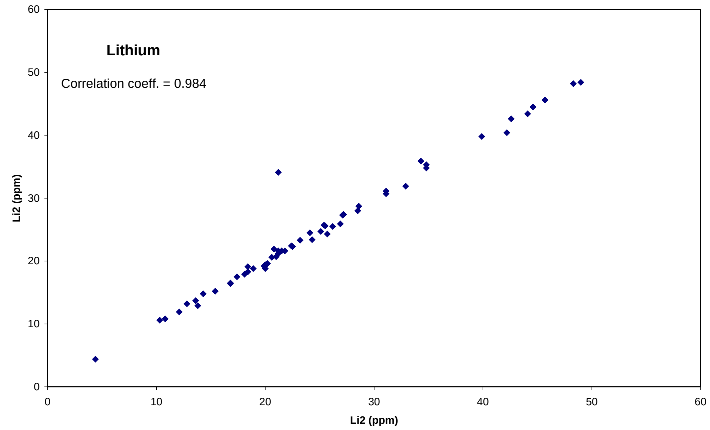

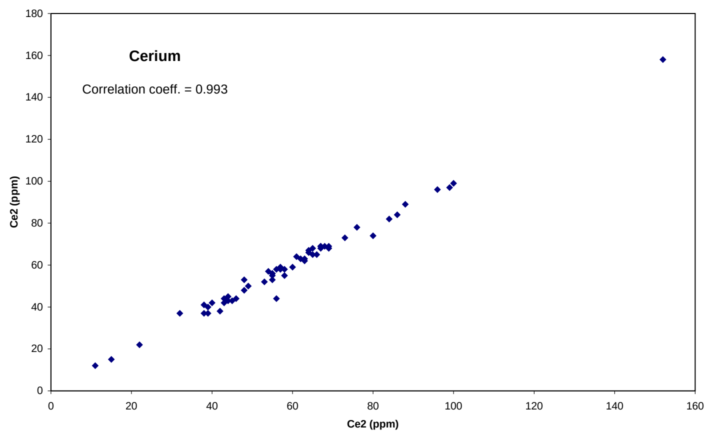

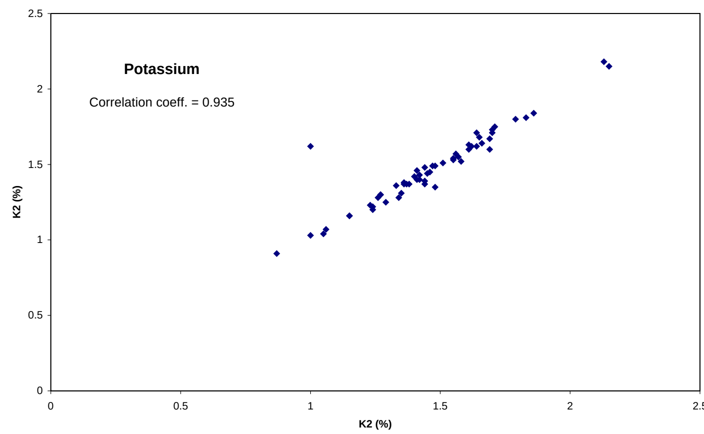

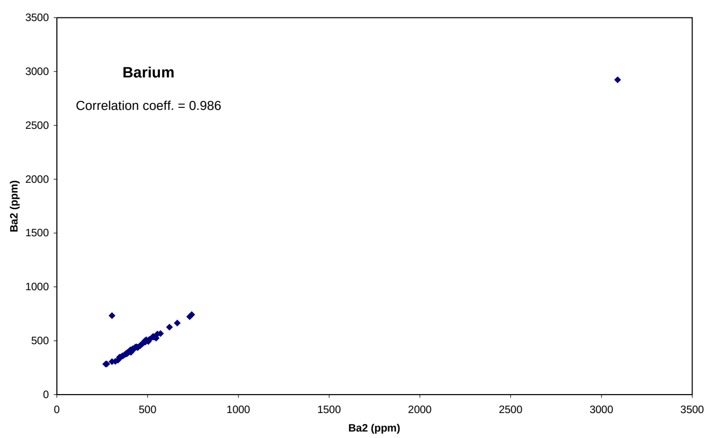

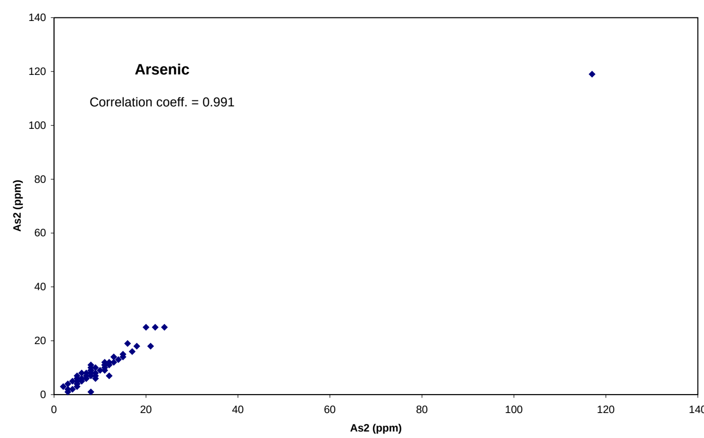

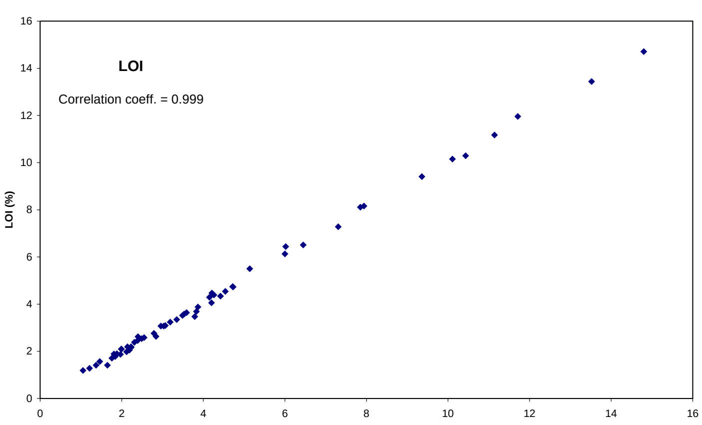

Appendix D: Comparison plots of field duplicates for elements analysed by INAA

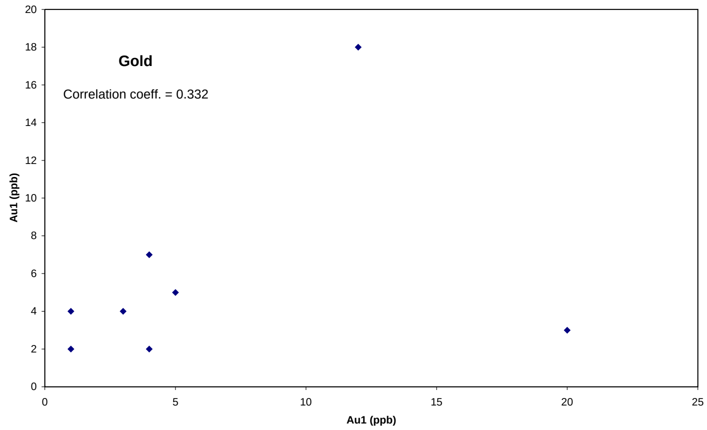

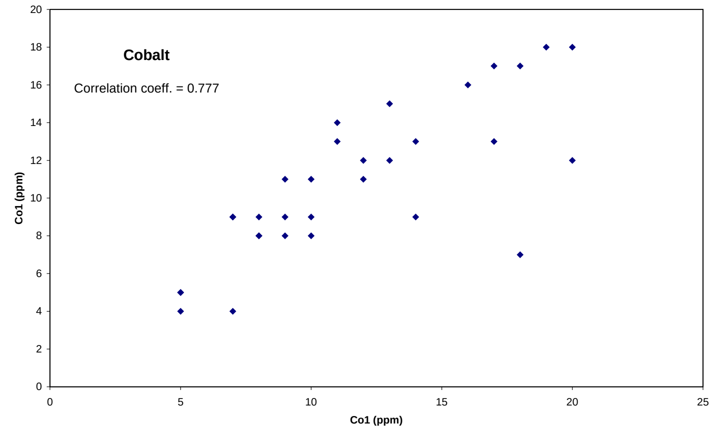

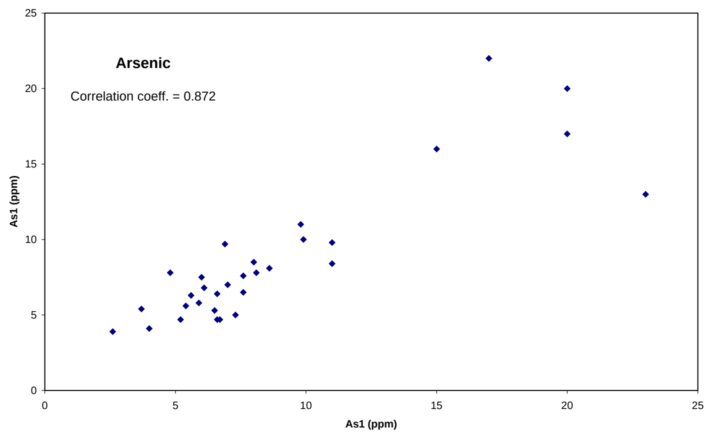

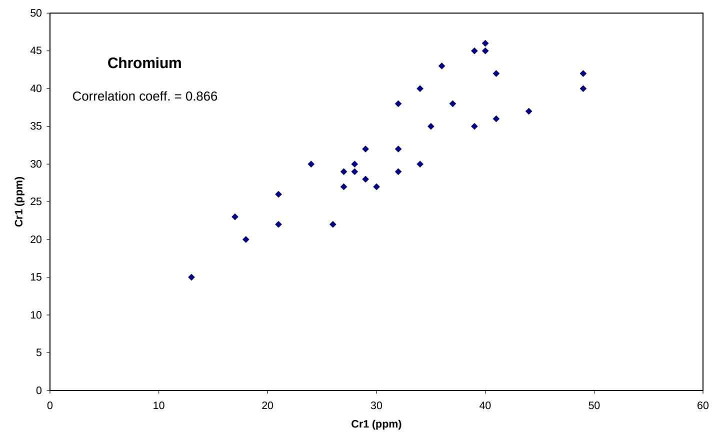

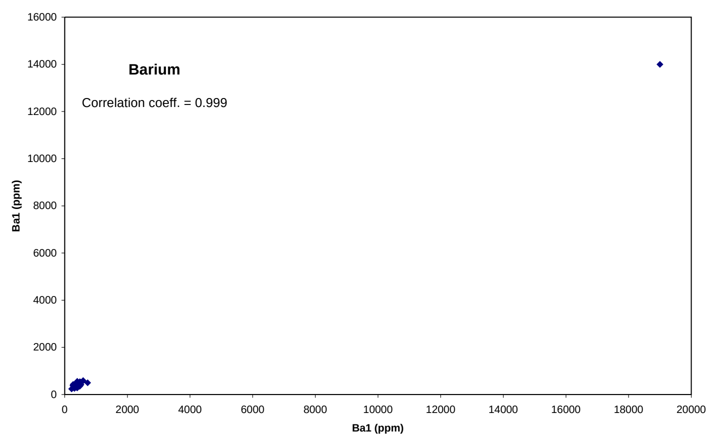

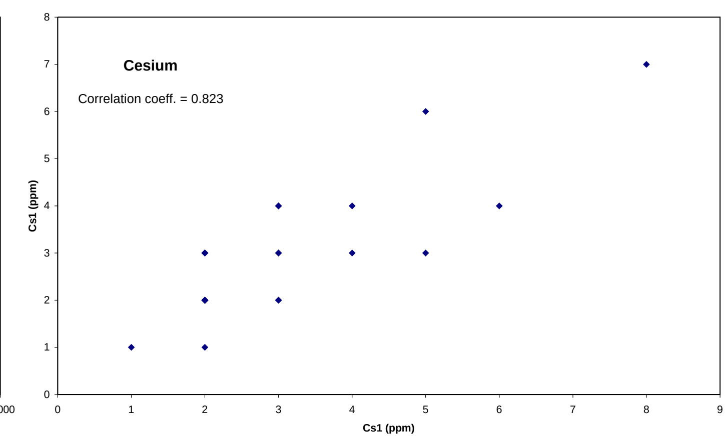

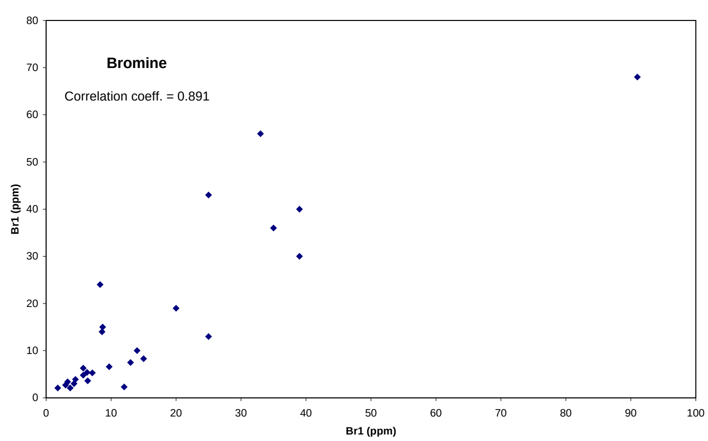

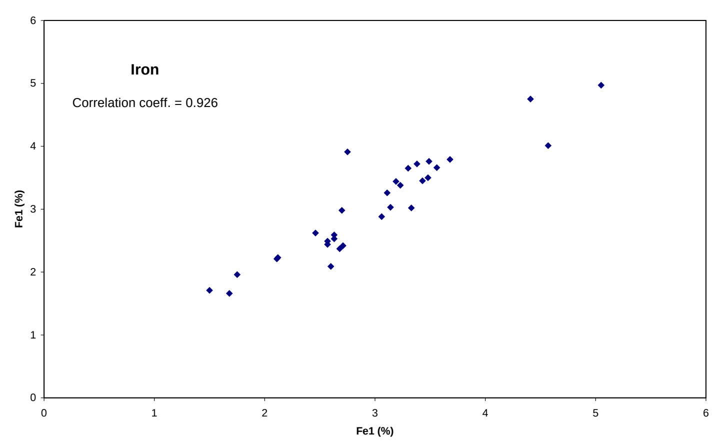

Appendix D: Cont.

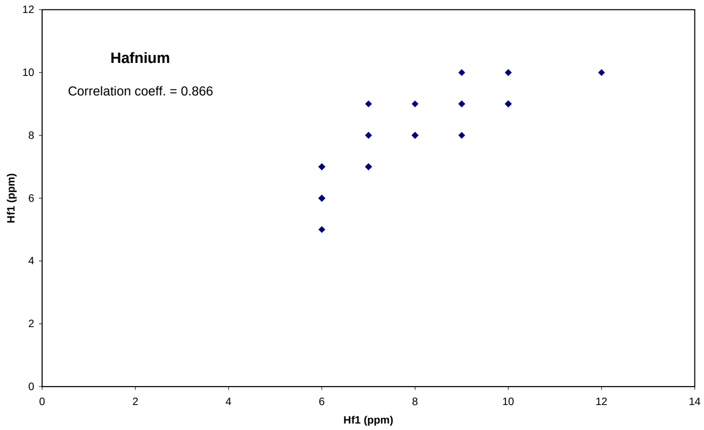

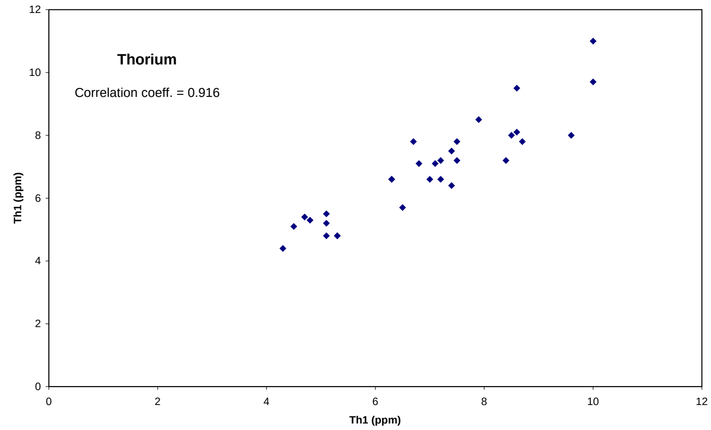

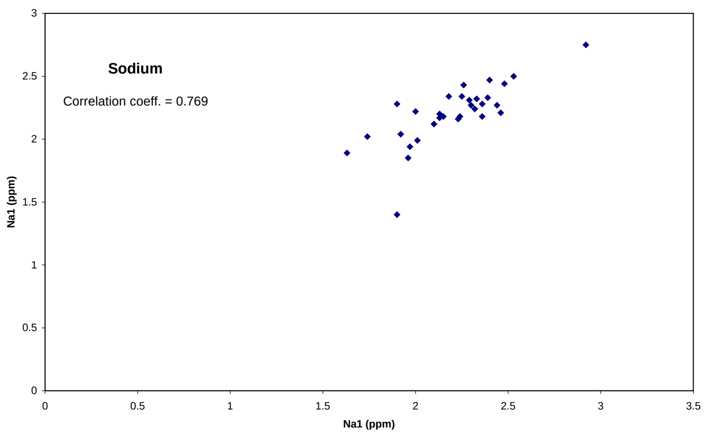

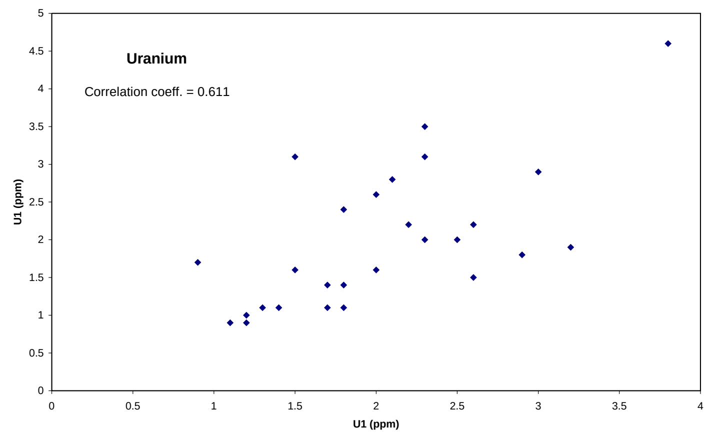

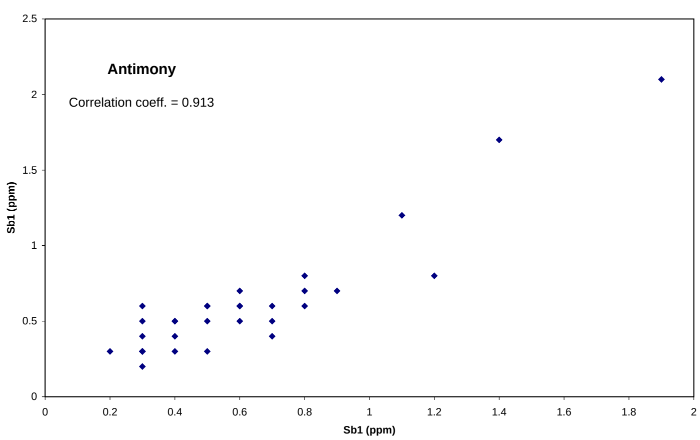

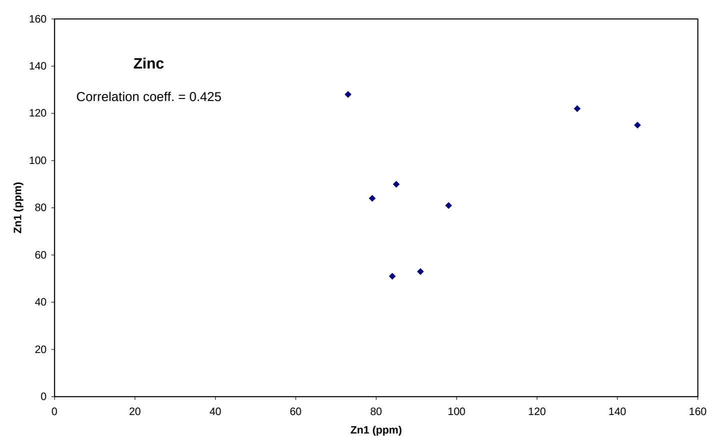

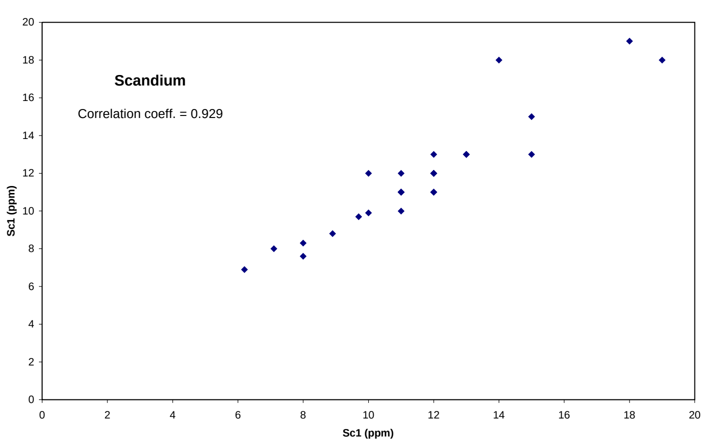

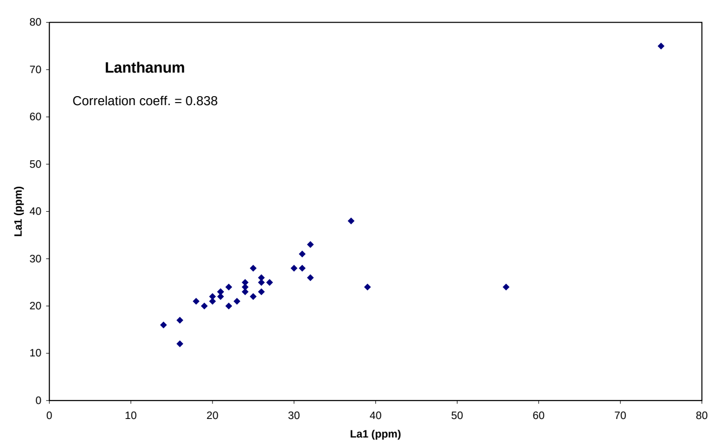

Appendix D: Cont.

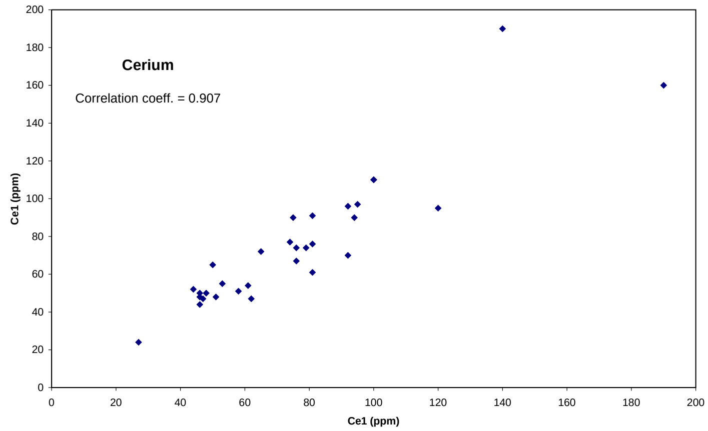

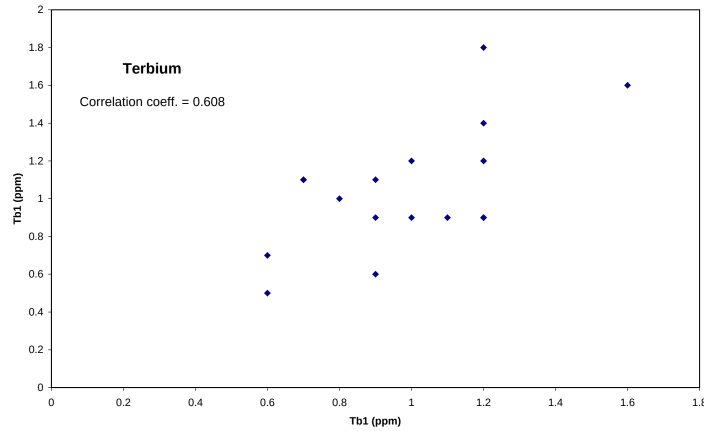

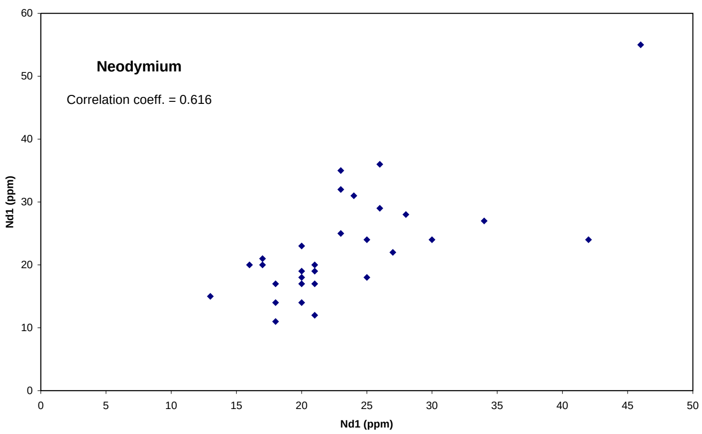

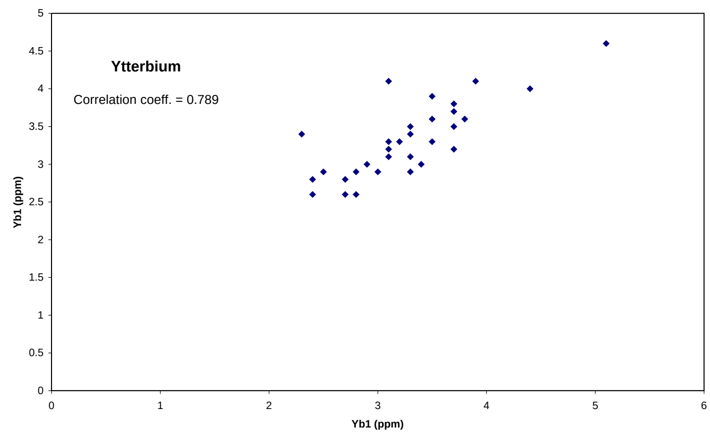

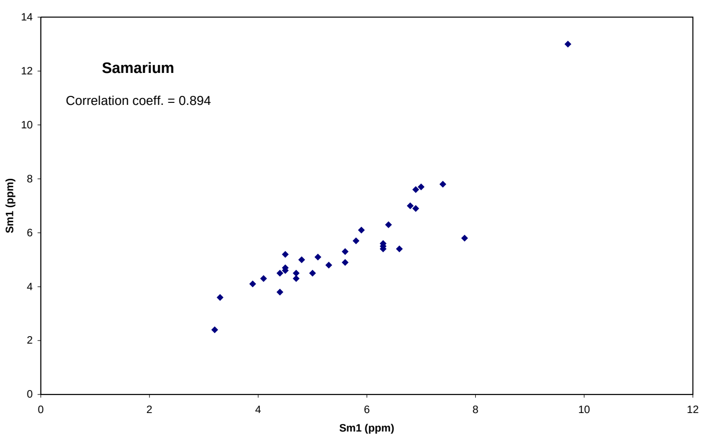

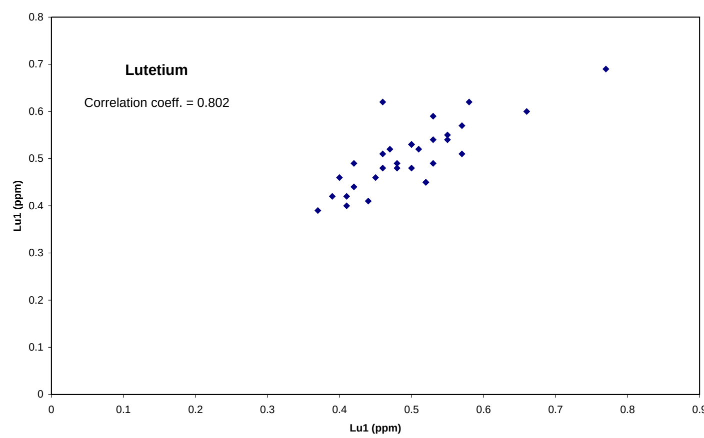

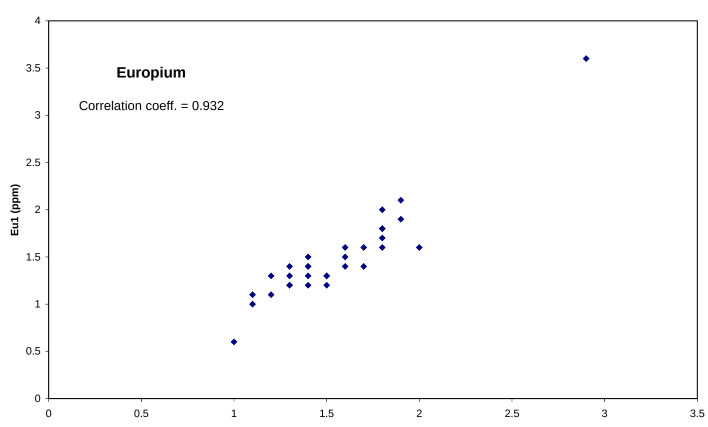

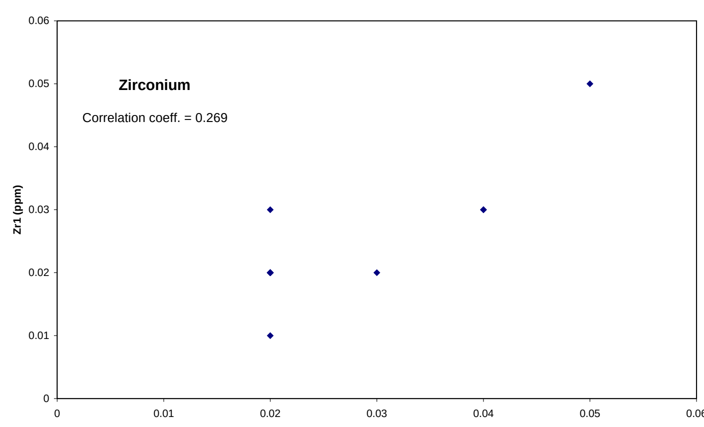

Appendix E: Comparison plots of field duplicates for elements analysed by ICP

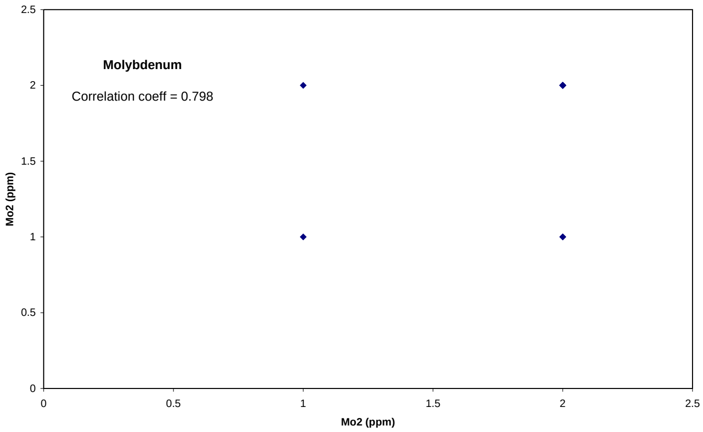

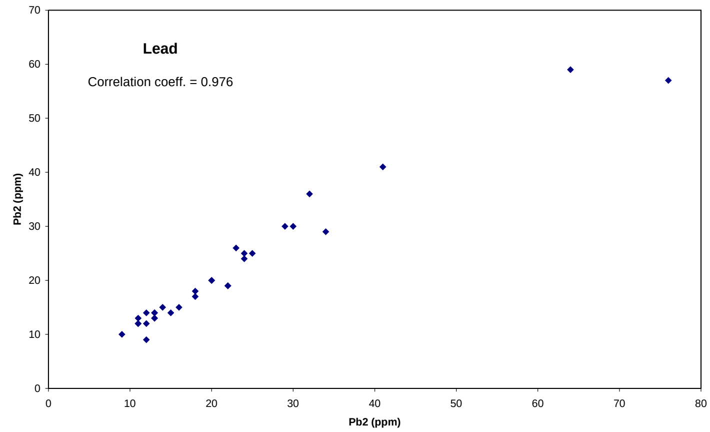

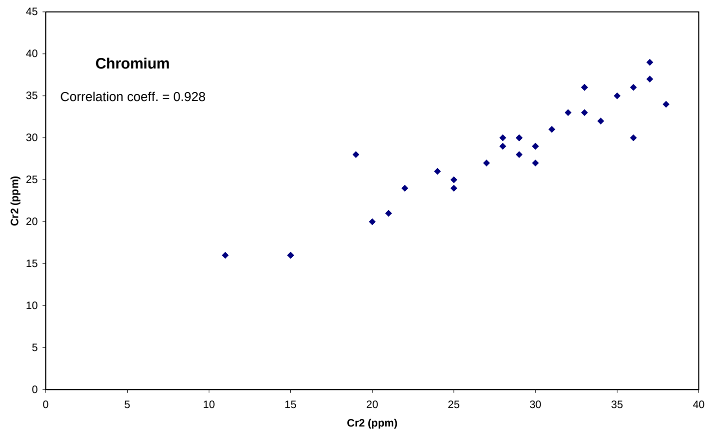

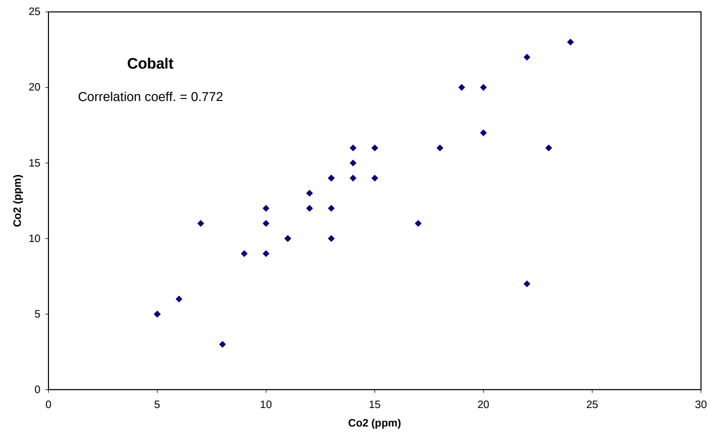

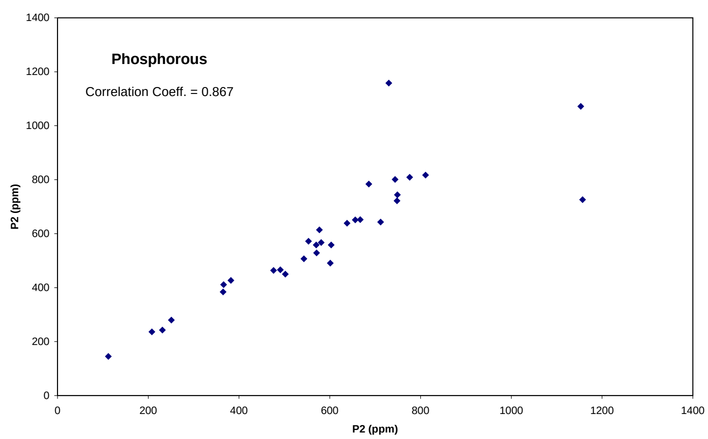

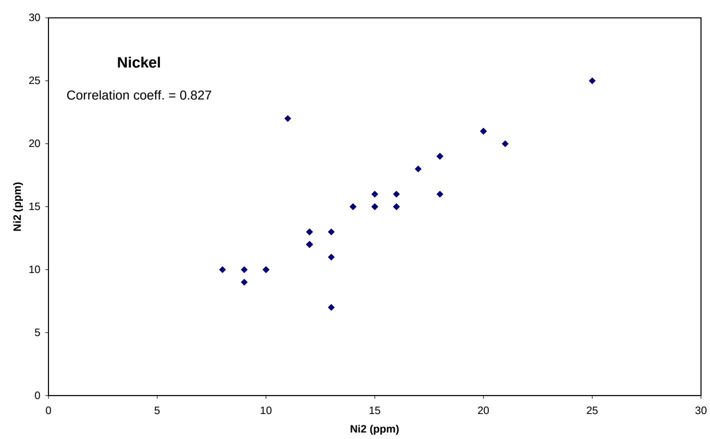

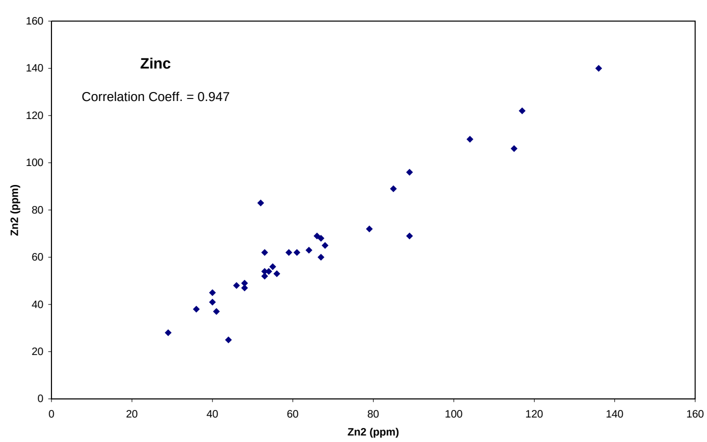

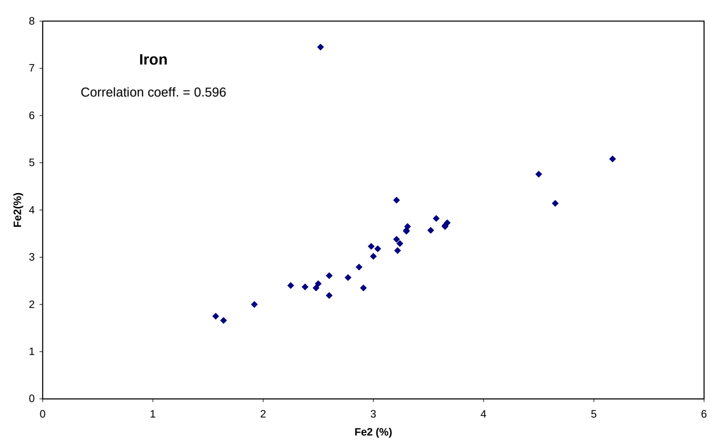

Appendix E: Cont.

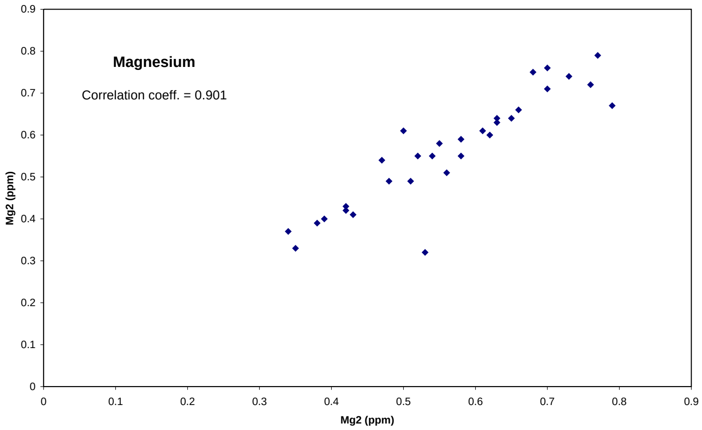

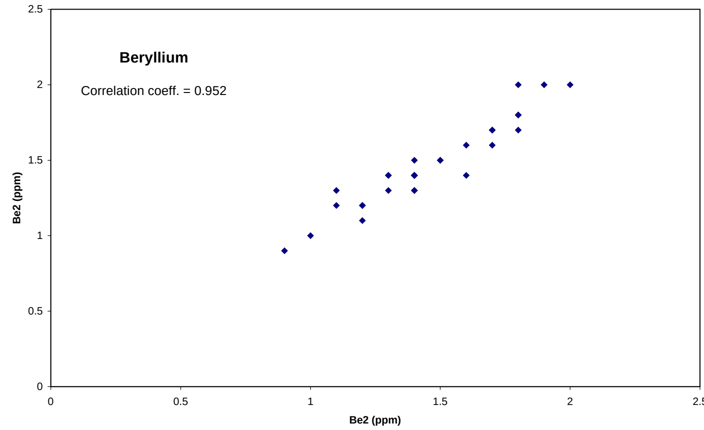

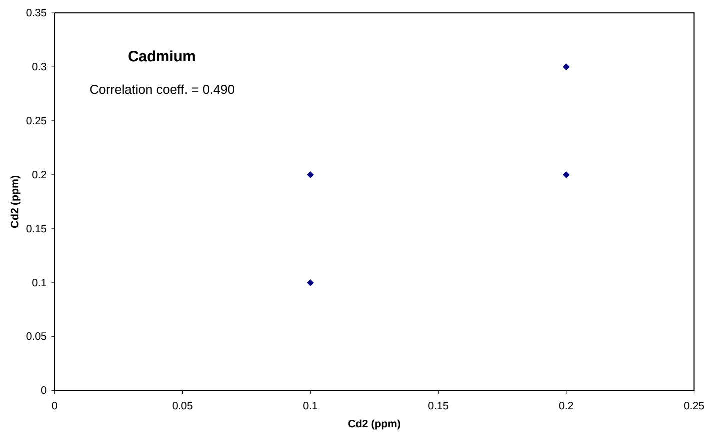

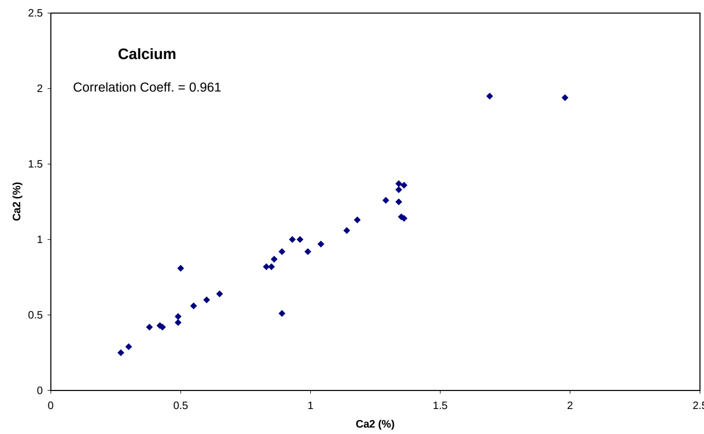

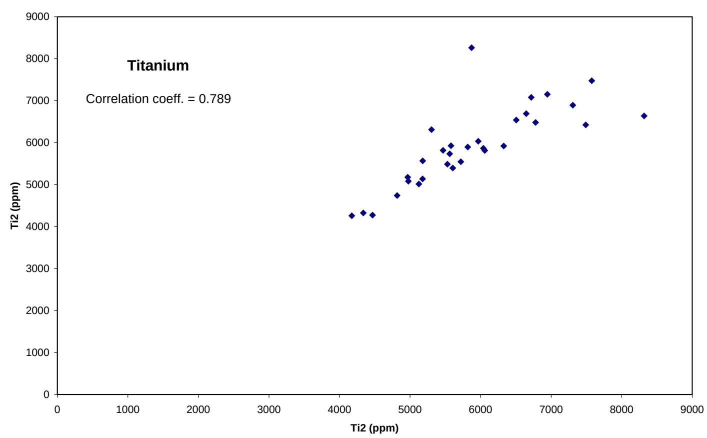

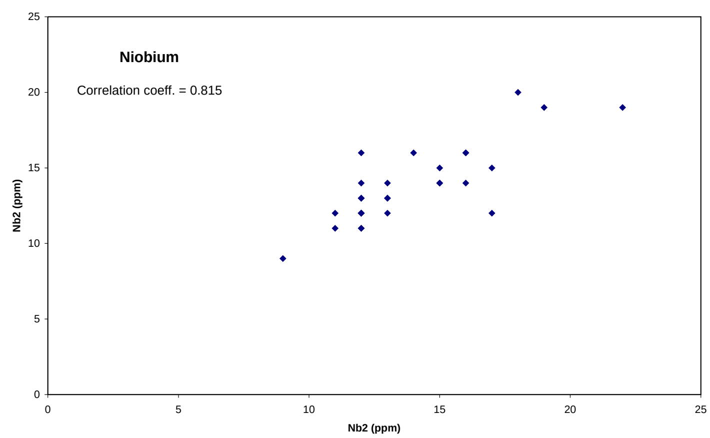

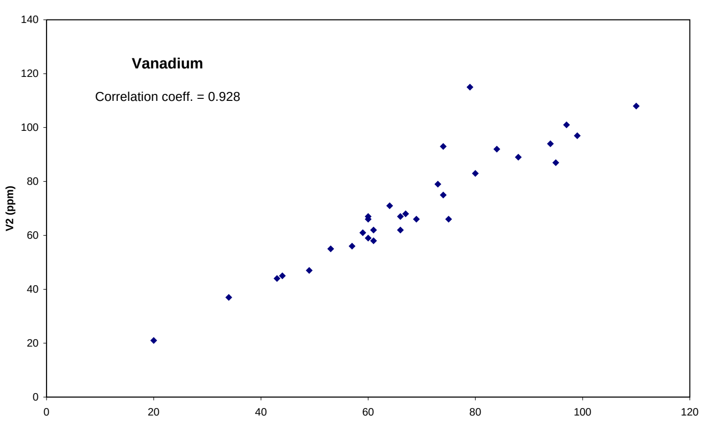

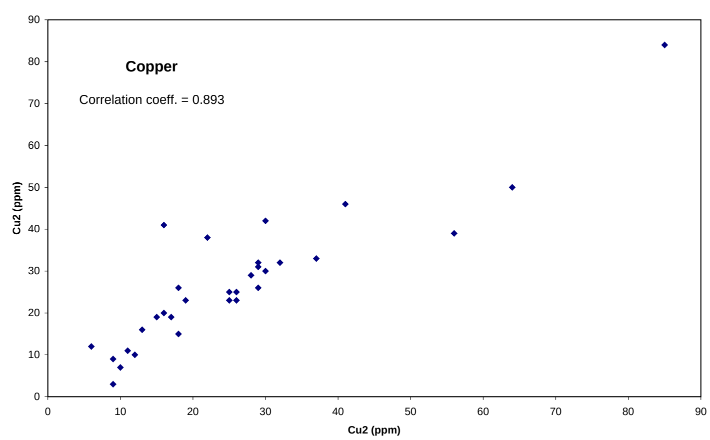

Appendix E: Cont.

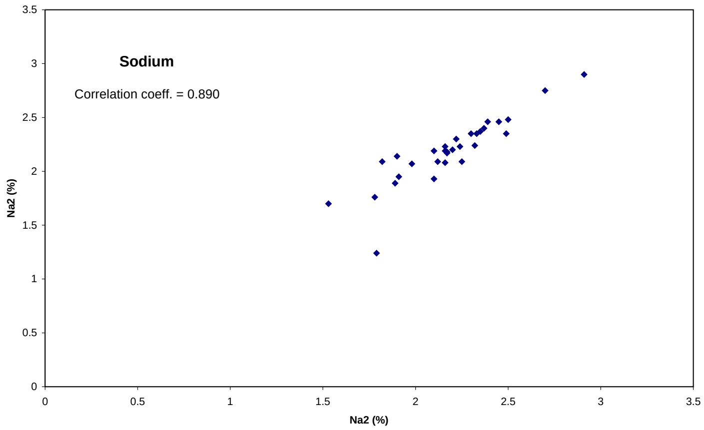

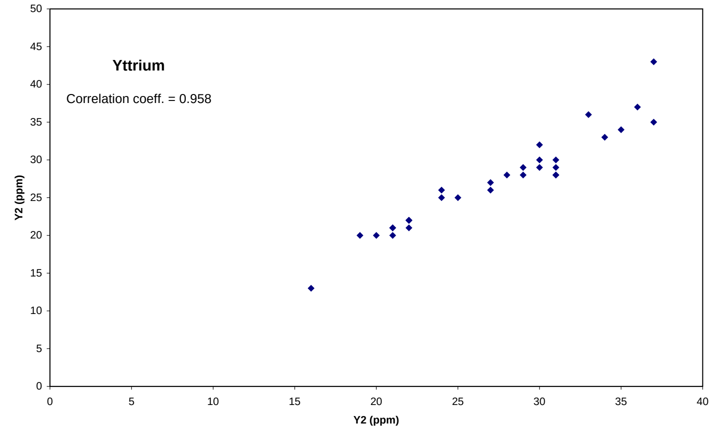

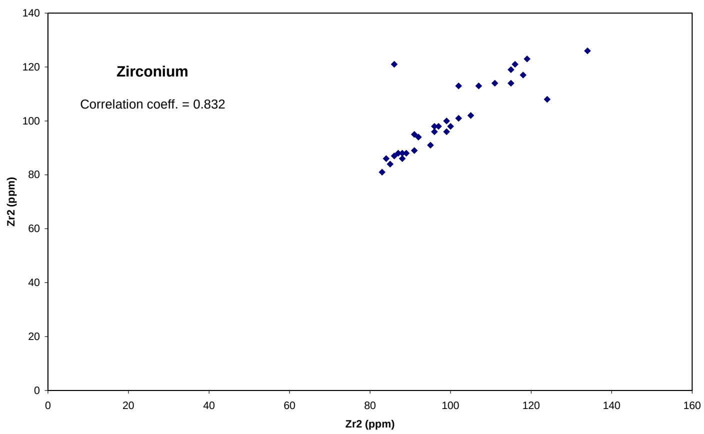

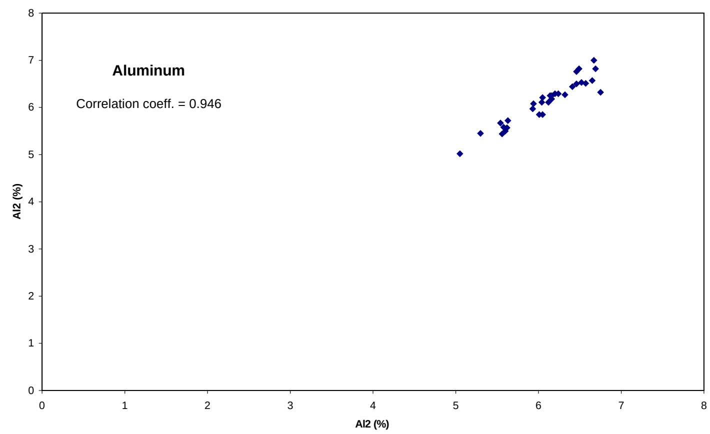

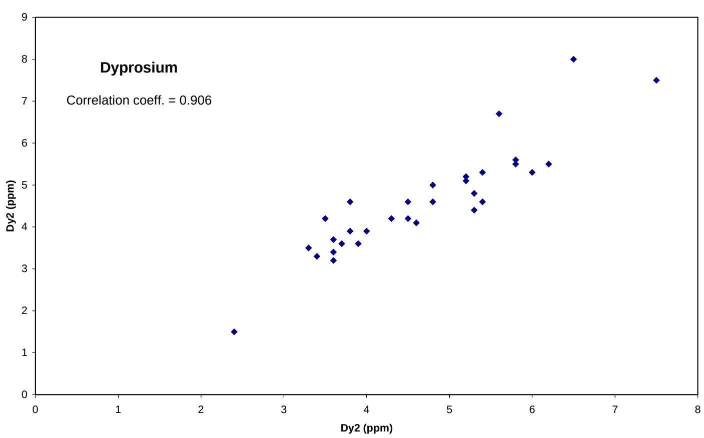

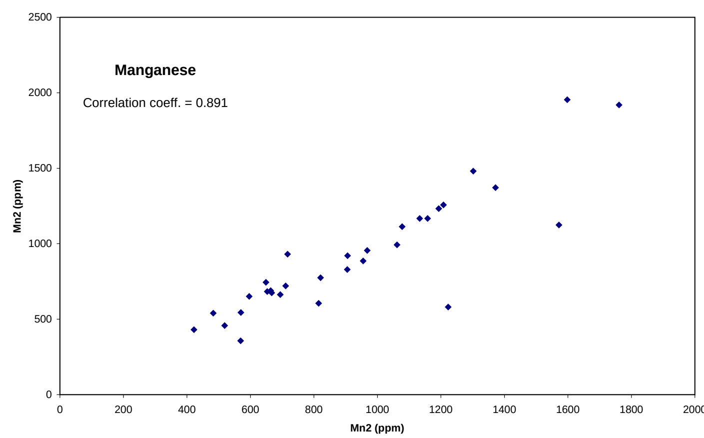

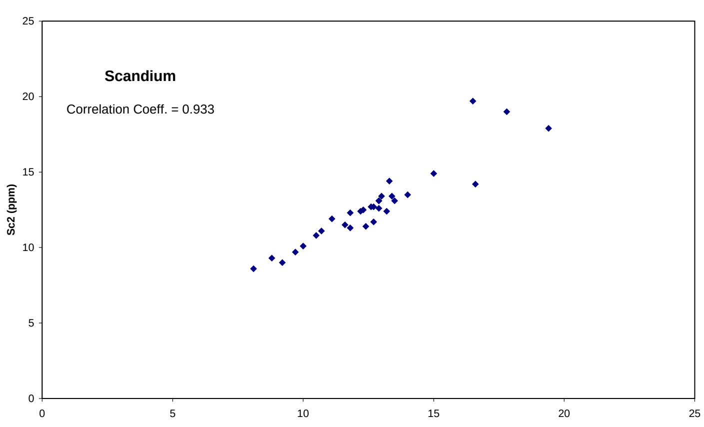

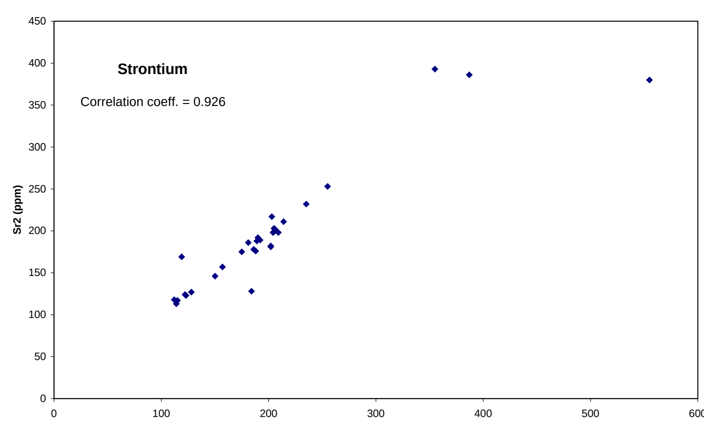

Appendix E: Cont.

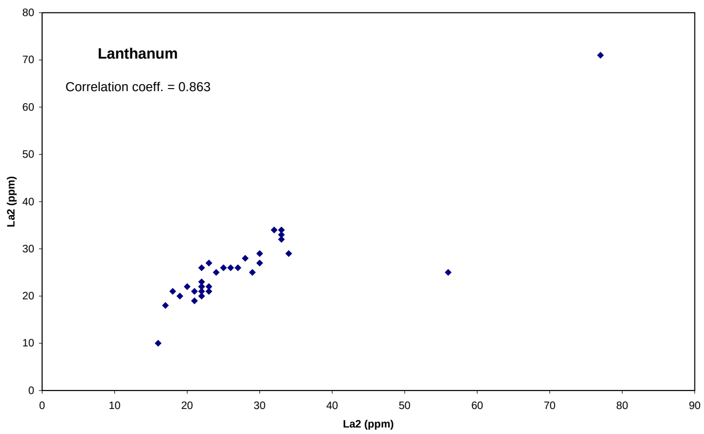

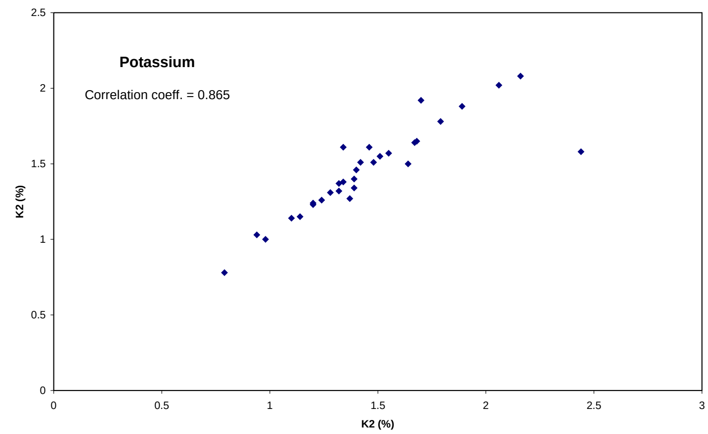

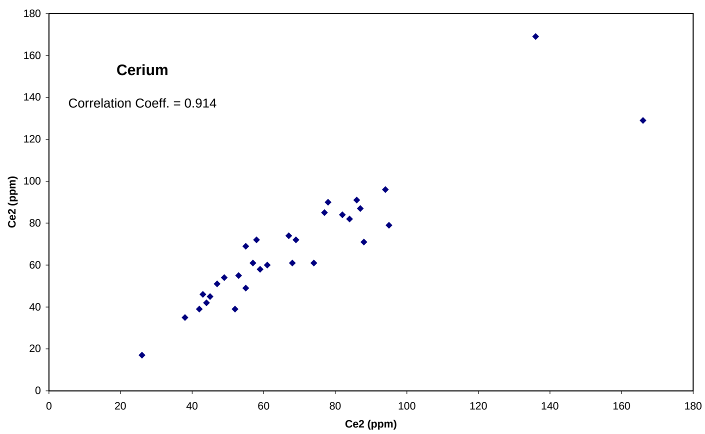

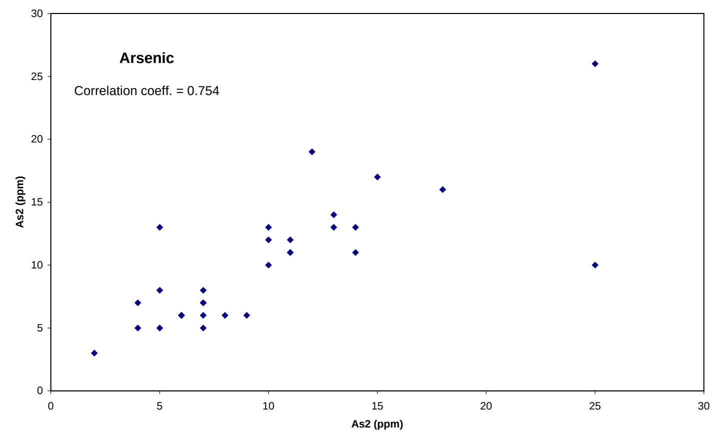

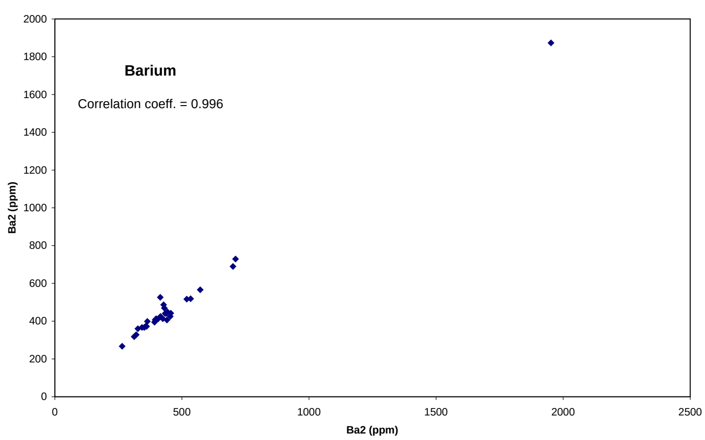

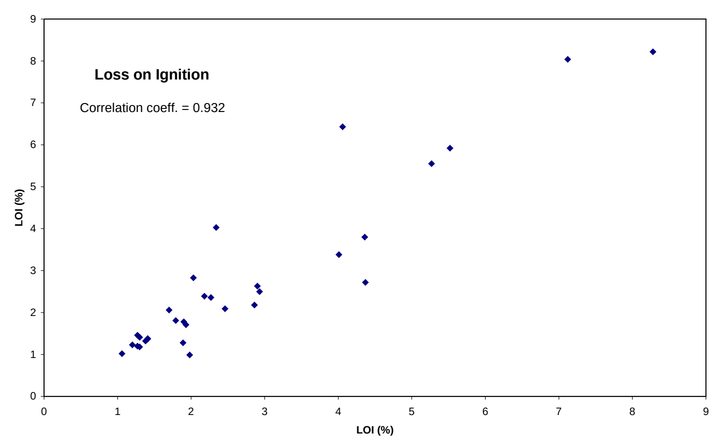

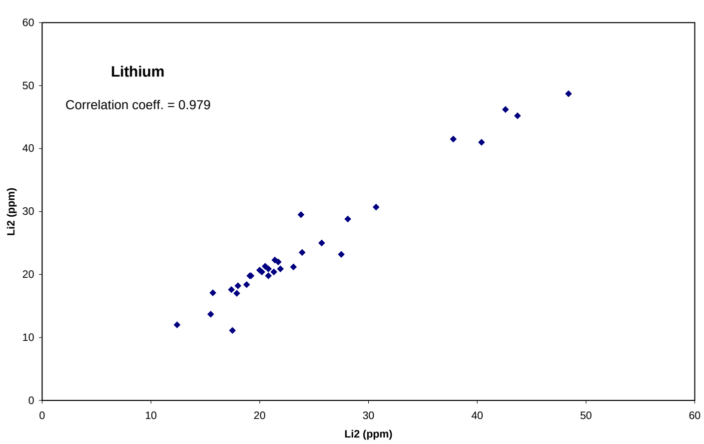

Appendix F:

List of Figures not included in text, but available on request.

Figure 18. Distribution of Aluminum in till

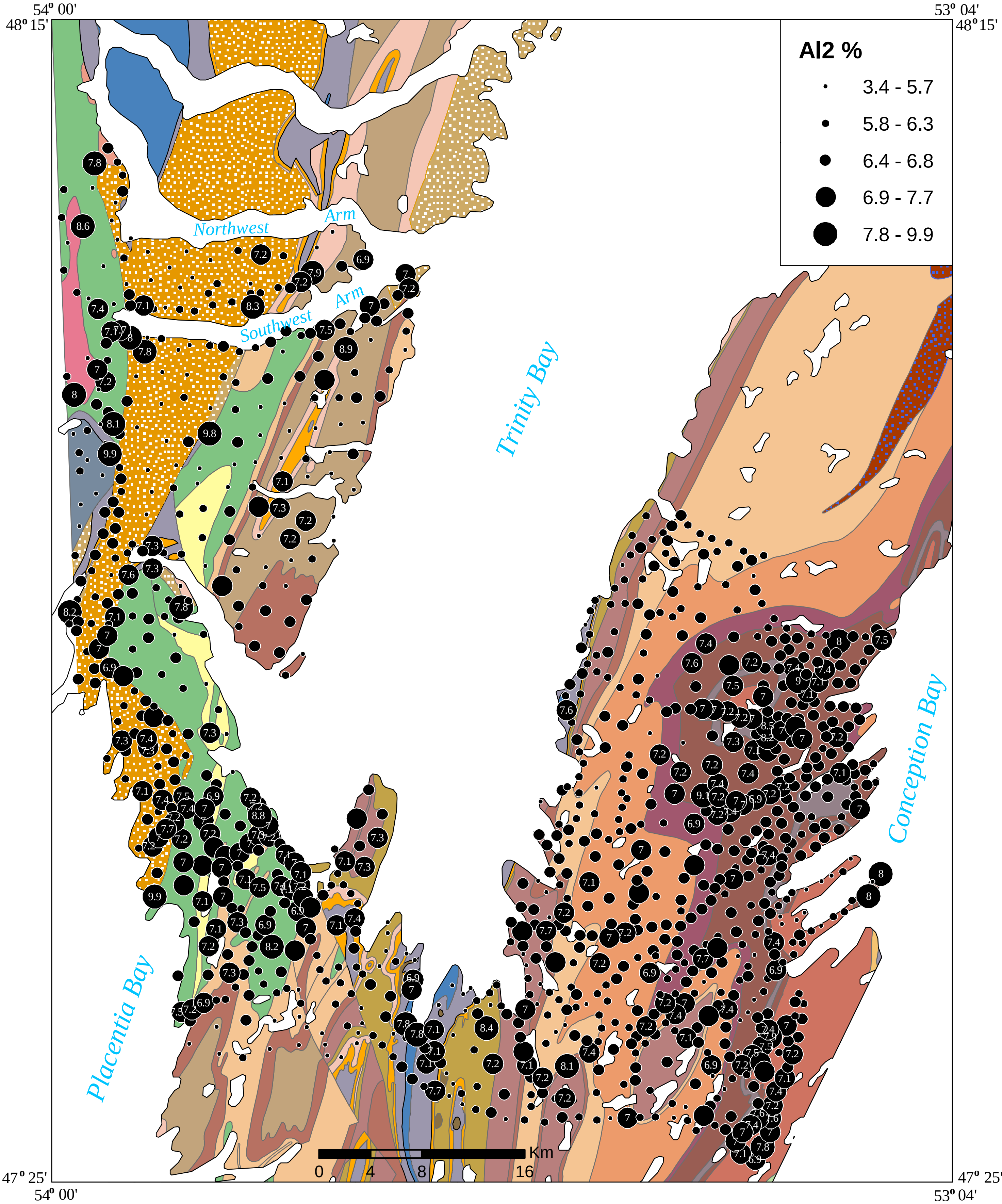

Open File NFLD 2824

Figure 19. Distribution of Beryllium in till

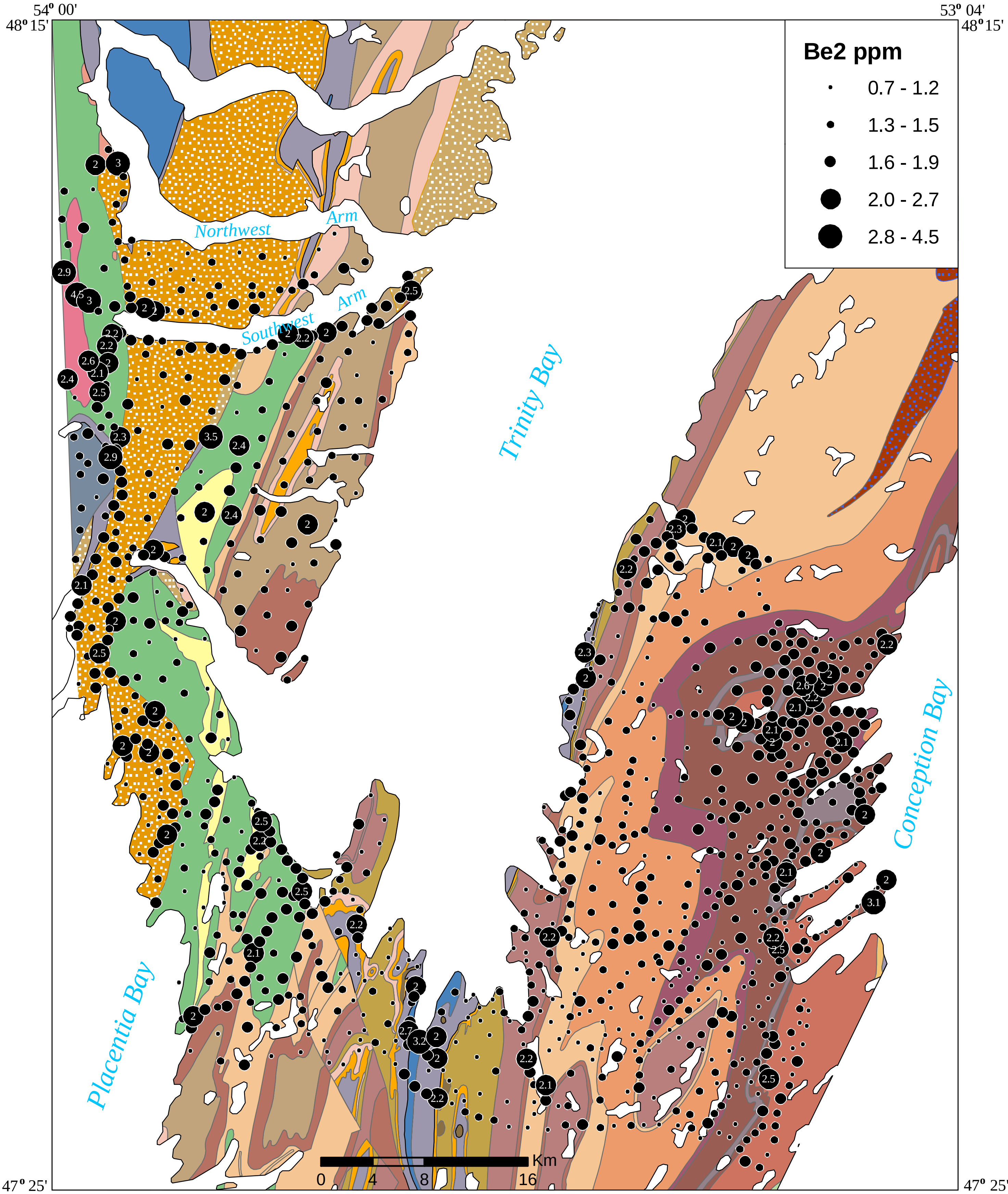

Open File NFLD 2824

Figure 20. Distribution of Bromine in till

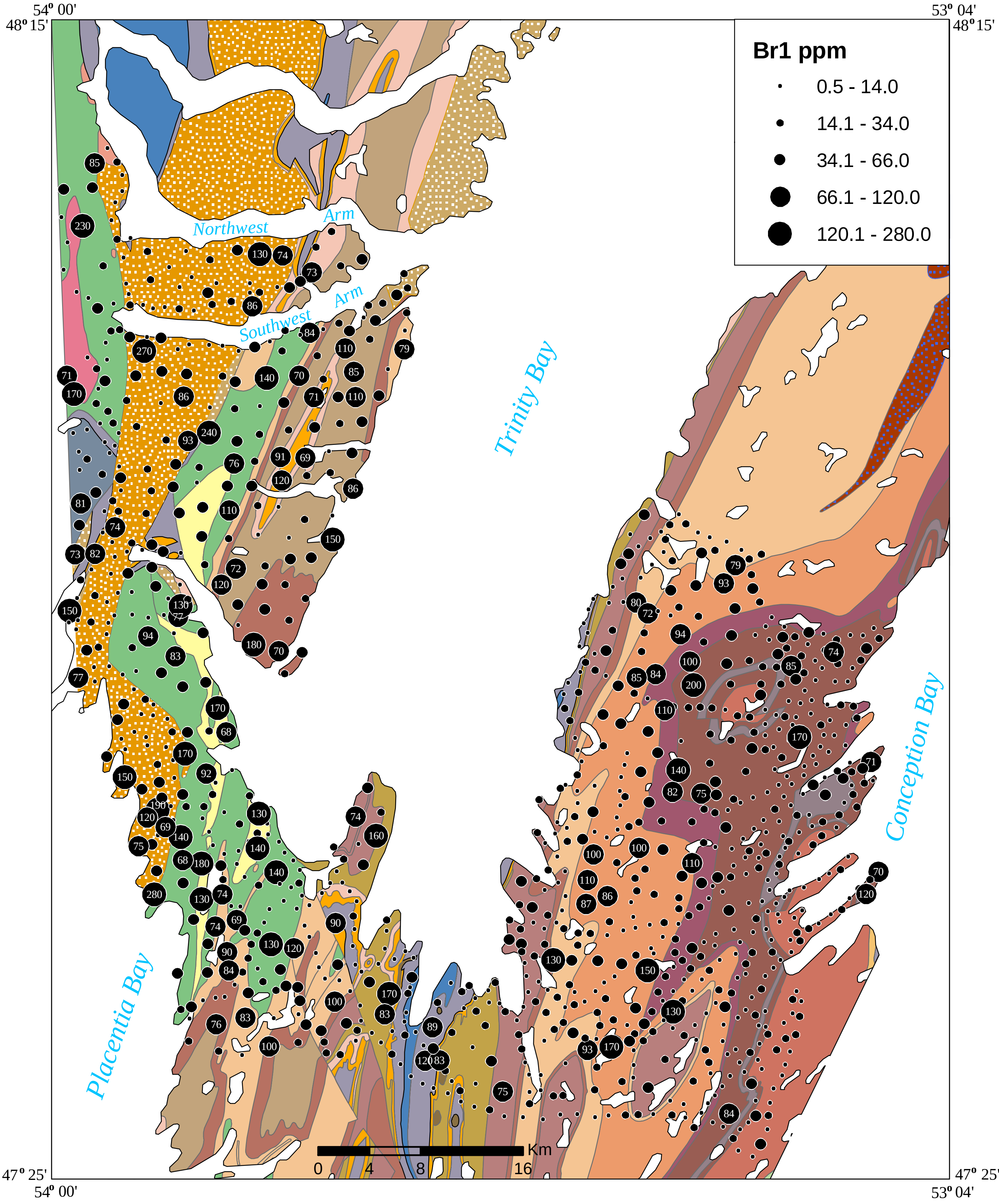

Open File NFLD 2824

Figure 21. Distribution of Calcium in till

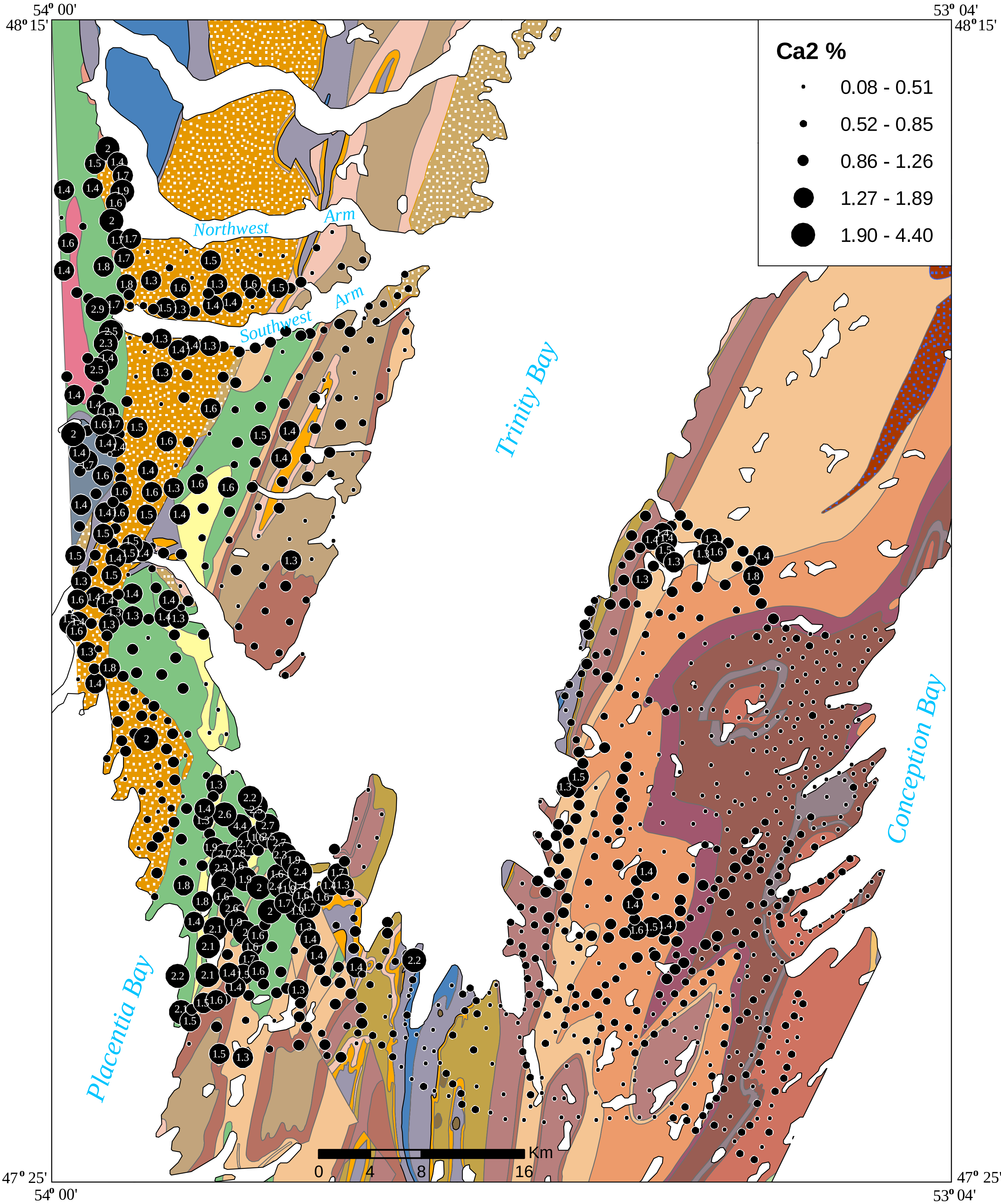

Open File NFLD 2824

Figure 22. Distribution of Cadmium in till

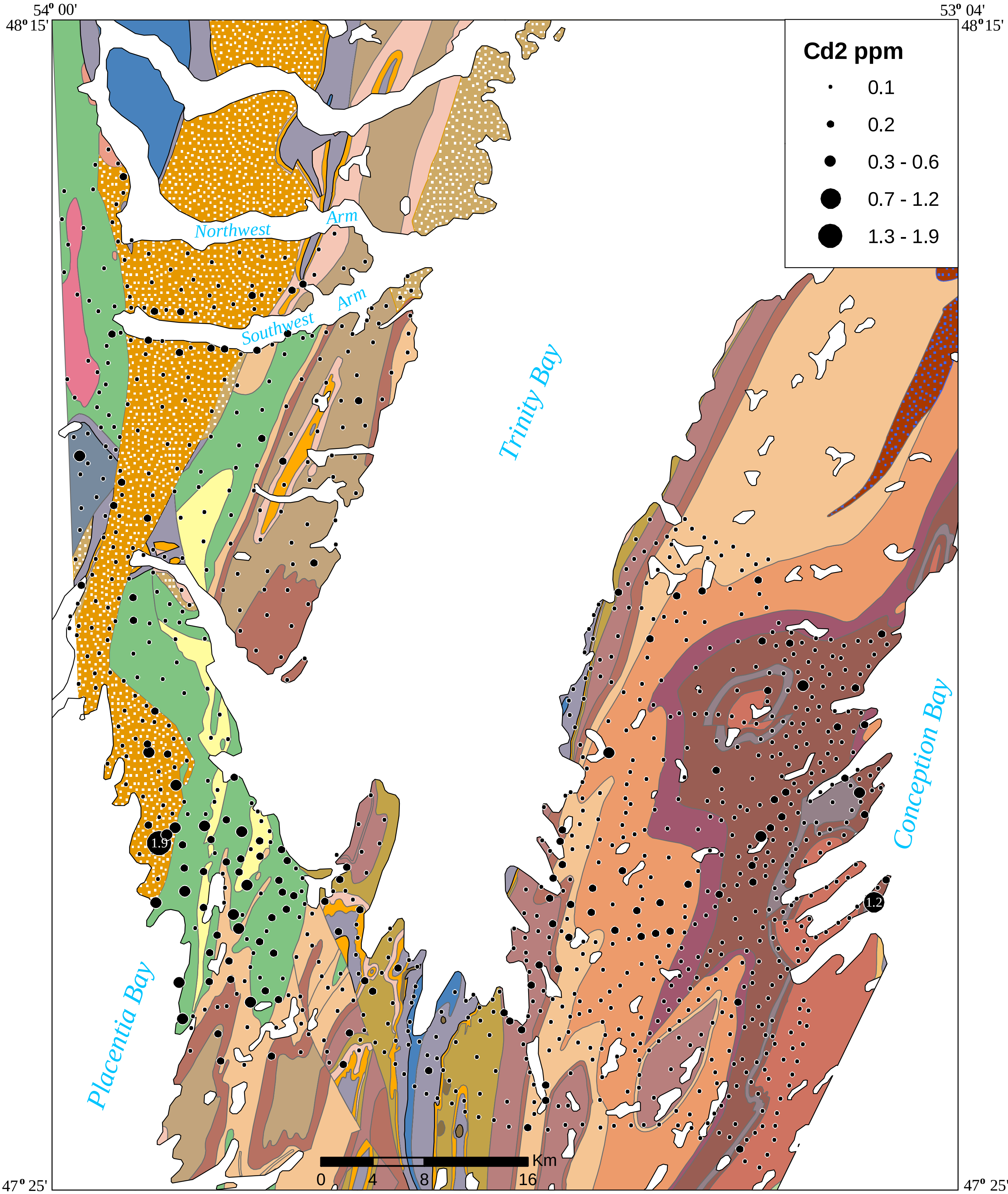

Open File NFLD 2824

Figure 23. Distribution of Cerium in till

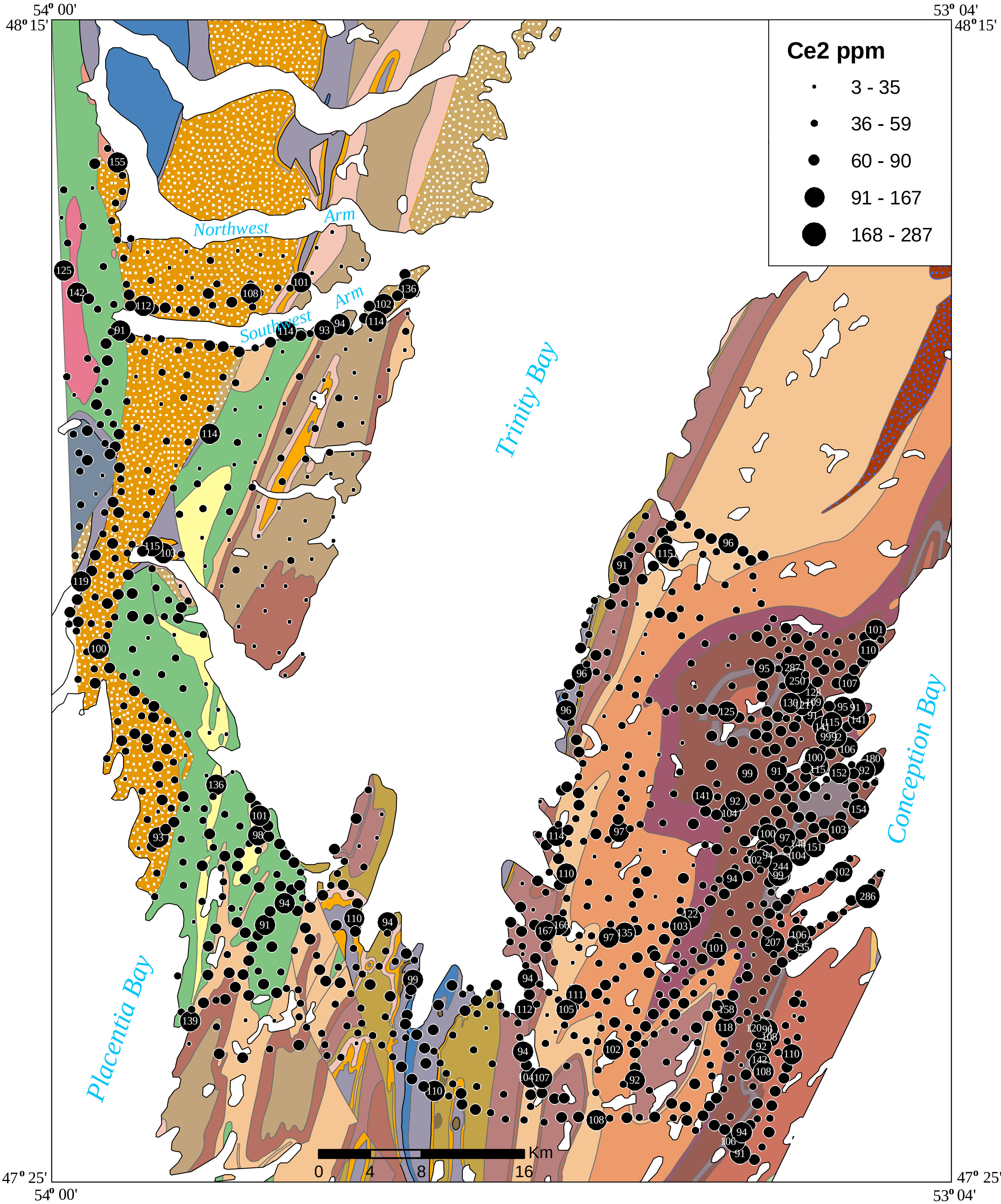

Open File NFLD 2824

Figure 24. Distribution of Cobalt in till

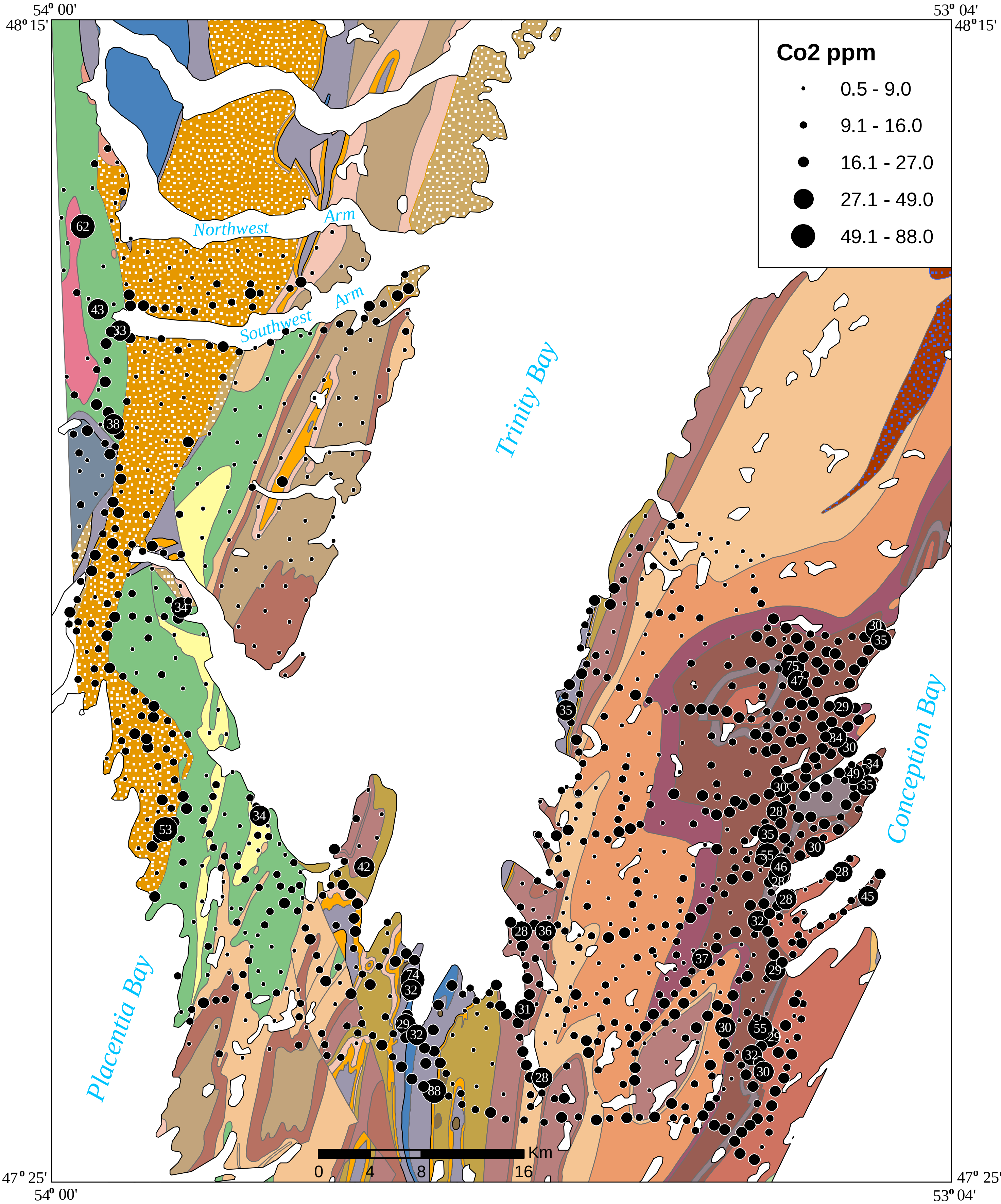

Open File NFLD 2824

Figure 25. Distribution of Cesium in till

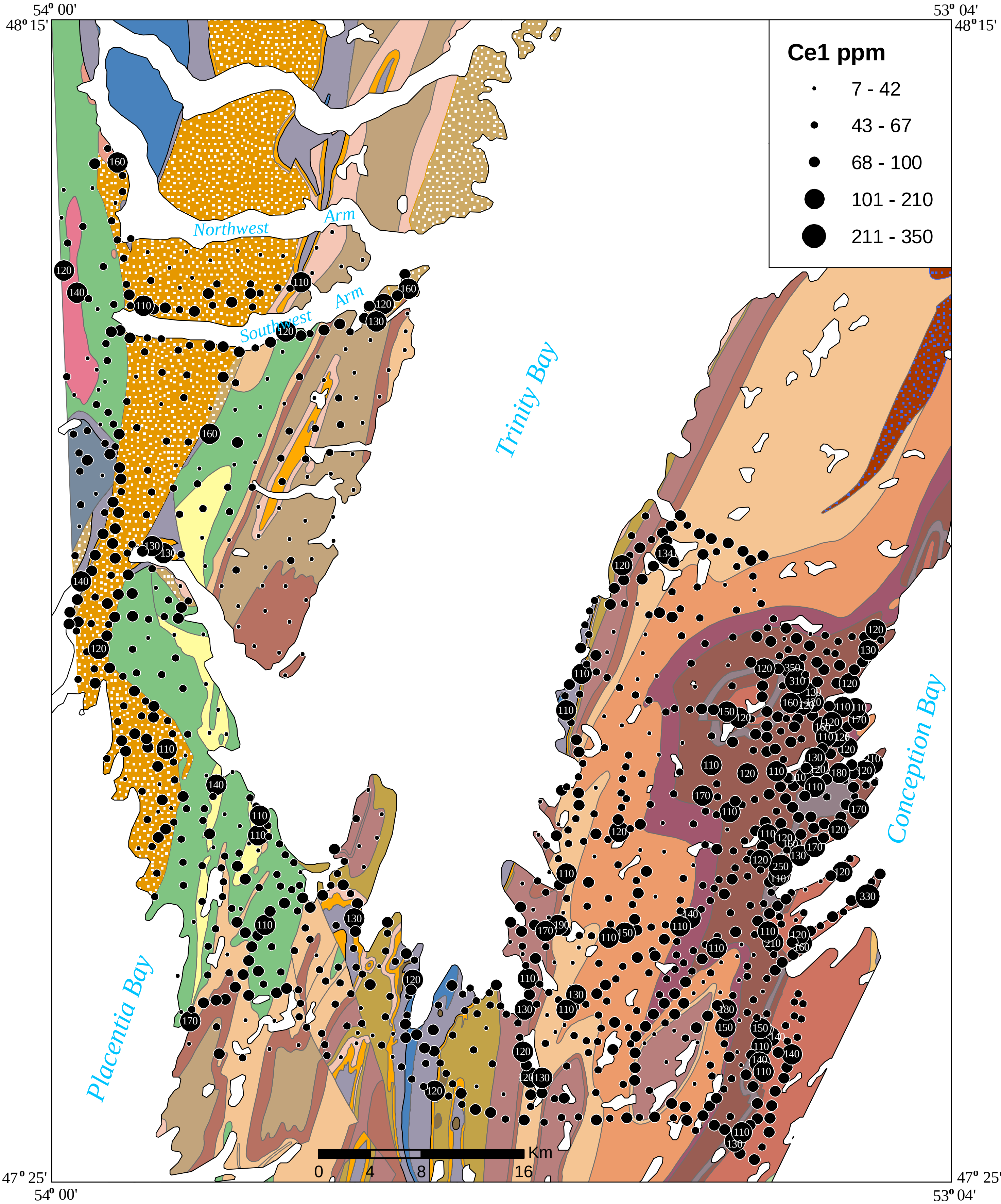

Open File NFLD 2824

Figure 26. Distribution of Dysprosium in till

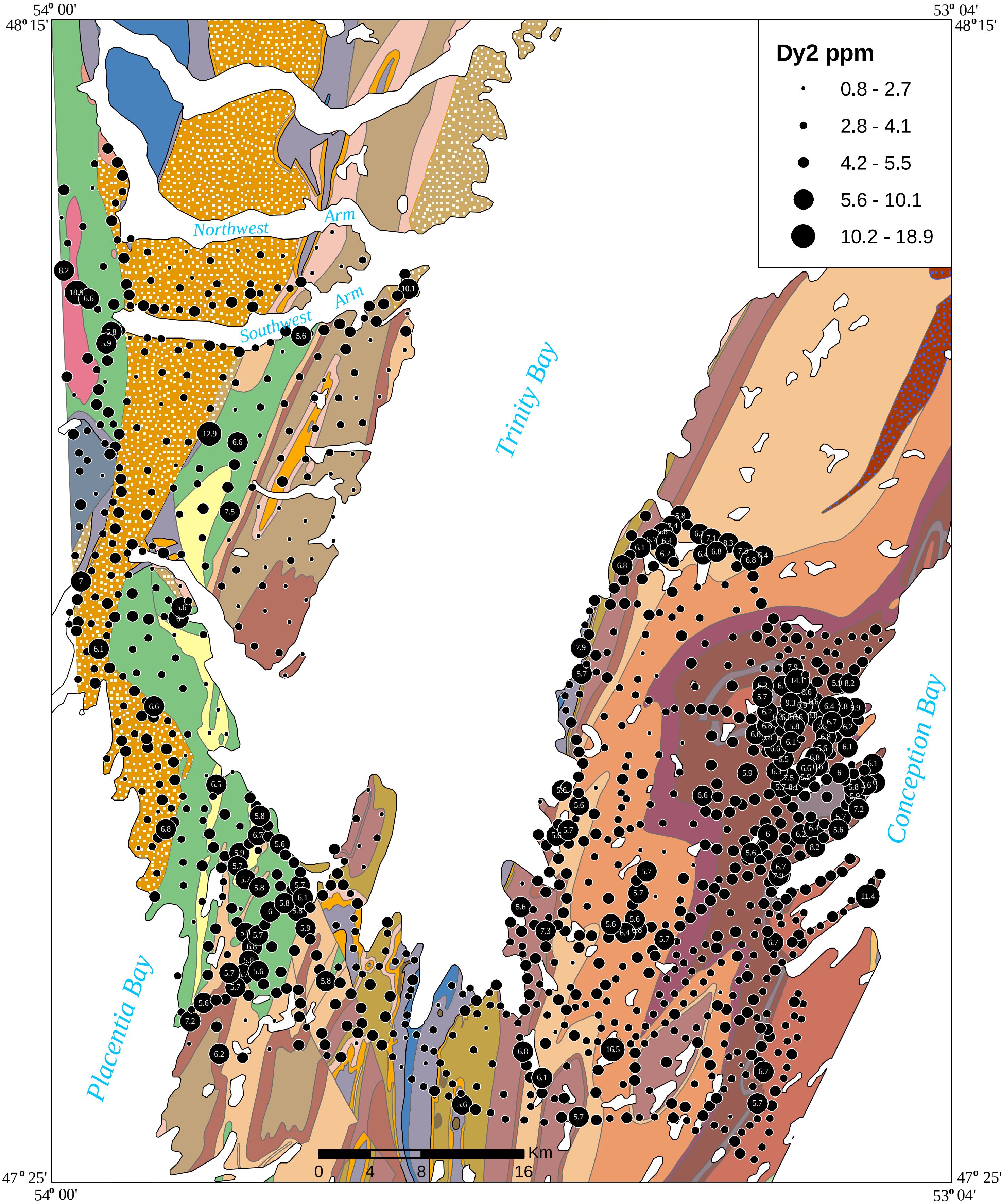

Open File NFLD 2824

Figure 27. Distribution of Europium in till

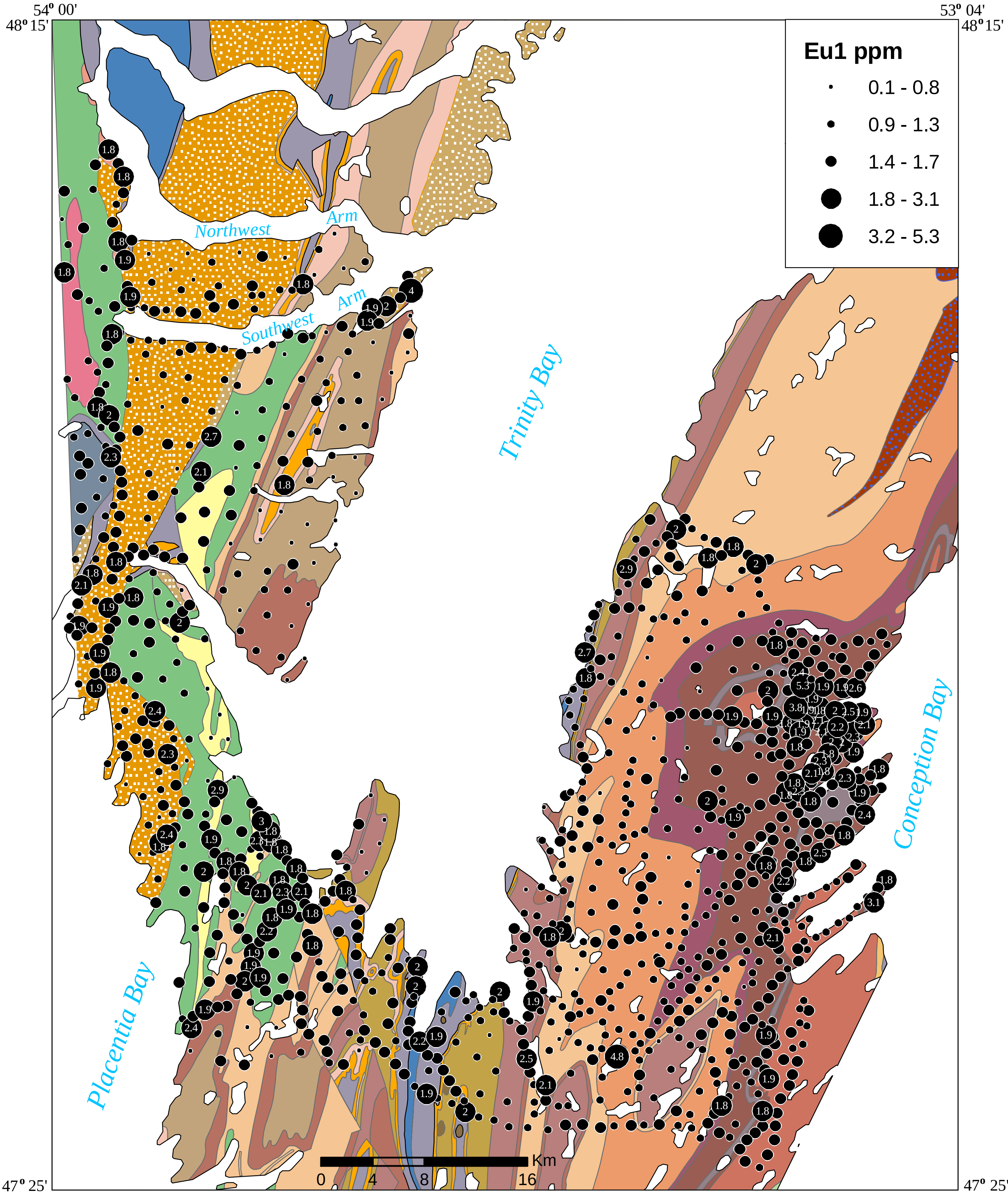

Open File NFLD 2824

Figure 28. Distribution of Iron in till

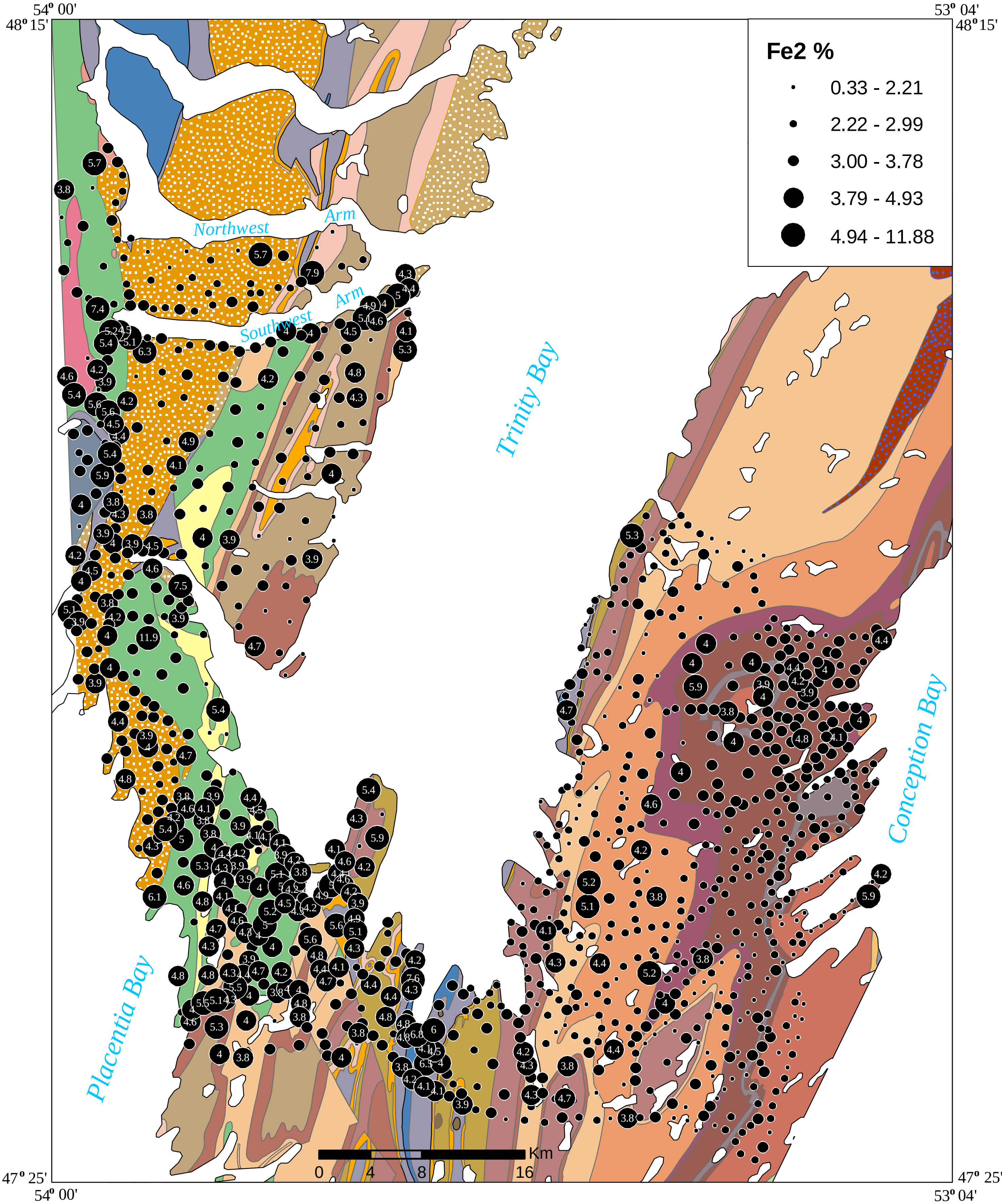

Open File NFLD 2824

Figure 29. Distribution of Hafnium in till

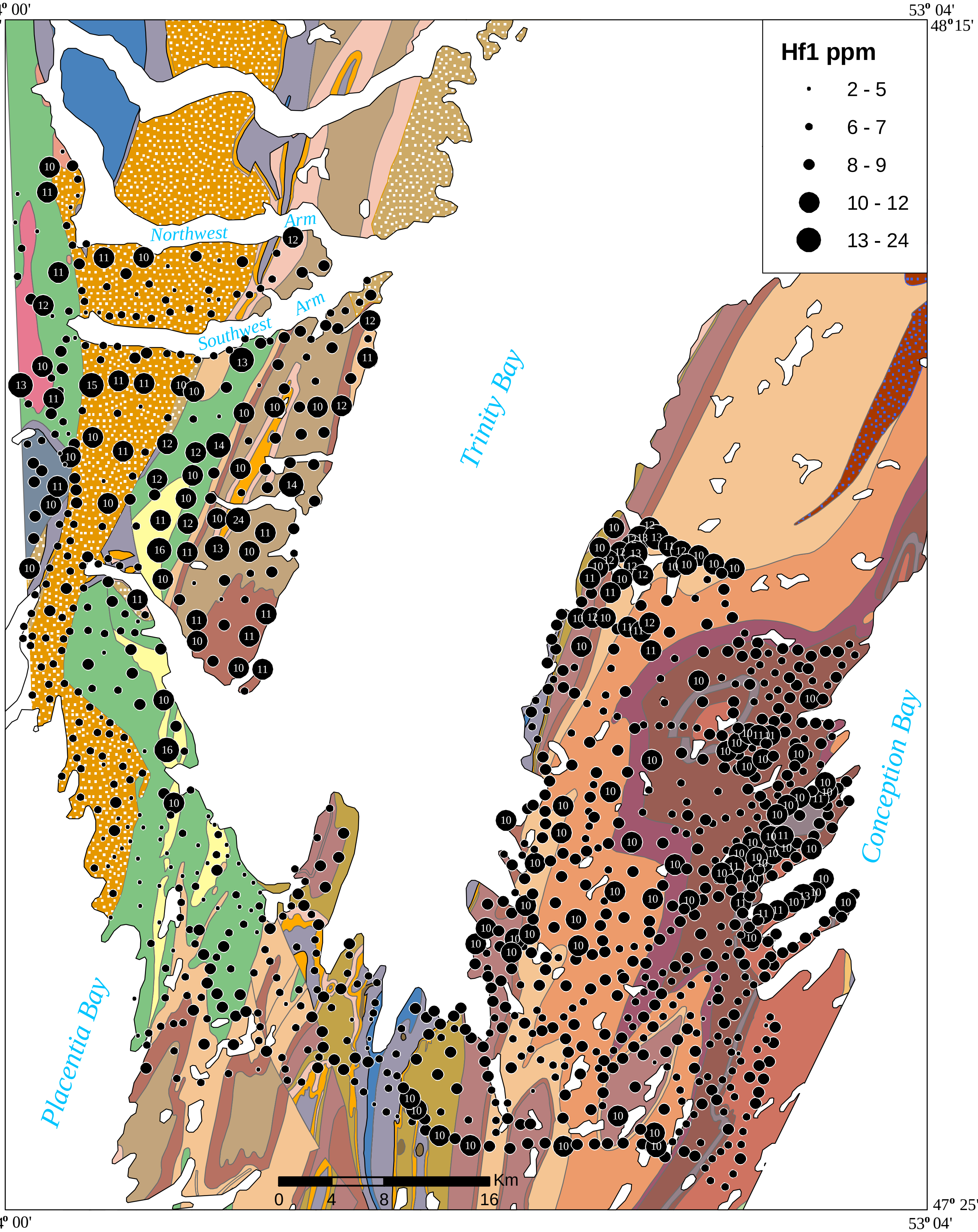

Open File NFLD 2824

Figure 30. Distribution of Mercury in till

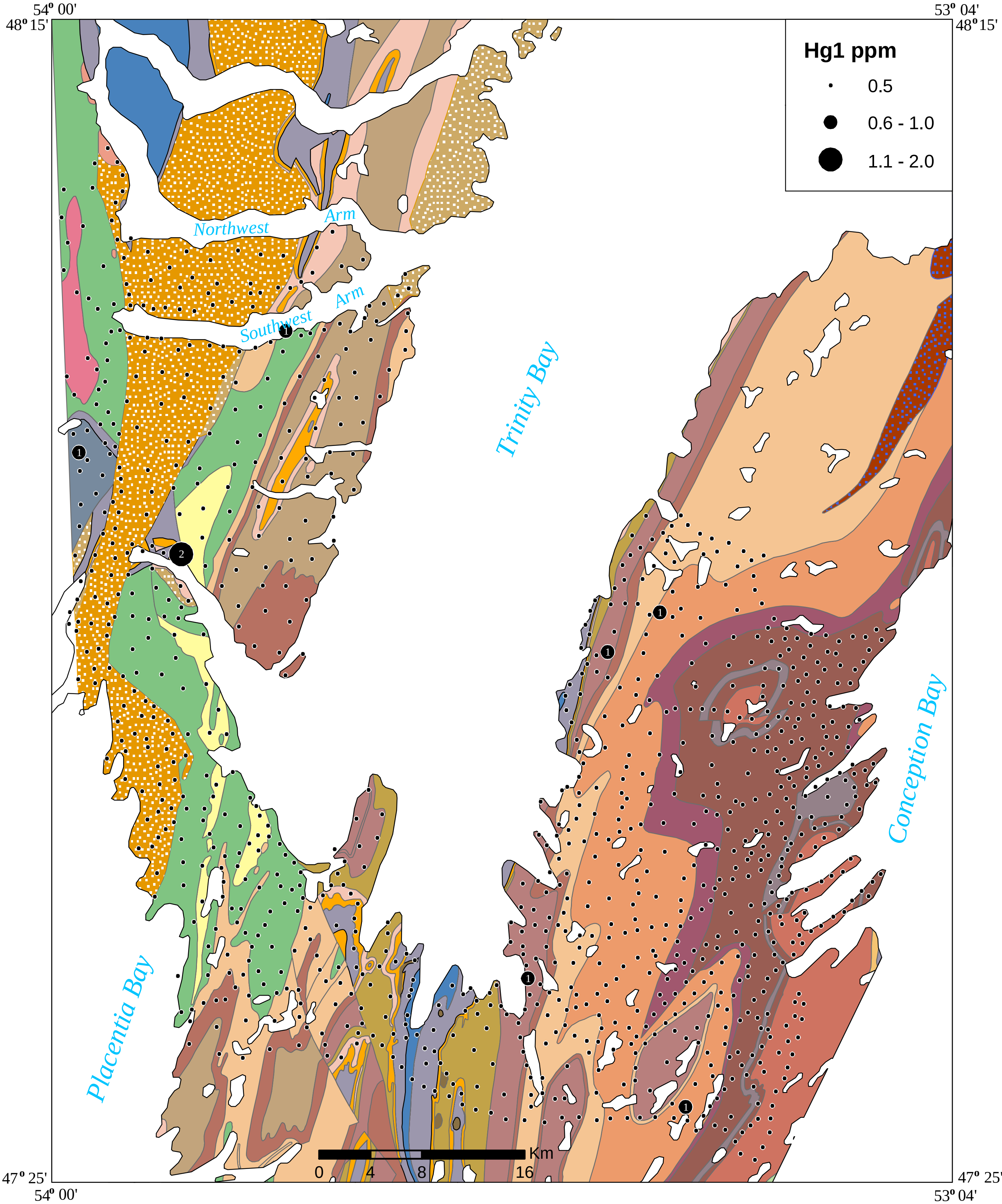

Open File NFLD 2824

Figure 31. Distribution of Iridium in till

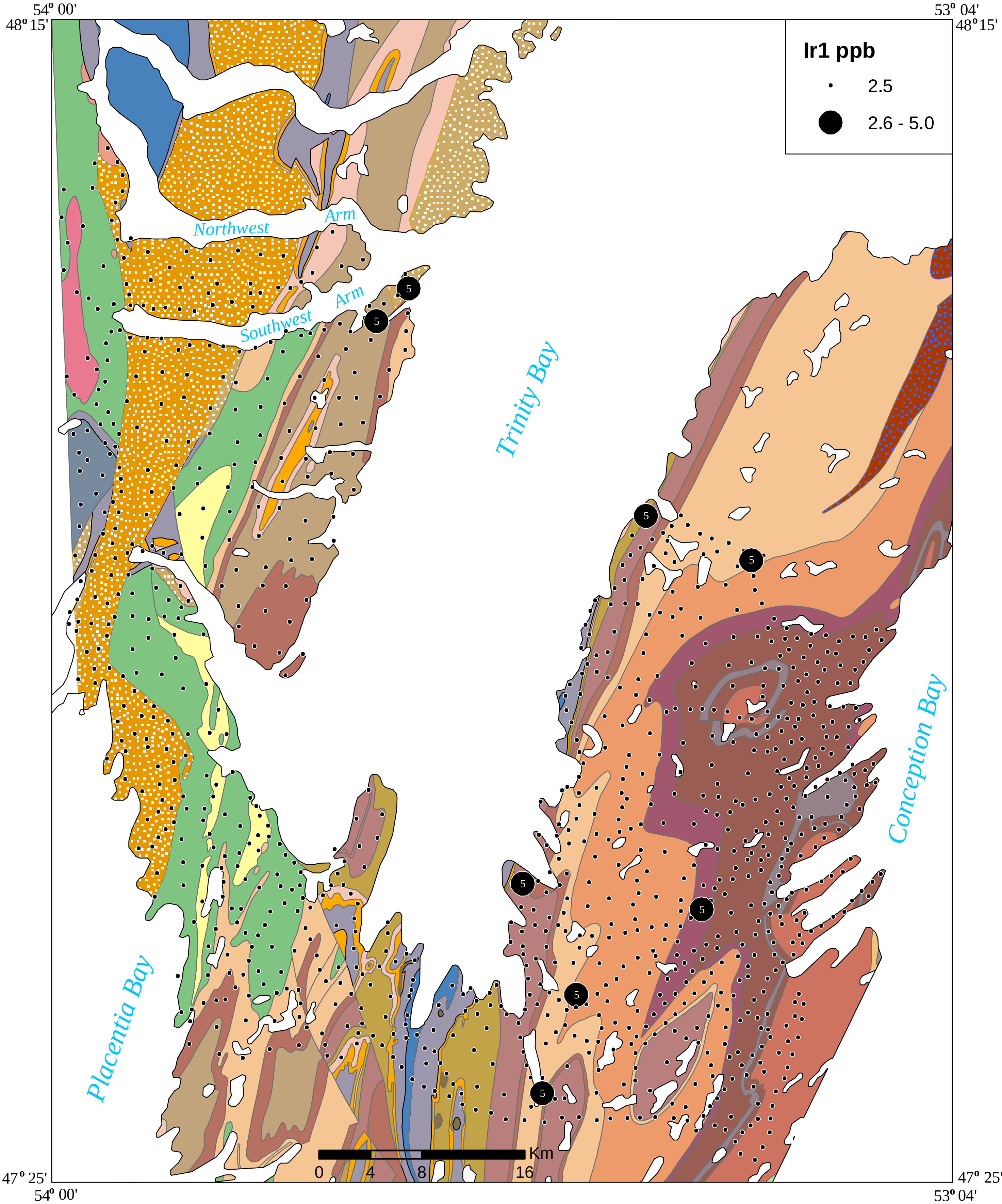

Open File NFLD 2824

Figure 32. Distribution of Potassium in till

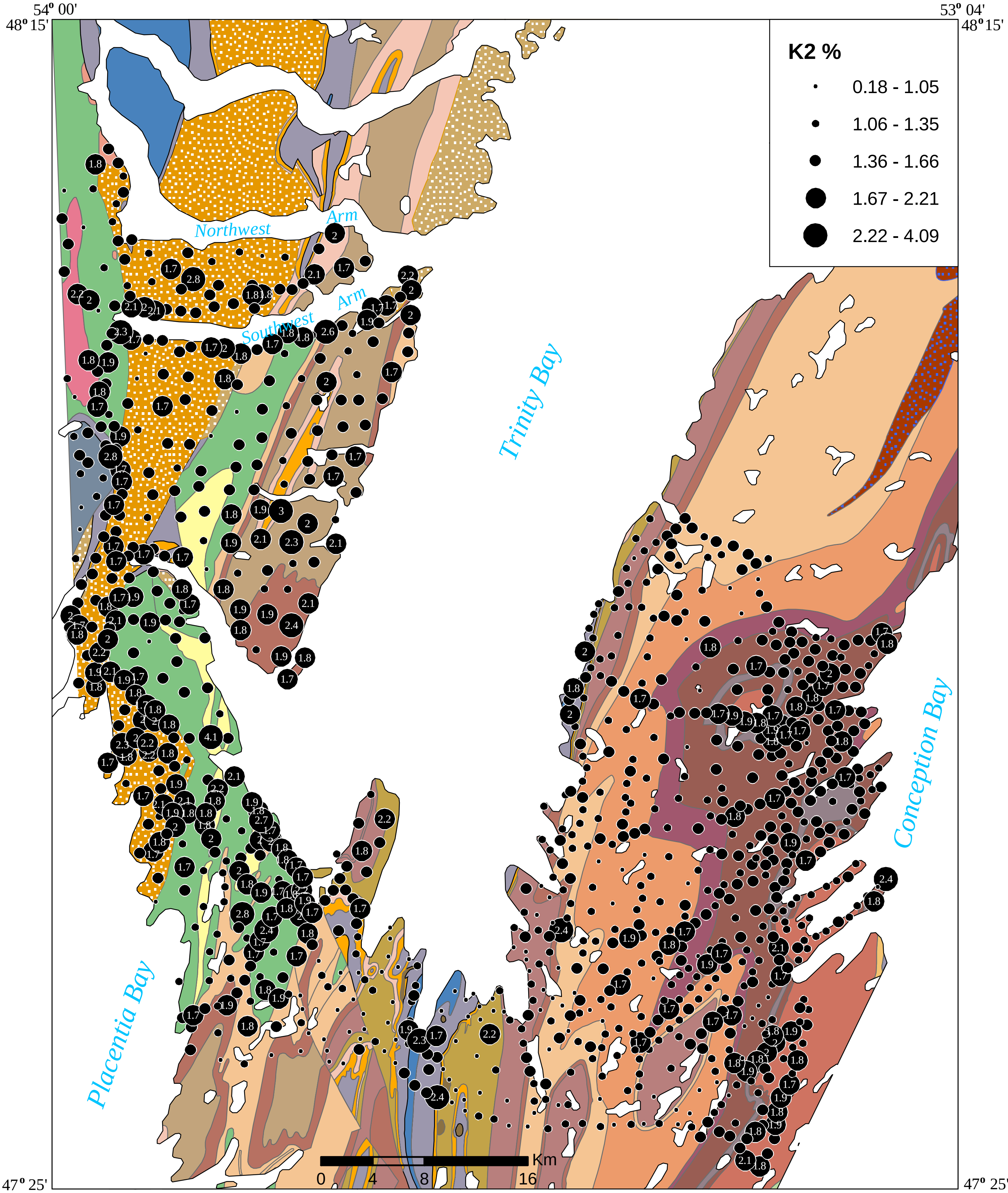

Open File NFLD 2824

Figure 33. Distribution of Lanthanum in till

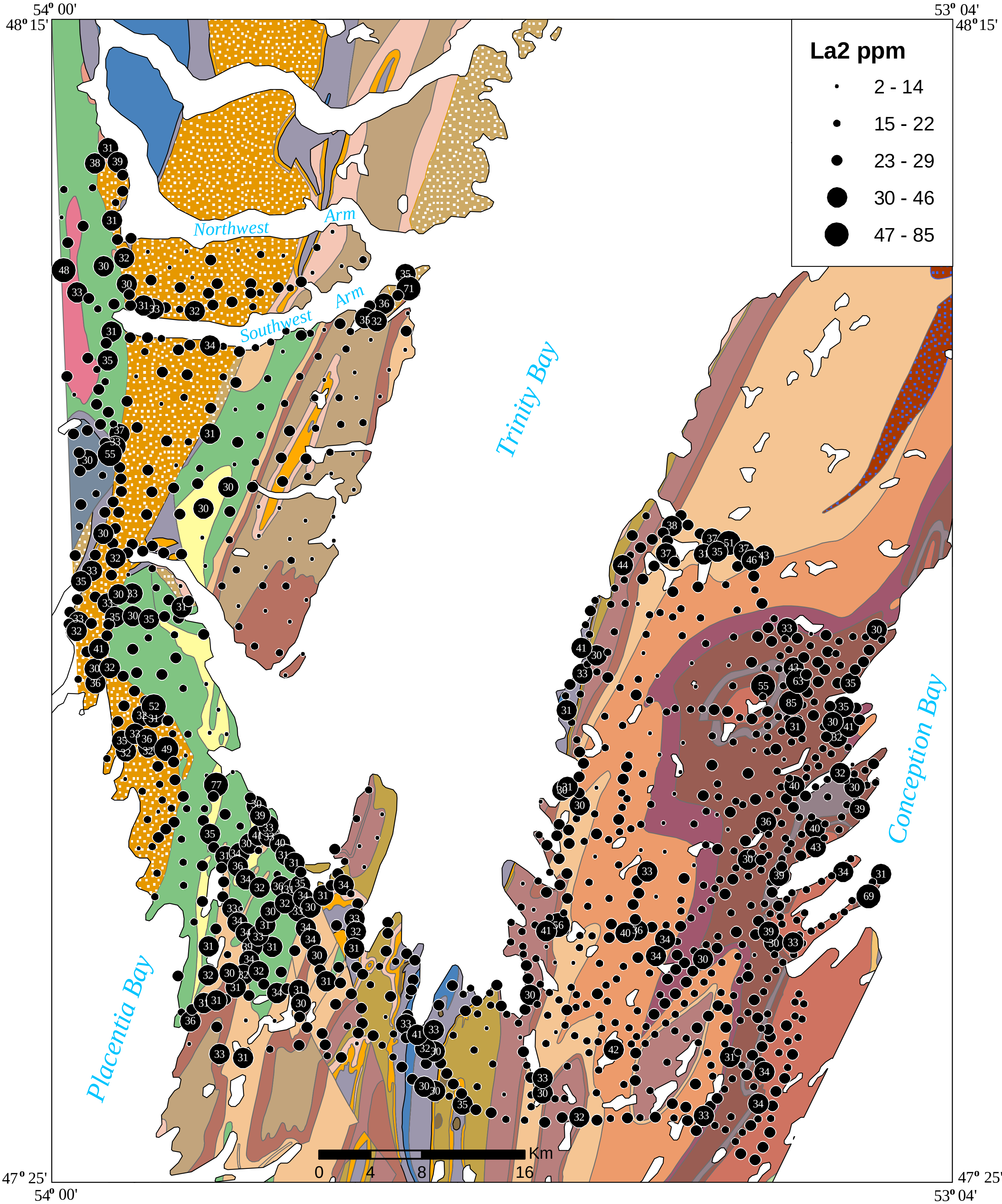

Open File NFLD 2824

Figure 34. Distribution of Lithium in till

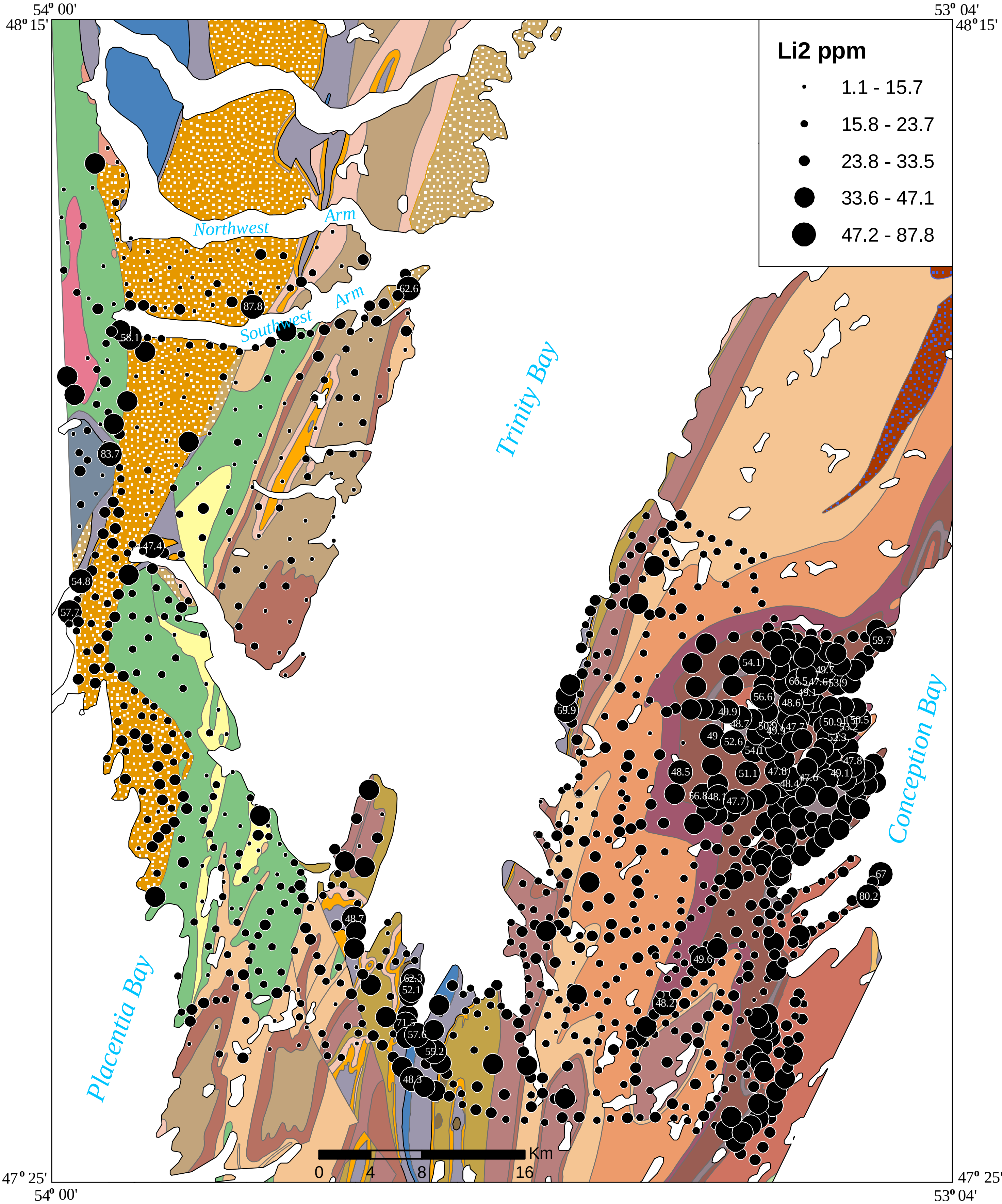

Open File NFLD 2824

Figure 35. Loss-on-Ignition in till

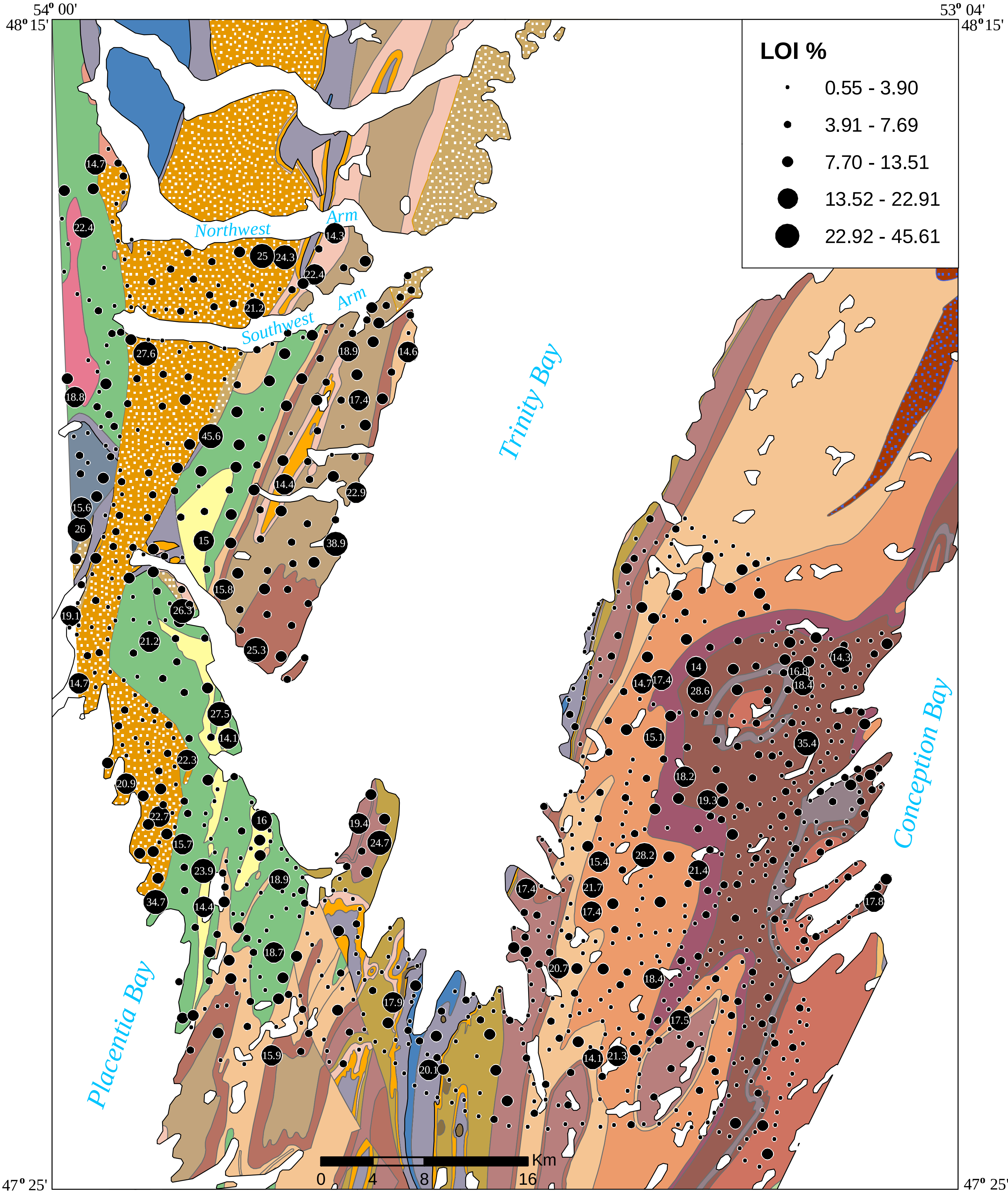

Open File NFLD 2824

Figure 36. Distribution of Lutetium in till

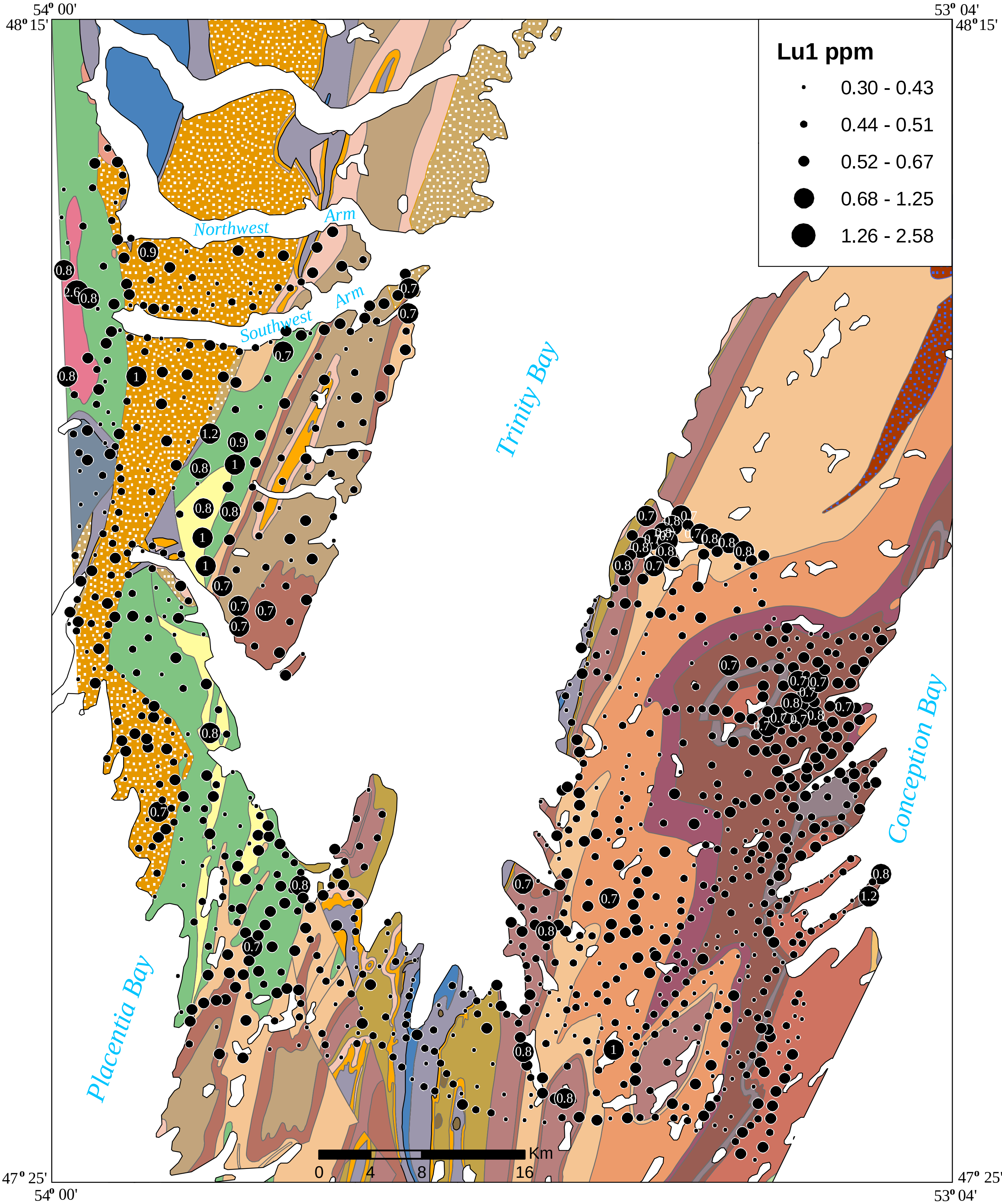

Open File NFLD 2824

Figure 37. Distribution of Magnesium in till

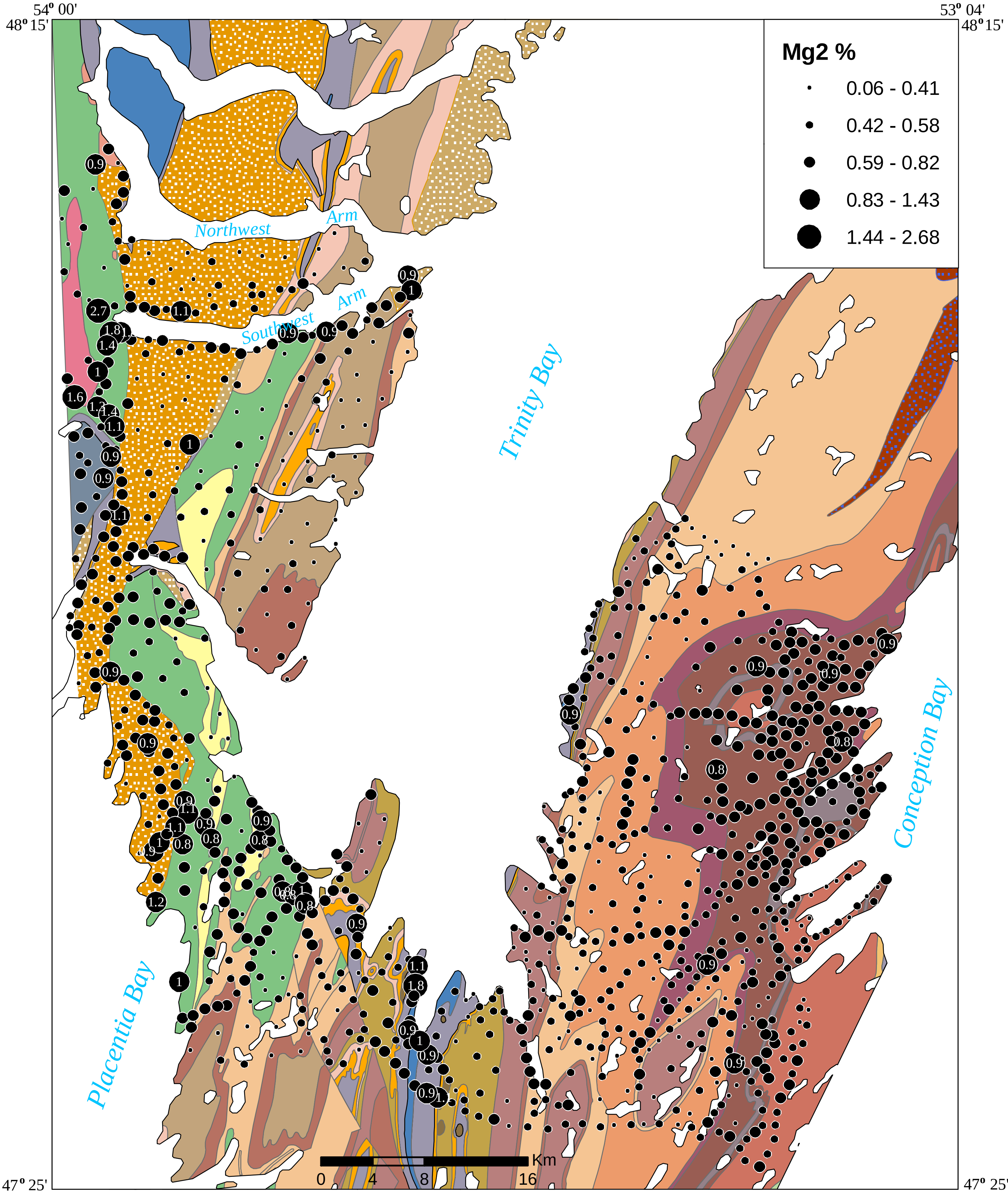

Open File NFLD 2824

Figure 38. Distribution of Molybdenum in till

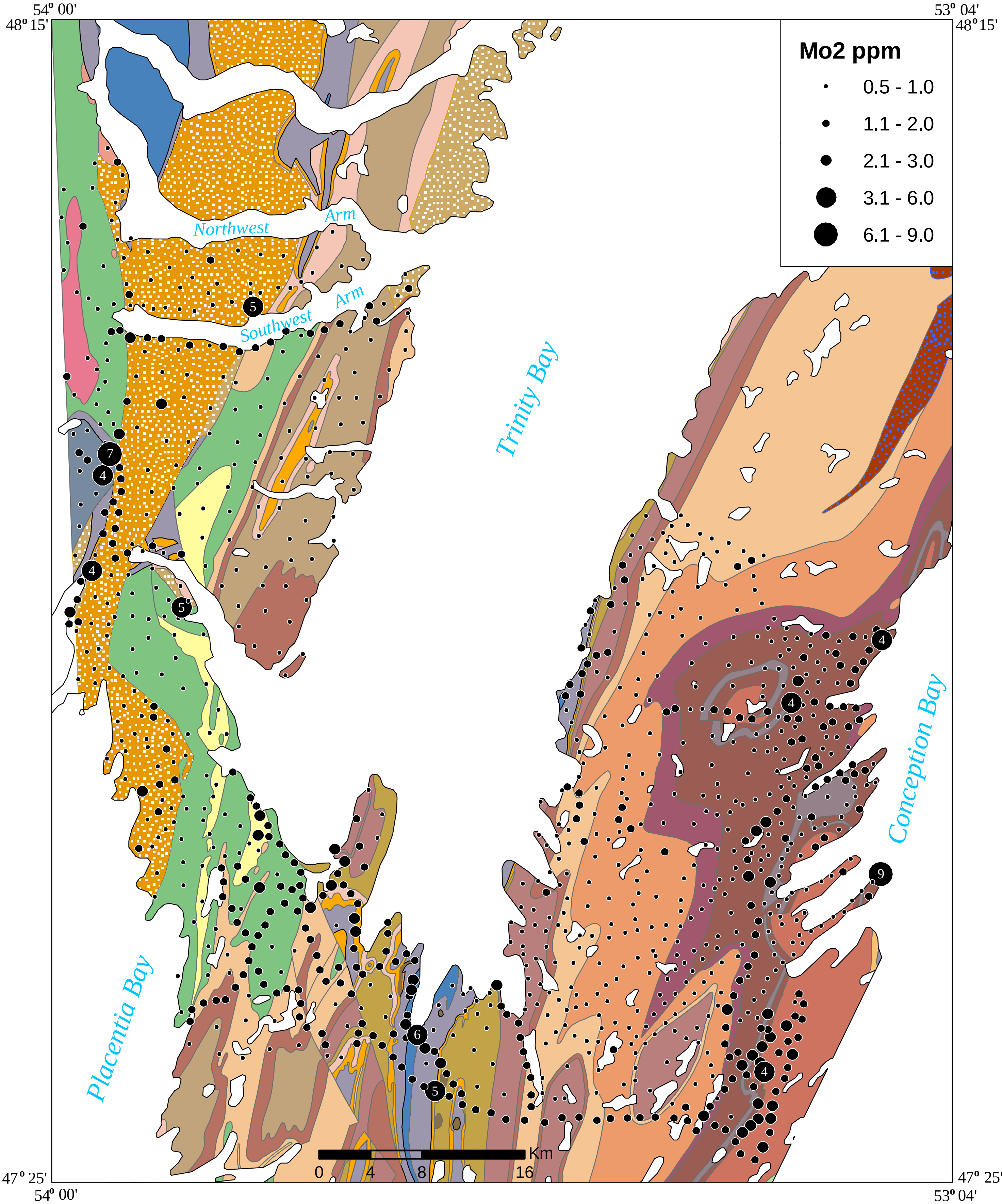

Open File NFLD 2824

Figure 39. Distribution of Sodium in till

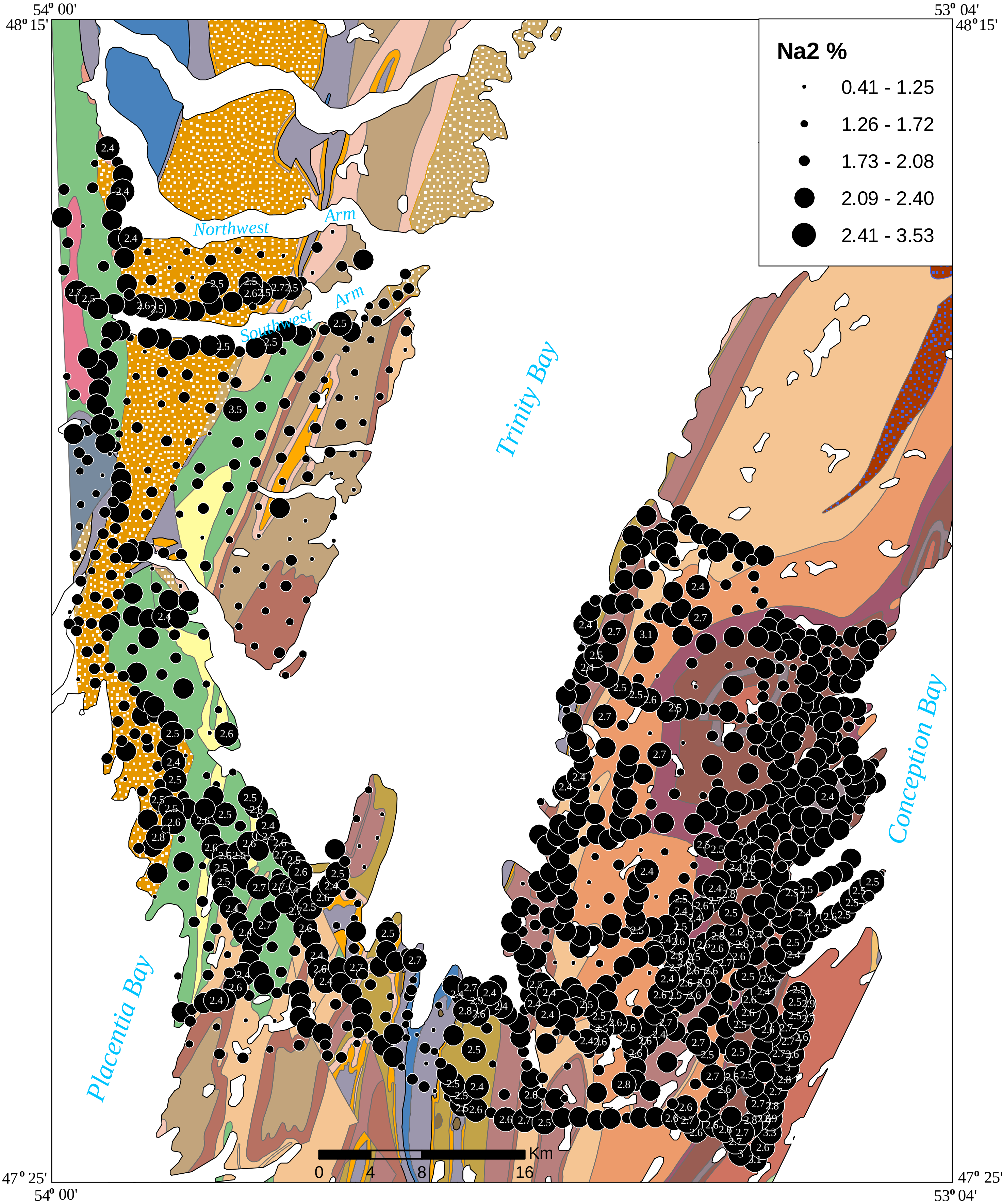

Open File NFLD 2824

Figure 40. Distribution of Niobium in till

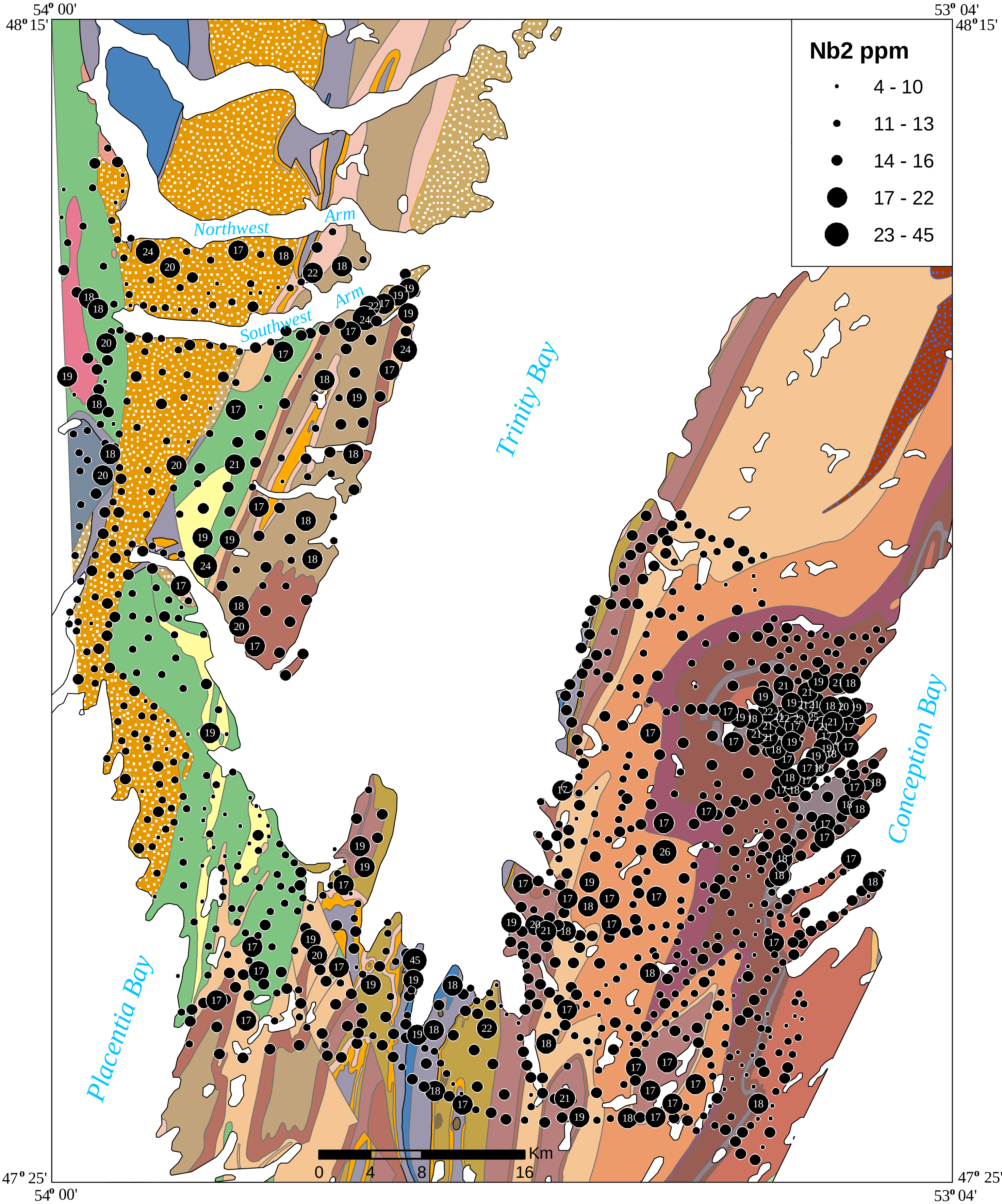

Open File NFLD 2824

Figure 41. Distribution of Neodymium in till

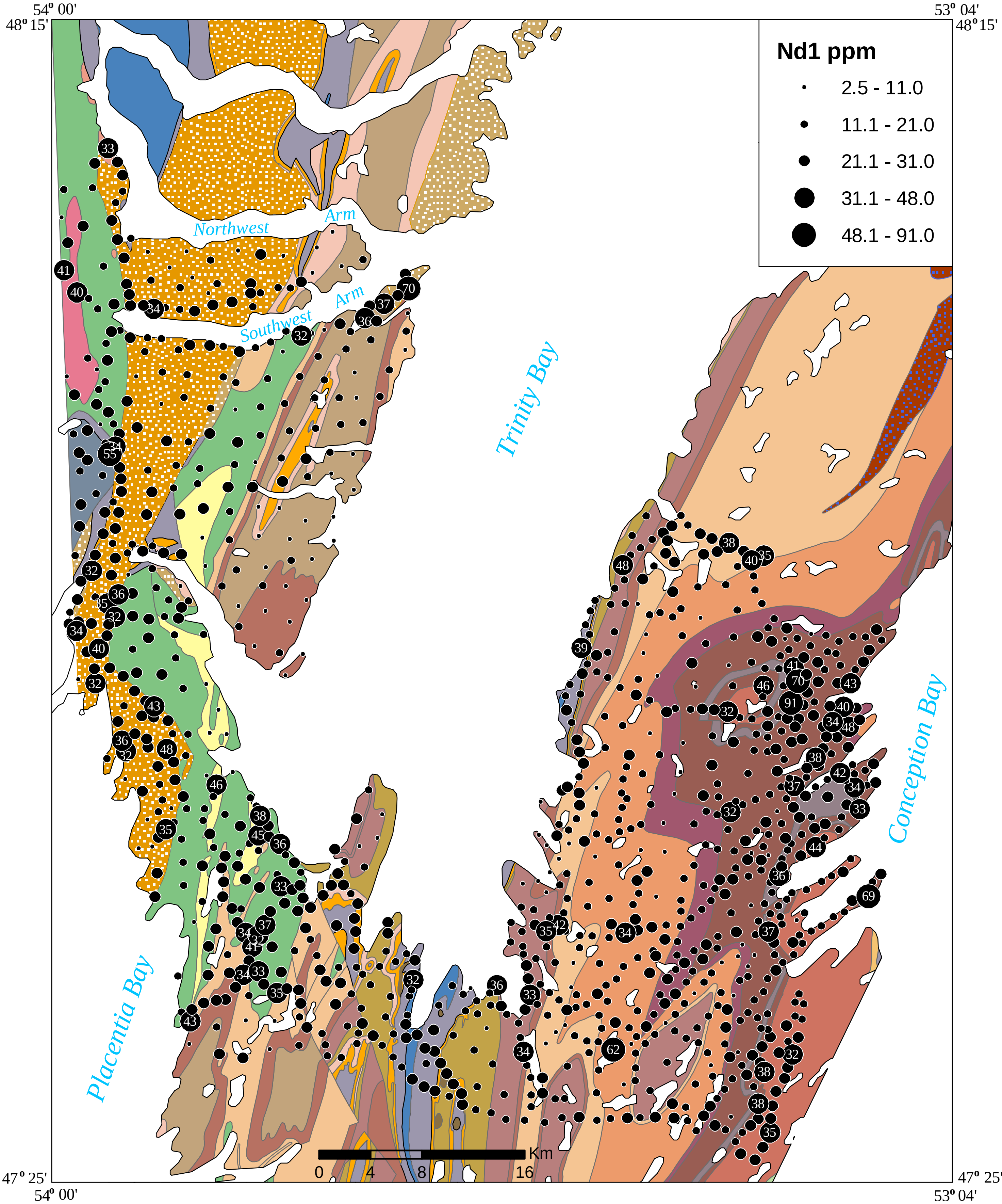

Open File NFLD 2824

Figure 42. Distribution of Phosphorous in till

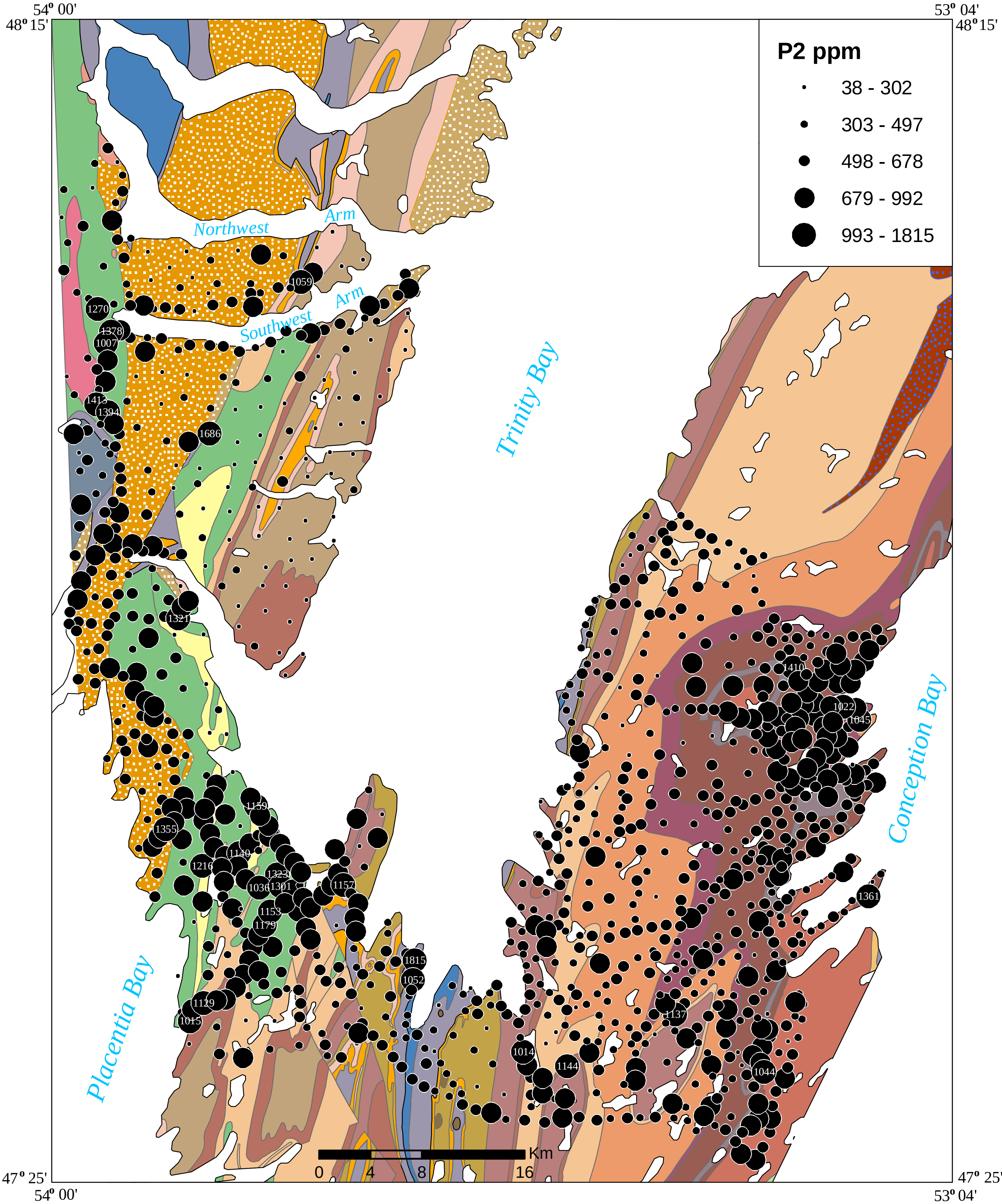

Figure 43. Distribution of Rubidium in till

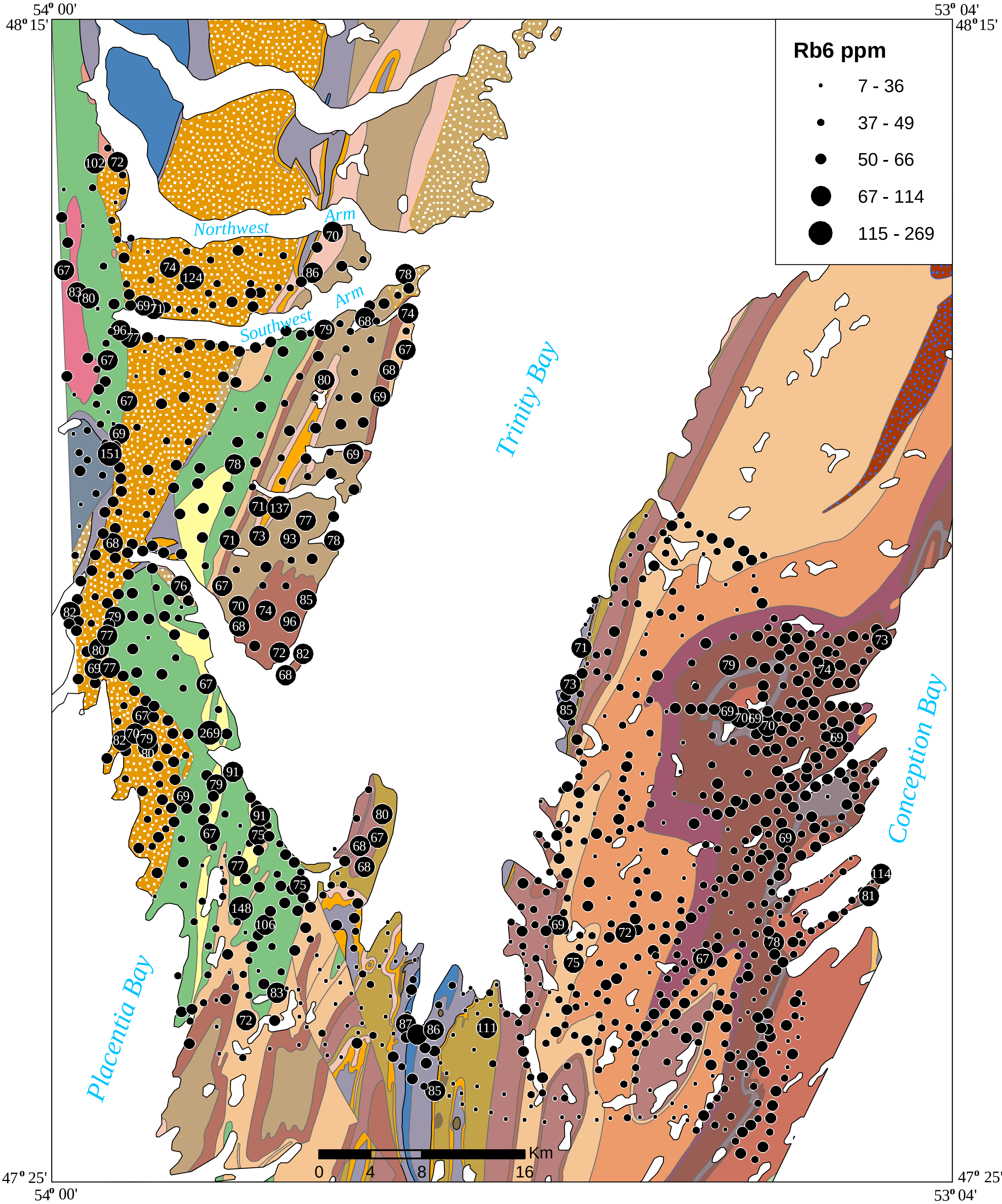

Open File NFLD 2824

Figure 44. Distribution of Scandium in till

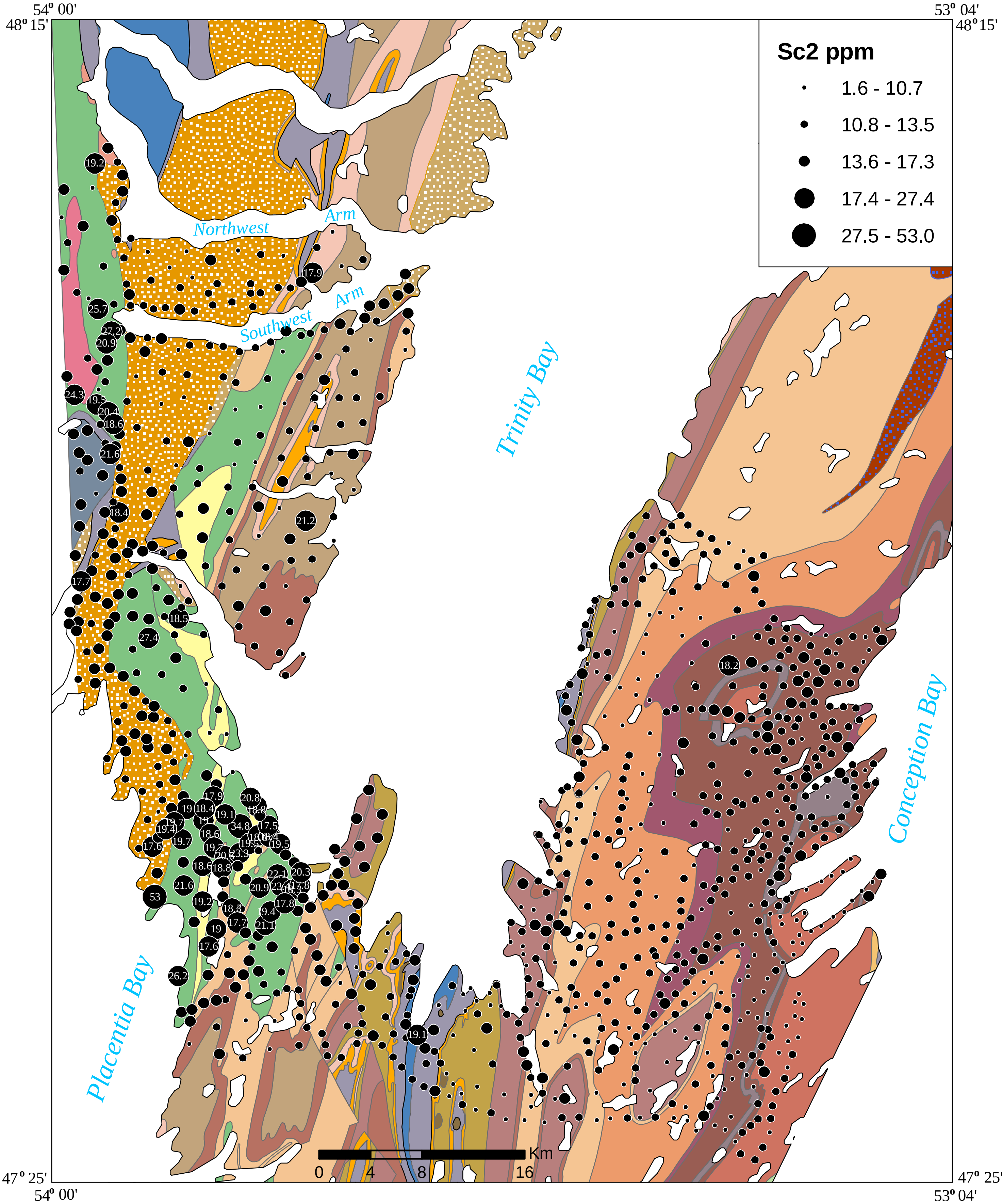

Open File NFLD 2824

Figure 45. Distribution of Selenium in till

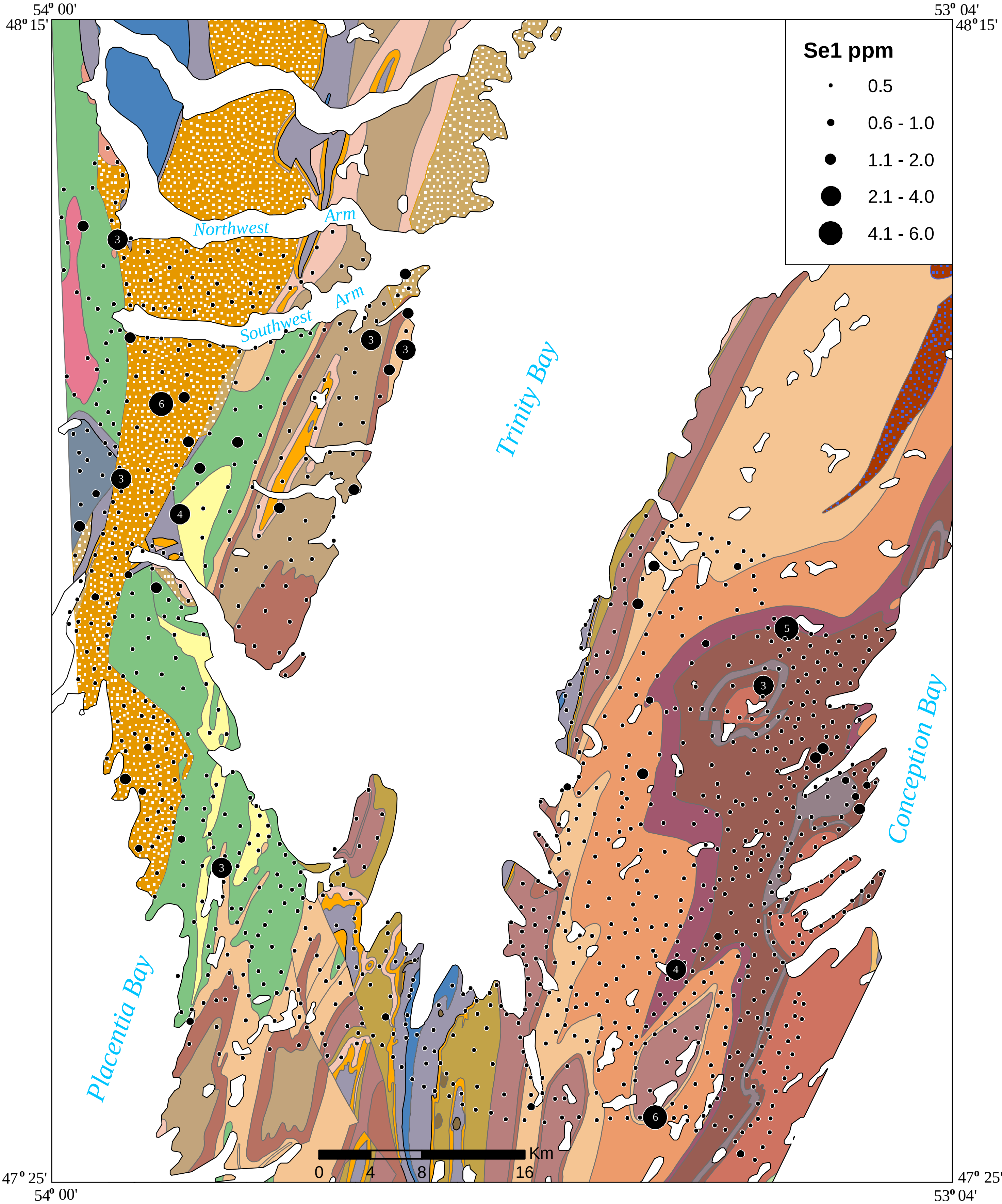

Open File NFLD 2824

Figure 46. Distribution of Samarium in till

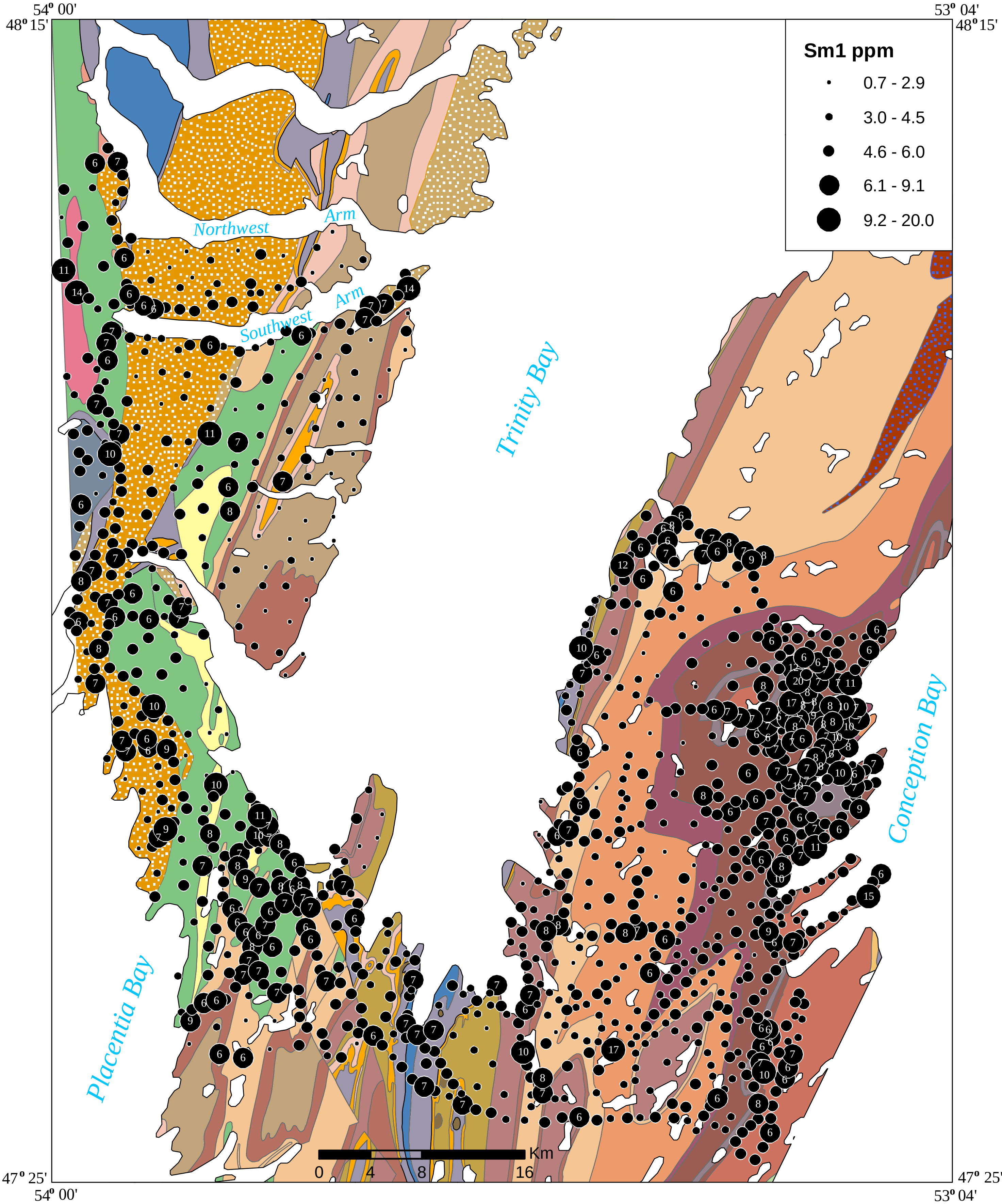

Open File NFLD 2824

Figure 47. Distribution of Tin in till

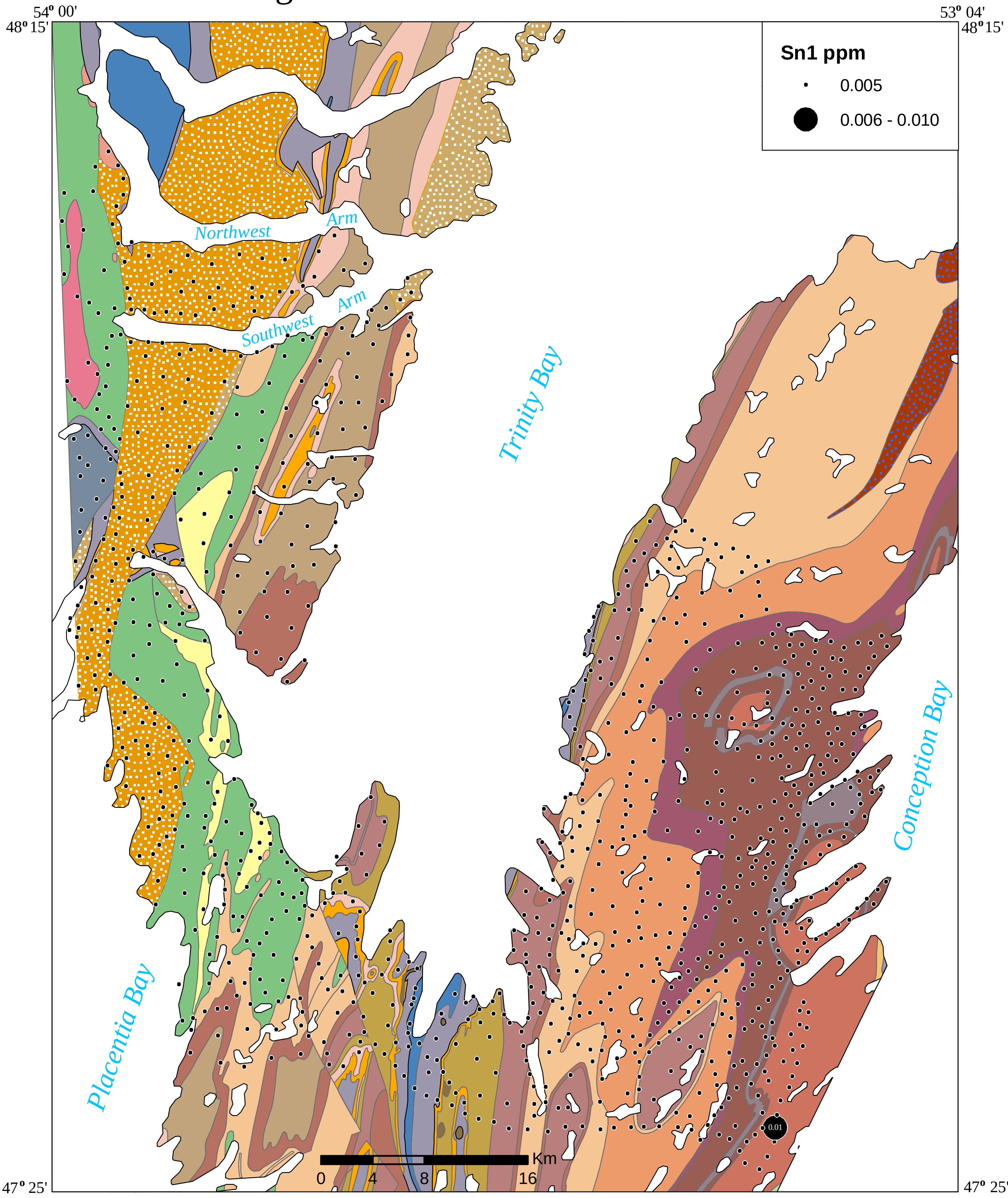

Open File NFLD 2824

Figure 48. Distribution of Strontium in till

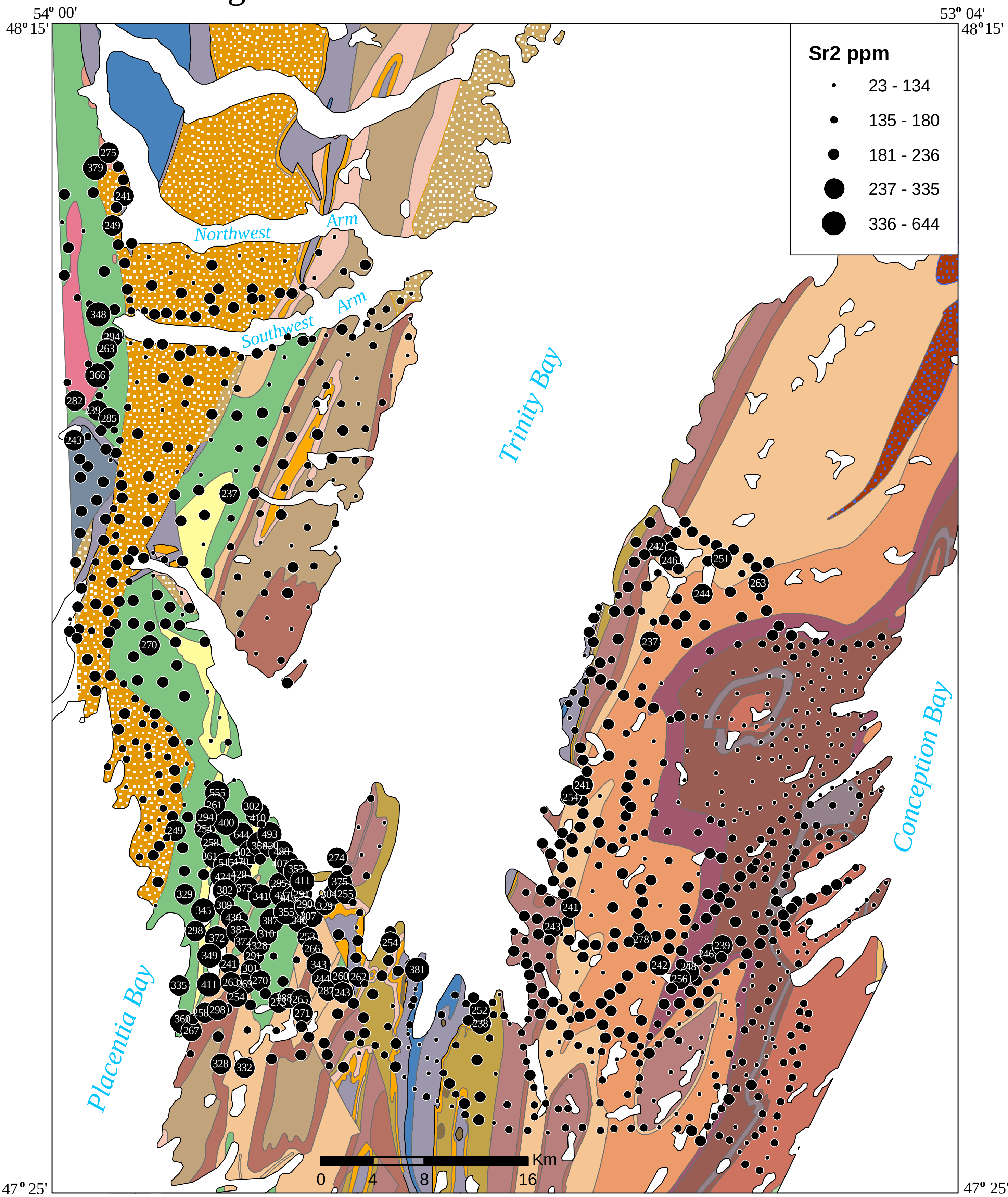

Figure 49. Distribution of Tantalum in till

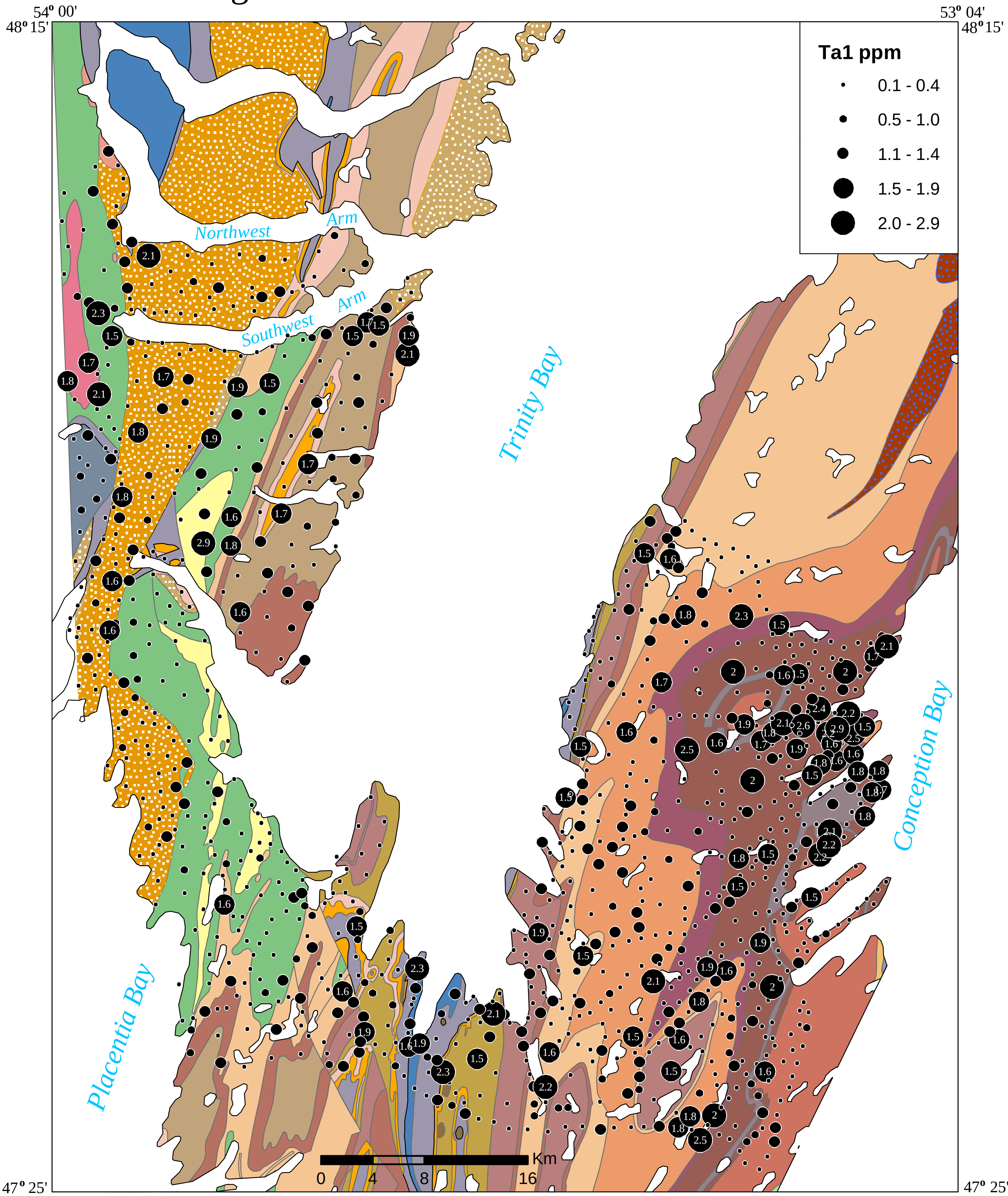

Open File NFLD 2824

Figure 50. Distribution of Terbium in till

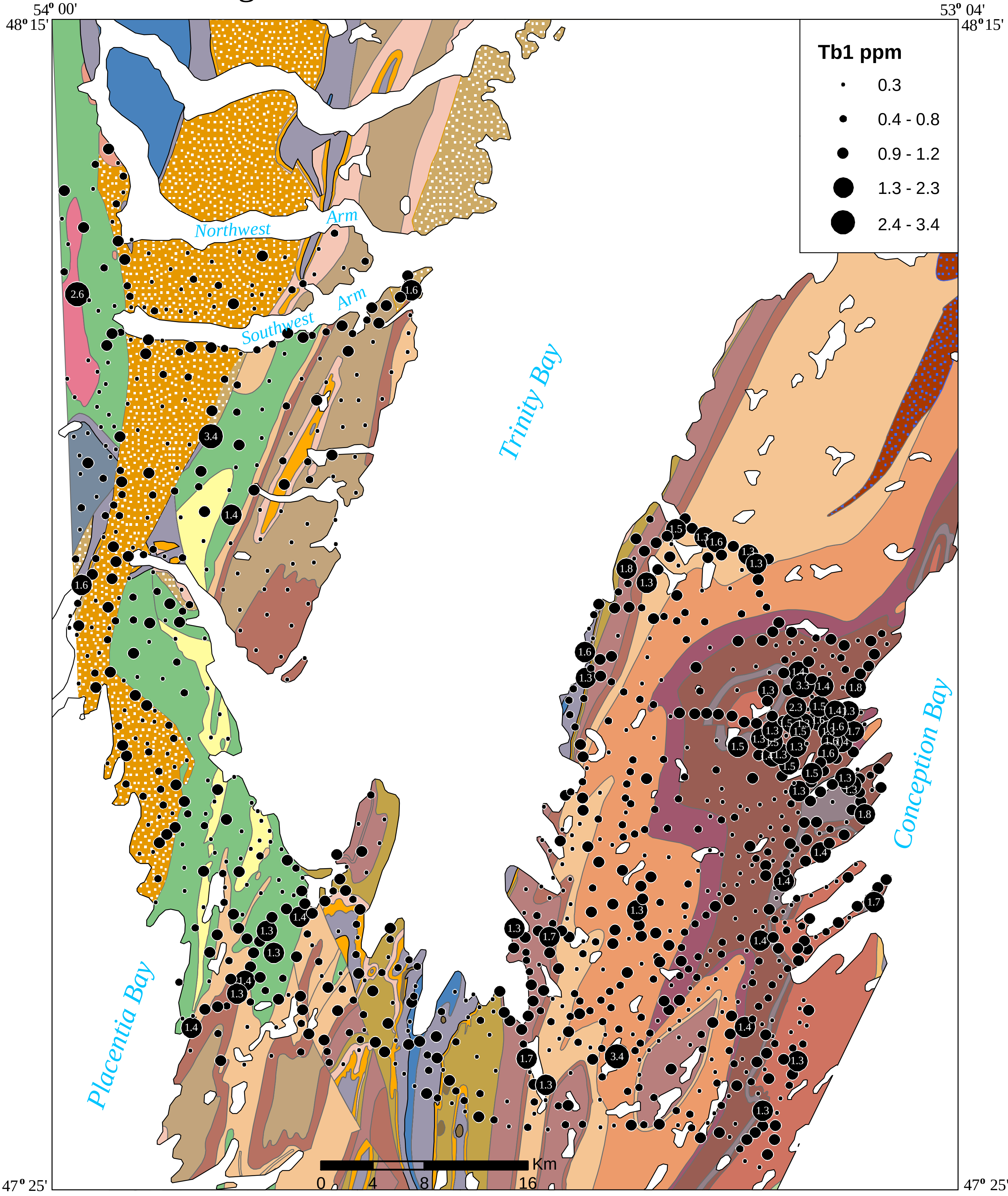

Open File NFLD 2824

Figure 51. Distribution of Thorium in till

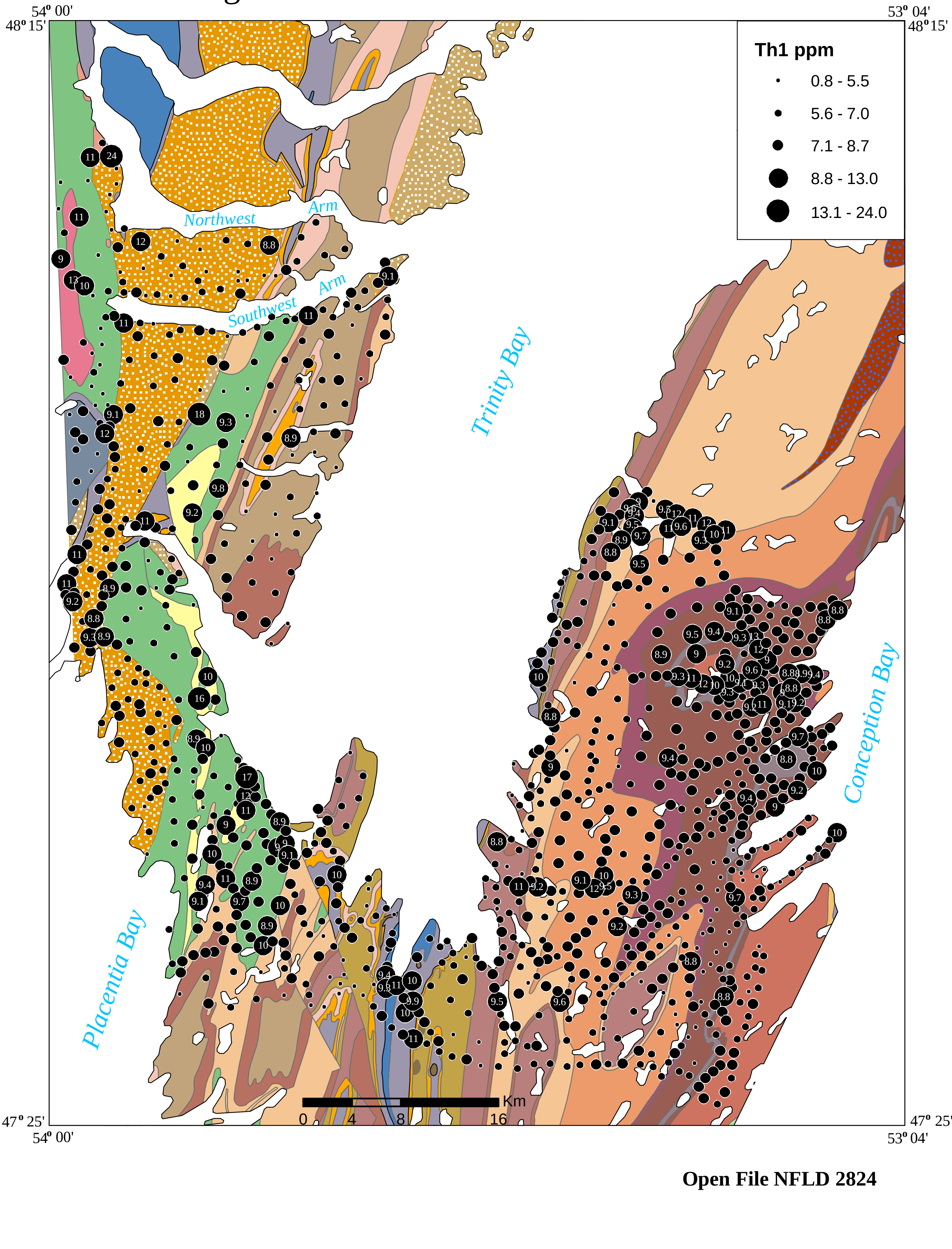

Open File NFLD 2824

Figure 52. Distribution of Titanium in till

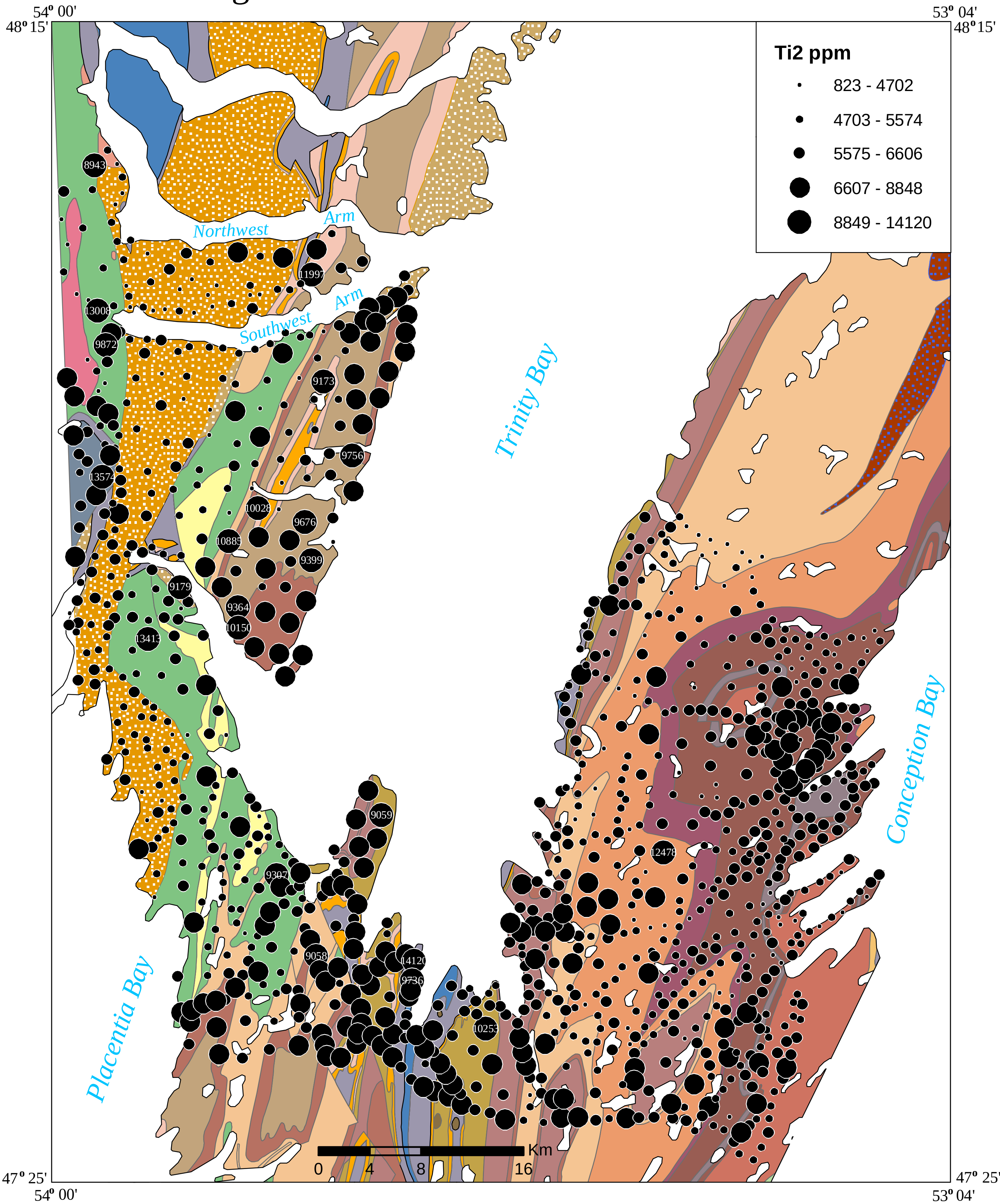

Open File NFLD 2824

Figure 53. Distribution of Uranium in till

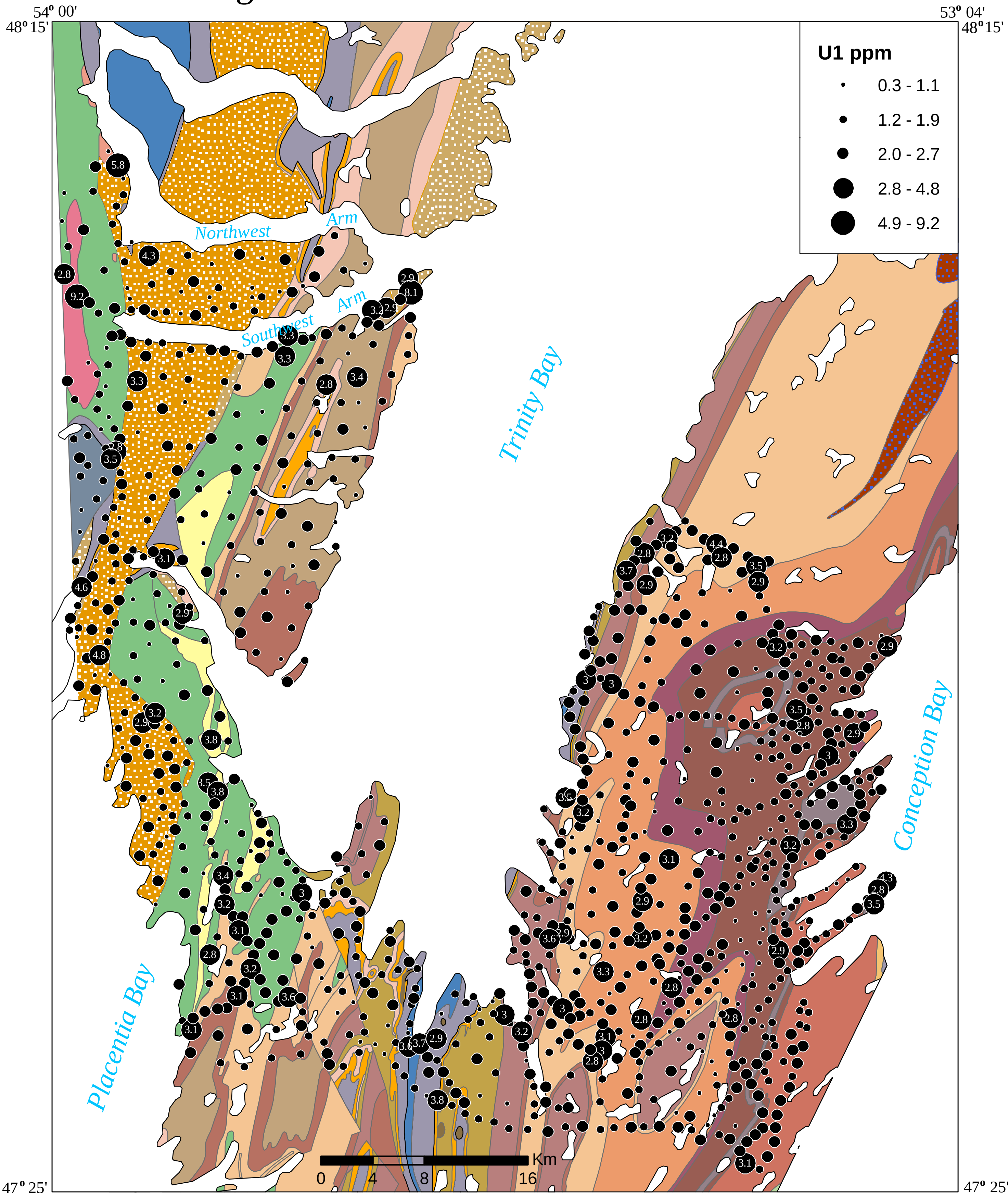

Open File NFLD 2824

Figure 54. Distribution of Tungsten in till

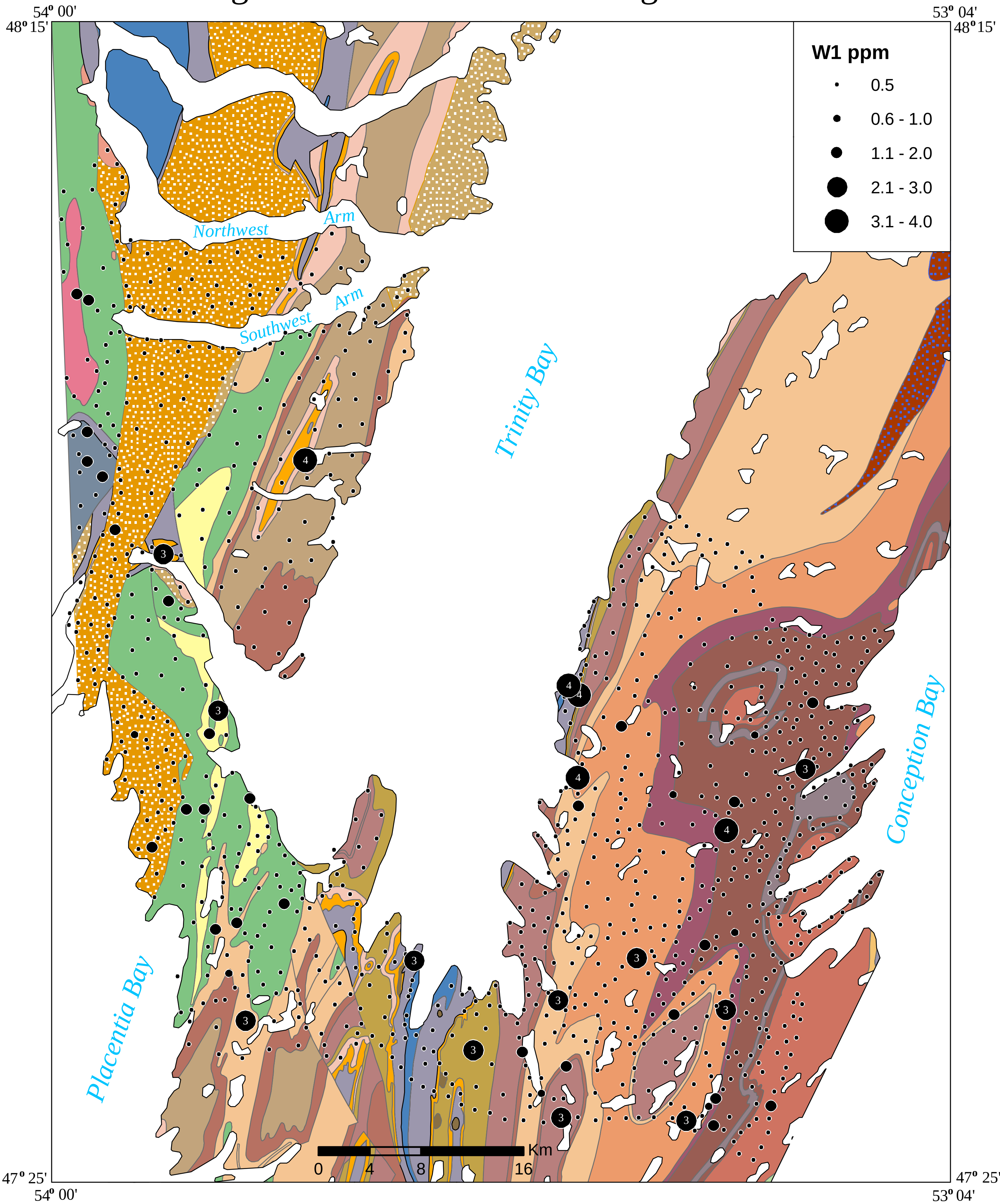

Open File NFLD 2824

Figure 55. Distribution of Yttrium in till

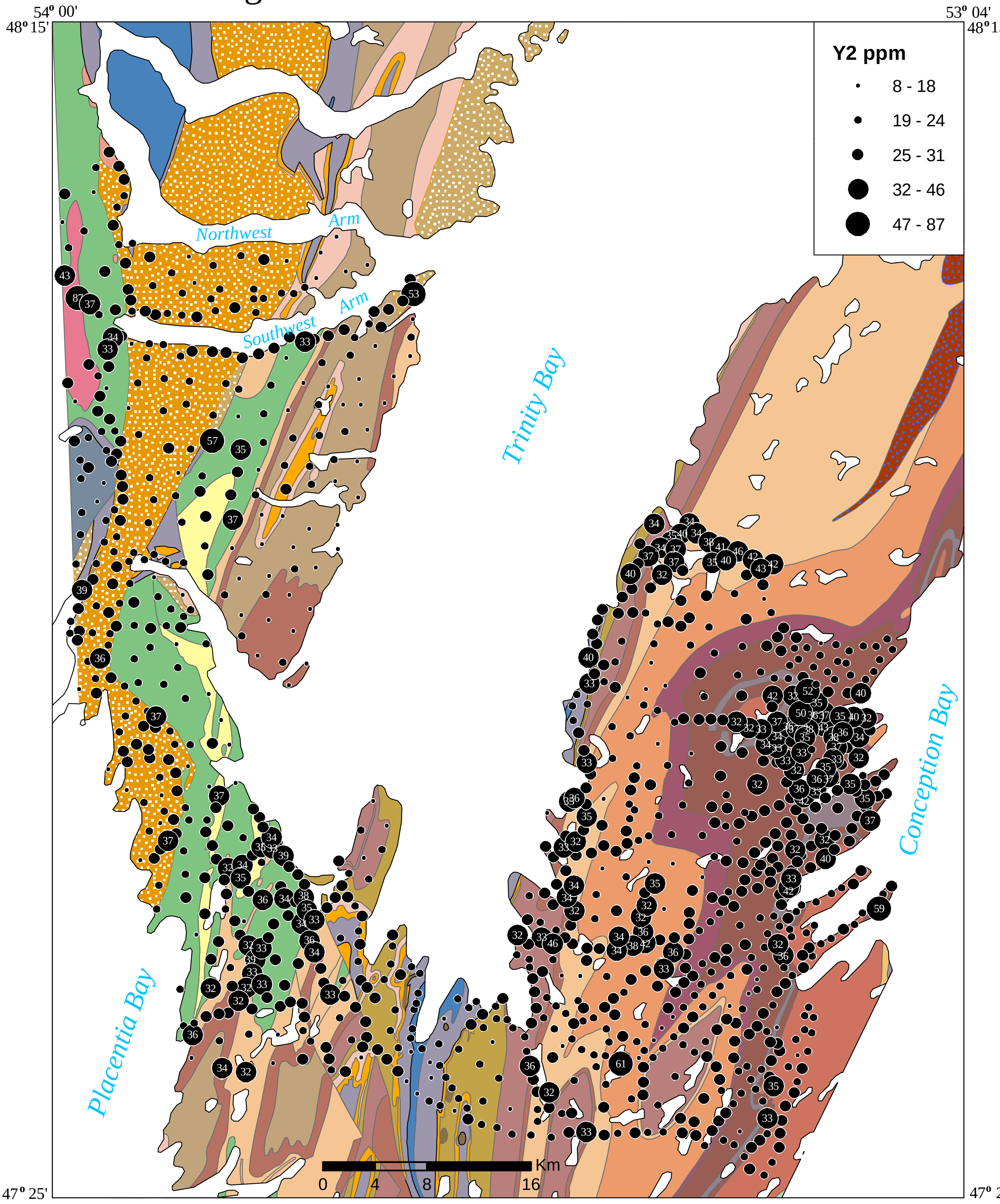

Open File NFLD 2824

Figure 56. Distribution of Zirconium in till

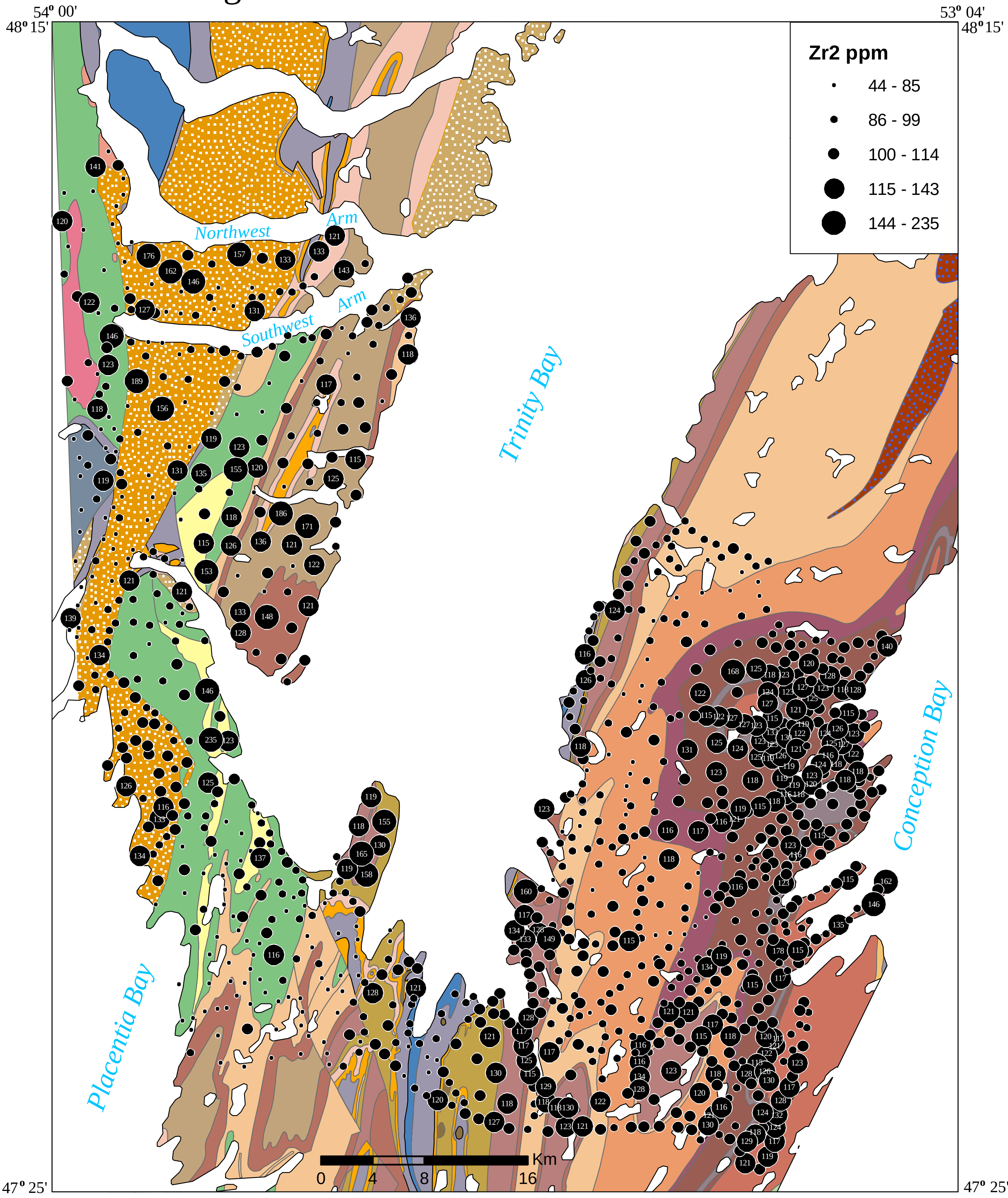

Open File NFLD 2824